Nondestructive Multivariate Classification of Codling Moth Infested Apples Using Machine Learning and Sensor Fusion

Nader Ekramirad
University of Kentucky, nader.ekramirad@uky.edu
Author ORCID Identifier:
https://orcid.org/0000-0001-9333-9713
Digital Object Identifier: https://doi.org/10.13023/etd.2022.342

STUDENT AGREEMENT:

I represent that my thesis or dissertation and abstract are my original work. Proper attribution has been given to all outside sources. I understand that I am solely responsible for obtaining any needed copyright permissions. I have obtained needed written permission statement(s) from the owner(s) of each third-party copyrighted matter to be included in my work, allowing electronic distribution (if such use is not permitted by the fair use doctrine) which will be submitted to UKnowledge as Additional File.

I hereby grant to The University of Kentucky and its agents the irrevocable, non-exclusive, and royalty-free license to archive and make accessible my work in whole or in part in all forms of media, now or hereafter known. I agree that the document mentioned above may be made available immediately for worldwide access unless an embargo applies.

I retain all other ownership rights to the copyright of my work. I also retain the right to use in future works (such as articles or books) all or part of my work. I understand that I am free to register the copyright to my work.

REVIEW, APPROVAL AND ACCEPTANCE

The document mentioned above has been reviewed and accepted by the student's advisor, on behalf of the advisory committee, and by the Director of Graduate Studies (DGS), on behalf of the program; we verify that this is the final, approved version of the student's thesis including all changes required by the advisory committee. The undersigned agree to abide by the statements above.

Nader Ekramirad, Student

Dr. Akinbode A. Adedeji, Major Professor

Donald Colliver, Director of Graduate Studies

NONDESTRUCTIVE MULTIVARIATE CLASSIFICATION OF CODLING MOTH INFESTED APPLES USING MACHINE LEARNING AND SENSOR FUSION

DISSERTATION

A dissertation submitted in partial fulfillment of the
requirements for the degree of Doctor of Philosophy in the
College of Agriculture, Food, and Environment and the College of Engineering
at the University of Kentucky

By
Nader Ekramirad
Lexington, Kentucky
Director: Dr. Akinbode Adedeji, Associate Professor of Food Process Engineering
Biosystems and Agricultural Engineering
Lexington, Kentucky

https://orcid.org/0000-0001-9333-9713

ABSTRACT

NONDESTRUCTIVE MULTIVARIATE CLASSIFICATION OF CODLING MOTH INFESTED APPLES USING MACHINE LEARNING AND SENSOR FUSION

Apple is the number one on the list of the most consumed fruits in the United States. The increasing market demand for high quality apples and the need for fast, and effective quality evaluation techniques have prompted research into the development of nondestructive evaluation methods. Codling moth (CM), *Cydia pomonella* L. (Lepidoptera: Tortricidae), is the most devastating pest of apples. Therefore, this dissertation is focused on the development of nondestructive methods for the detection and classification of CM-infested apples. The objective one in this study was aimed to identify and characterize the source of detectable vibro-acoustic signals coming from CM-infested apples. A novel approach was developed to correlate the larval activities to low-frequency vibro-acoustic signals, by capturing the larval activities using a digital camera while simultaneously registering the signal patterns observed in the contact piezoelectric sensors on apple surface. While the larva crawling was characterized by the low amplitude and higher frequency (around 4 Hz) signals, the chewing signals had greater amplitude and lower frequency (around 1 Hz). In objective two and three, vibro-acoustic and acoustic impulse methods were developed to classify CM-infested and healthy apples. In the first approach, the identified vibro-acoustic patterns from the infested apples were used for the classification of the CM-infested and healthy signal data. The classification accuracy was as high as 95.94% for 5 s signaling time. For the acoustic impulse method, a knocking test was performed to measure the vibration/acoustic response of the infested apple fruit to a pre-defined impulse in comparison to that of a healthy sample. The classification rate obtained was 99% for a short signaling time of 60-80 ms. In objective four, shortwave near infrared hyperspectral imaging (SWNIR HSI) in the wavelength range of 900-1700 nm was applied to detect CM infestation at the pixel level for the three apple cultivars reaching an accuracy of up to 97.4%. In objective five, the physicochemical characteristics of apples were predicted using HSI method. The results showed the correlation coefficients of prediction (R_p) up to 0.90, 0.93, 0.97, and 0.91 for SSC, firmness, pH and moisture content, respectively. Furthermore, the effect of long-term storage (20 weeks) at three different storage conditions (0 °C, 4 °C, and 10 °C) on CM infestation and the detectability of the infested apples was studied. At a constant storage temperature the detectability of infested samples remained the same for the first three months then improved in the fourth month followed by a decrease until the end of the storage. Finally, a sensor data fusion method was developed which showed an improvement in the classification performance compared to the individual methods. These findings indicated there is a high potential of acoustic and NIR HSI methods for detecting and classifying CM infestation in different apple cultivars.
KEYWORDS: Apples, Codling moth, Sensor fusion, Vibro-acoustic, Hyperspectral imaging, Machine learning

Nader Ekramirad

06/17/2022

Date

NONDESTRUCTIVE MULTIVARIATE CLASSIFICATION OF CODLING MOTH INFESTED APPLES USING MACHINE LEARNING AND SENSOR FUSION

By
Nader Ekramirad

Dr. Akinbode Adedeji
Director of Dissertation

Dr. Donald Colliver
Director of Graduate Studies

06/17/2022
Date

DEDICATION

I dedicate my dissertation work to my family, my wife, and my newborn son. A special gratitude to my lovely wife, Mobarakeh whose love, energy and patience made life easier for me through regulating our life during the challenging last months of my dissertation.

ACKNOWLEDGMENTS

I would like to thank you the following people for their help and support in the process of my Ph.D. work at the department of Biosystems and Agricultural Engineering, University of Kentucky. First, special thanks to my advisor Dr. Akinbode Adedeji whose full support, mentorship and leadership made this accomplishment possible. I deeply value the opportunity to work with Dr. Adedeji during this project. His concerns and ideas toward world's food quality and security, and agricultural sustainability have been and will be a strong driving force for me to pursue my research in this area. I also want to thank my committee members for their eye-opening points and ideas throughout this work. Especially, Dr. Kevin Donohue who provided me with technical knowledge in acoustic signal processing and many useful advice and suggestions throughout this project. Also, I would like to thank Dr. Raul Villanueva and his team in Department of Entomology for their excellent contribution in the project. Additionally, I would like to thank Dr. Tim Stombaugh and Dr. Joshua Jackson for their contributions to my committee and their critical evaluation of my research. I would like to appreciate my friends and coworkers Dr. Alfadhl Y. Khaled, Chad Parrish, Lauren Doyle, and Julia Loeb who helped me a lot in many aspects of my research. Last but not least, I would like to extend my sincere thanks to my parents for their love and support. Without their help, this achievement would not have been possible.

TABLE OF CONTENTS

LIST OF TABLES

LIST OF FIGURES

CHAPTER 1. INTRODUCTION

Apple (*Malus domestica*) is one of the most widely grown and valuable fruits in the global market. There is a growing demand for fruits generally, especially apples (organic cultivars mostly) due to increased awareness of consumers on the positive health implications of fruit consumption and its impact on their wellness. Additionally, post COVID-19 pandemic, the production of fresh apples is projected to witness a compound annual growth rate (CAGR) of 4.0% during 2022-2027 to meet the global market demand. They are commercially grown in 32 states with a total production of 11 billion pounds in 2019, which makes the United States the second largest apple producer country in the world (USDA Economic Research Center, 2020). Apple is ranked first on the fruit consumption list in the U.S. with an average value of about 26 pounds per person (USDA Economic Research Center, 2015). As a high-value crop with improved cultivars selling at premium prices, apple production value in the United States was over $3 billion in 2018 (USDA Economic Research Center, 2020). Among the 200 unique apple varieties grown in the U.S., the top 10 varieties are Red Delicious, Gala, Granny Smith, Fuji, Golden Delicious, Honey Crisp, McIntosh, Rome, Cripps, and Pink Lady (U.S. Apple Association 2018). Approximately 25% of apples produced in the United States are exported to some top destinations such as Mexico, Canada, India, Taiwan, United Arab Emirates, Hong Kong, Vietnam, Indonesia, Saudi Arabia, and Thailand (U.S. Apple Association 2018). However, there are relatively small amount of fresh apples imported to the U.S. in the late season which account for five percent of total yearly consumption (U.S. Apple Association 2018).

The multi-billion-dollar US apple industry is dealing with some challenges in meeting more stringent regulatory restrictions such as zero-tolerance level for insect infestation in shipments, as well as ever-increasing public awareness and concern over health and the environment (Ag Marketing Resource Center, 2021). Besides, there is a fast-growing consumer demand for high-quality apples that are raised under certified organic farming systems. Organic apples are among the top three most-demanded fresh fruits (Ag Marketing Resource Center, 2021). New standards are prohibiting traditional approach to pest management; it is therefore imperative to develop new management and monitoring techniques needed for quality assurance of fruit crops like apples.

Insect pests are the main destructive organisms harbored by the fruits, affecting their quality negatively (Singh & Sharma, 2018). Insects pose significant economic losses in post-harvest agroindustry due to shipment rejections, shipment restrictions, quality reduction, and price drops (Arthur et al., 2010). Insect management in post-harvest systems to reduce the insect pest risk to exported fresh fruits is usually achieved through phytosanitary measures and quarantine treatments as well as some alternative treatments such as irradiation, fumigation and Controlled Atmosphere/Temperature Treatment System (CATTS) (Hallman & Hellmich, 2009; Neven et al., 2006). Although pests hardly persist under commercial storage conditions using these alternative measures, the application of these methods is limited due to the inaccessibility of technology, noncompliance with organic standards and environmental health, and cost or complexity of operation compared to existing methods (Arthur et al., 2010). For instance, methyl bromide, which is currently used in many countries for fumigation of CM in combination with cold storage treatment, is subject to phase-out requirements of the 1987 Montreal

Protocol on Ozone Depleting Substances (Jamieson et al., 2018). CATTS, an example that has been assessed as a disinfestation measure to control CM larvae inside apples, leads to deterioration in external and internal quality attributes of apple fruits and needs further refinement of its protocols (Jamieson et al., 2018). On the other hand, there is a lack of appropriate monitoring and identification methods for the early detection of immature insects in post-harvest systems to prevent the whole batch of shipments from being rejected at the export destination (Kumar & Vishwakarma, 2018; Singh & Sharma, 2018). Thus, effective nondestructive monitoring and detecting techniques are needed to prevent post-harvest losses in the region of origin and to avoid the biological and economic consequences of insect pest invasion in domestic and international destinations.

Codling moth (CM), *Cydia pomonella* L. (Lepidoptera: Tortricidae), one of the 100 worst invasive alien species worldwide, is the most detrimental apple pest with the potential of infesting 100% of an orchard (Witzgall et al., 2008). Moreover, recent machine learning based models have predicted the continuation of widespread global distribution of CM especially in Europe, Asia, and North America, based on global accessibility data, apple yield data, elevation data and 19 bioclimatic variables along with the ecological characteristics (Jiang et al., 2018). In fact, despite the limited flight capability of the CM, they are very likely to distribute over long distances through transportation. As a result, export markets in many countries, especially in Asia, enforce a zero-tolerance policy for this pest. These Asian countries are the major destinations for most U.S. apples. Therefore, there is an urgent need to develop robust, accurate, and effective nondestructive techniques for the detecting of CM-infested fruits in the export and import borders to prevent ecological and economical losses.

There are several different nondestructive techniques such as near-infrared (NIR) spectroscopy, machine vision, hyperspectral imaging (HSI), thermography, X-ray, magnetic resonance imaging (MIR), and E-nose/E-tongue that can be used for detection of insect infestation in fruits. There are some advantages and limitations of these techniques relevant to detecting insect infestation in fruits. For example, since HSI provides high-fidelity spatial-spectral information over a wide range of the light spectrum (Lower et al., 2017), it is preferred for identifying the symptoms of surface infestation which cannot be accurately detected with a regular RGB camera because of interference from the sample's surface color (Cubero et al., 2011; Ruiz-Altisent et al., 2010). Moreover, unlike the visible color vision method which cannot be used for the detection of internal defects, HSI in NIR range is capable of providing some internal biochemical information related to insect infestation in fruits (Pu et al., 2015). Another example of nondestructive detection approaches is acoustic method, which is automatic, sensitive, mostly inexpensive, and efficient for the detection of hidden insects damages inside agricultural commodities (Mankin et al., 2011). Thus, in this study, acoustic and HSI methods have been identified because of their complementary advantages for the detecting and classifying of CM-infested apples.

Fruits and vegetables, in general, have complicated and dynamic textures with different characteristics. As a result, only limited information on fruit samples will be obtained using an individual sensing technique (Zhou et al., 2020). Thus, merging the data from different sensors can give comprehensive information of the characteristics of fruits and improve the prediction accuracy through a better understanding of internal and external states of the samples. Besides, CM infestation leads to deterioration in both external and internal physicochemical characteristics of apples. Therefore, individual sensing techniques will only capture one (or a few) of the many aspects of infestation damage. For example, HSI provides physical and chemical information from the surface up to a few mm depth into the fruit tissue and flesh (Liu et al., 2019); however, it is not able to acquire data from the core of apples. On the other hand, vibrational acoustic methods can be used to monitor and detect the infested samples through sensing either the activities of the insect deep into fruit, or the internal physicochemical changes related to the infestation. Thus, in this study, it was proposed to investigate the application of the sensor fusion approach (HSI and acoustic) along with machine learning methods for detecting CM infestation in apples to harnessing the merits of both methods to improve the classification performance of the machine learning models for higher accuracy.

1.1 Rationale and Significance

The development of effective nondestructive methods for detecting infested apples is of great importance for boosting the reliability and efficiency of monitoring quarantine pests in countries such as the United States with a huge amount of apple import and export. The USDA indicates that the inspection of plant materials for their internal quality is mostly conducted manually in a random and destructive manner, which is labor-intensive, tedious, costly, and subjective (USDA annual report, 2017). Furthermore, the traditional destructive evaluation methods cause huge losses from unusable infected samples and it is grossly ineffective. Therefore, the significance of this study impinges on improvement in the approach to pest detection in apple to replace the current cumbersome method. This will lead to improvement in apple quality assessment, particularly in detecting CM-infested apples, moving from an invasive and random method of detection to an objective, and nondestructive technique. There is a potential to expand and apply the results of this study to post-harvest insect infestation detection in other fruits. Currently, there is no known nondestructive method used for the detection and classification of CM-infested apples. The proposed approach in this study will set the stage for the development of technologies that will lead to near-perfect detection of CM infestation in apples.

1.2 Hypothesis

We hypothesize that:

1. Low-frequency vibro-acoustic signal pattern of CM larval activity is recognizable and can be used for detecting and classifying the infested apples with active larvae.
2. External stimulation, such as heat, can affect the intensity of the larval activities and lead to enhanced detection of CM infestation.
3. High-frequency acoustic impulse response from infested apples is different from the signals from healthy ones and contains distinguishable statistical features.
4. Physicochemical quality attributes of apples change as a result of storage as well as the infestation process, and can be predicted using a nondestructive hyperspectral method.
5. HSI method can accurately detect external and internal defects in CM-infested apples.
6. Sensor fusion of acoustic and HSI methods combined with machine learning will improve the classification rate of CM-infested apples in comparison to either of the individual methods.

1.3 Objectives

The main goal of this study is to detect and classify CM-infested apples using a sensor fusion approach (acoustic and hyperspectral imaging techniques), along with different pattern recognition and machine learning methods.

1.3.1 Specific Objectives

The following are the specific objectives of this study:

Objective One: To identify the source of the detectable vibrational (vibro)-acoustic signals coming from CM-infested apples through:

Objective Two: To develop pattern recognition and classification models for the detection and classification of vibro-acoustic signals of CM-infested apples.

Objective Three: To detect CM-infested apples using high-frequency acoustic impulse response test.

Objective Four: To classify CM-infested apples through identification and detection of external and internal defects using the HSI method.

Objective Five: To build calibration models for the prediction of some important physicochemical quality attributes of apples during storage using a nondestructive hyperspectral imaging method.

Objective Six: To study the detectability of CM-infested apples over 20 weeks of storage to define the condition threshold for the most effective detection of apple infestation.

Objective Seven: To develop a sensor fusion model using the acoustic and HSI features through machine learning methods to improve the classification rate of CM-infested apples.

CHAPTER 2. LITERATURE REVIEW

2.1 Overview

Insects cause enormous damage to fruits, vegetables, and field crops each year, leading to major production and economic losses in the agricultural production and food industry worldwide. Insect pests are responsible for approximately 10–20% of yield losses in major crops worldwide, and even far more in developing countries, reaching about 50% of annual horticultural production loss in Africa, which is a $22.5 billion industry (Badii et al., 2015). The havoc caused by insect pests in trans-border trade, with increased global trade network, is enormous. The detection of these insect pests before they get into the supply chain is still a major challenge for the industry. The U.S. loses about $40 billion yearly due to the presence of these organisms of quarantine concern (Gulati et al., 2016; Pimentel et al., 2005). On the other hand, insect affecting crops in the field such as budworms, or caterpillars are hard to control (Liu et al., 2017). Insect feeding often occurs cryptically within fruits and vegetables without showing an obvious external symptom until they are nearly fully rotten. This is the case of the codling moth (*Cydia pomonella* (L.), Lepidoptera: Tortricidae), one of the most devastating pests in apples. This insect has four main stages in its life cycle; egg, larva, pupa, and adult moth (Greenwood, 2000). The larval phase is its most devastating phase when it feeds on the flesh and pulp of fruits it was laid on. When the point of entry is the calyx, the damage is difficult to detect with the subjective method of assessment common in most apple processing plants, and this is why nondestructive detection becomes important (Rady et al., 2017; Greenwood, 2000). Early detection when eggs are laid on the surface of the produce is also very important.

In order to prevent the economic and ecological losses from alien insect pests, increasingly stringent quarantine measures are being put in place by governments. As an example, Fruits and Vegetables Import Requirements (FAVIR) of the US government require preclearance of horticultural consignments in the exporting countries as well as inspections at the ports of arrival for any live larva or pupa of quarantine pests. In general, a biometrically designed statistical sampling is applied to conduct phytosanitary physical inspections against any quarantine-significant insect in fruit and vegetable commodities. In 2017, around 194 million pounds of fresh fruits and vegetables were inspected and cleared for shipment to the United States (USDA Annual Report, 2017). Based on the United States Department of Agriculture (USDA) report about the US plant inspection stations in 2017, the inspection of plant materials is mostly conducted physically, along with some modern technologies such as digital imaging, X-ray and molecular detection tools for low-volume plants, plant cuttings, and seeds. As a result, automatic, fast, and reliable noninvasive methods of detection are needed to monitor quarantine pest existence and the internal quality of the fruits and vegetables in high-volume shipments (USDA Annual Report, 2016).

The rapid advancement in electronic technology and data analytics with greater computing power, along with their increased application in the agricultural field, have introduced new methods for non-destructive quality assessment of fruits and vegetables. A range of techniques have been reported for non-destructive detection of insect infestation such as near-infrared (NIR) spectroscopy (Moscetti et al., 2015; Peshlov et al., 2009; Saranwong et al., 2011; Wang et al., 2010), acoustic methods—sound/noise/vibration (Li et al., 2018; Liljedahl & Abbott, 1994; Mankin et al., 2011), imaging—visible light sensing (Blasco et al, 2017), imaging—hyperspectral (Cen et al., 2013; Lu et al., 2017), nuclear magnetic resonance (Zhang & McCarthy, 2013), X-ray (Chuang et al., 2011; Haff & Toyofuku, 2008), volatile emission, and others (Burns & Ciurczak, 2007; Nicolaï et al., 2014; Rajendran, 2005; Sun, 2010). In this chapter, the life cycle of the CM will be discussed and then all known techniques used for postharvest nondestructive detection of internal insect infestation in fruits and vegetables will be summarized. The merits as well as the limitations of each method will be profiled, several examples of applications are presented, and challenges and opportunities for the future of non-destructive detection of internal insect infestations are discussed.

2.2 Characteristics and Life Cycle of Codling Moth

CM is mostly found on pome fruits such as apples, pears, and stone fruits (peaches and nectarines). The life cycle of CM strongly depends on climatic and environmental factors. Female moths usually lay eggs on the fruit. The CM egg is oval, flat, about 2 mm long, and almost transparent. The eggs hatch in 8 to 14 days and turn into neonate larvae which are about 2 to 3 mm long with a black head and creamy white body. The newly hatched larva enters a fruit and feeds on the flesh as it grows to mature larva. The larva is pinkish to white in color with a brown head and can reach 3/4 inch (Figure 2.1). The CM has five larval instars regardless of temperature conditions, where the optimal temperature and humidity for larval development are 27 – 32 ºC and 75%, respectively. At a temperature below zero degrees, the larvae become totally inactive; however, if the temperature is increased to the optimal levels, the larvae become active again. After completing the fourth larval instar, the mature fifth instar larvae exit the fruit and develop to a pupae outside the fruit under the tree bark, crevices, or sheltered areas in the tree in suitable climatic conditions.

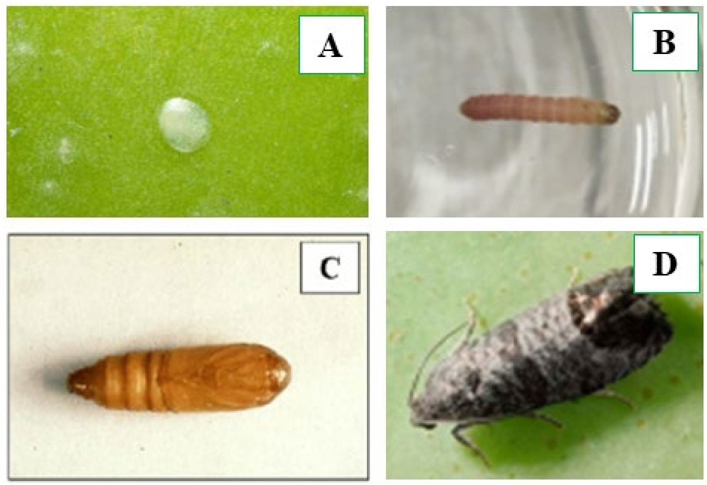

Figure 2.1 Codling moth egg (A), larva (B), pupa (C), and adult (D)

The pupae are 10–12 mm long and can be as wide as 3 mm, and of a light brown color. Then the pupae transform into a moth. After emergence male and female moths mate and eggs are laid on the fruit again and the cycle continues. The adult is about 3/8 inch, gray, with distinctive bronze areas on the bottom 1/3 of the wing.

Based on the life cycle of CM, the larval phase is the most devastating stage for pomes fruits. This is when the pest causes internal damage, sometimes with no visible external damage because the point of entrance is obscure – usually through the calyx. This makes it extremely difficult to detect and classify CM infection in postharvest processing plants (Figure 2.2). In most cases, CM larva enters through the calyx opening without making any extra holes in the flesh of the fruit (Greenwood, 2000). However, in some cases, there are some tiny holes on apple skin or some residuals/frass on its surface, which are hard to detect through batch manual inspections. Thus, there is a great possibility of infested fruits entering shipment or storage facilities. Moreover, early detections of eggs laid on the surface of the apple fruits are very important to stop the persistence of the infestation in the post-harvest supply chain. The latter shows the necessity for the development of a fast, reliable, and nondestructive method to detect cryptic infestations of CM in apples at different stages of larval development.

Figure 2.2 External and internal view of a typical CM-infested apple

2.3 Nondestructive Methods for Insect Pest Detection

2.3.1 Spectroscopic Techniques

Spectroscopy methods provide operational information about the chemical and physical characteristics of fruits and vegetables by obtaining reflectance, transmittance, absorbance, or scattering of polychromatic or monochromatic radiation from the surface of the sample in the ultraviolet (UV), visible (Vis), and NIR regions of the electromagnetic spectrum. But the application of NIR region (780 to 2500 nm) is particularly compelling because it is sensitive to overtones and combinations of chemical bonds such as C–H, O–H, and N–H, which are abundantly present in foods. Moreover, NIR spectroscopy has the capacity of measuring multiple quality attributes of foods simultaneously (Sun, 2010).

Some researchers have proven the high potential of NIR spectroscopy for the detection of insects or insect damage in food commodities, such as blueberries (Peshlov et al., 2009), cherries (Xing et al., 2008), figs (Burks et al., 2000), green soybeans (Sirisomboon et al., 2009), jujubes (Wang et al., 2010), chestnuts (Moscetti et al., 2014), and other foods (Burns & Ciurczak, 2007; Nicolaï et al., 2014; Rajendran, 2005; Singh et al., 2010).

While the technical configurations such as sensor type and resolution of the equipment used for spectroscopy affect the measurement, the two most significant factors affecting the detection of insect infestation are wavelength range and optical measurement mode (interactance, reflectance, and transmittance) (Jamshidi, 2020). According to a recent meta-analysis conducted by Jamshidi (2020) summarizing different studies for non-destructive detection of internal insect infestation in fruits using the spectroscopy technique, the spectral range of visible/shortwave near-infrared (350–1100 nm) showed lower classification accuracy compared to NIR or Vis/NIR (total error of 21.71% in comparison to errors of 13.30%, or 13.65%, respectively). Furthermore, the results showed that applying the interactive mode for spectroscopy achieved lower errors in classifying infested fruits from healthy ones (error of 6.66% compared to errors of 15.73% and 16.04% for reflectance and transmittance modes, respectively) (Jamshidi, 2020).

In fact, the detection of insect infestation by NIR spectroscopy can be achieved through either direct detection of insects and larvae due to their hemolymph, lipids, and chitin content (Moscetti et al., 2014), or indirect identification of the changes in the spectral properties of infested tissues resulting from internal browning or darkening, dehydration, or microbial contamination. Since NIR spectra (especially at the short wavelength and high-frequency region of 850 to 1888 nm) are capable of penetrating the fruit peel and tissue, useful information can be acquired by measuring the interaction (energy attenuation) between the IR energy and the food samples. On the other hand, the high moisture content of fruits and vegetables makes it difficult for the light in the long wavelength near infrared range of 1100–2500 nm to penetrate through the whole fruit, especially in very large samples. Consequently, the short wavelength NIR spectroscopy is normally used in the internal quality assessment of fruits to detect the presence of insects via changes of chemical and optical properties of whole fruit caused by insect infestation.

2.3.2 Visible Light Sensing

In the last four decades, machine vision systems have been extensively investigated to replace the human role in several agricultural applications, including sorting, detecting defects and diseases, and characterizing other quality attributes of agricultural products (Chen & Sun, 1991; Patel et al., 2012). Visible light sensors at a wavelength from 380 to 750 nm falls in the range that is generally used for detecting external or surface features (Liu et al., 2017). A summary of works on computer vision used for detecting insect infestation in fruits and vegetables are shown in Table 2.1.

Table 2.1 Studies on detection of insect infestations in fruits and vegetables using visible color cameras

Sensor Type	Crop	Insect Type	Machine Learning Technique	Classification Results	Reference
RGB camera	Citrus	Scale insect (*Coccoidea*)	MIA	92.8%	(López-García et al., 2010)
RGB camera	Citrus	Thrips (Thysanoptera), Scales, and Medfly (*Ceratitis capitata*) egg	BDA	73–86%	(Blasco et al., 2009)
RGB camera	Citrus	Medfly	BDA	NA	(Blasco et al., 2016)
RGB camera	Citrus	Thrips, Scales, and Medfly egg	ROSA	93.4–100%	(Blasco et al., 2007)

RGB camera	Citrus	Thrips, Scales, and Medfly egg	LDA	43.2–78.1%	(Blasco et al., 2007)
Line scan cameras	Pistachio	Insect damage	DF	74–91.8%	(Pearson et al., 2001)

MIA: multivariate image analysis; BDA: Bayesian discriminant analysis; LDA: Linear discriminant analysis; ROSA: region-oriented segmentation algorithm; DF: discriminant function; RGB – Red, Green, and Blue color spaces; NA – not applicable.

Although the studies listed on Table 2.1 mainly focused on citrus fruits and two types of insect infestation, it is also clear that the idea of using color images to detect surface defects is effective as long as the infested tissue has different color or texture properties. Nonetheless, the use of visible color vision is not beneficial for the detection of internal defects as such problems cannot be recognized (Cubero et al., 2011; Ruiz-Altisent et al., 2010). Moreover, some symptoms of surface infestation cannot be accurately detected with a color vision camera because of interference from the sample's surface color. This requires using a more accurate and wavelength-based technique, such as hyperspectral or multispectral imaging systems (Cubero et al., 2011; Ruiz-Altisent et al., 2010).

2.3.3 Hyperspectral Imaging

The HSI technique is a relatively recent approach that is gaining extensive use in agricultural production systems and food processing for noninvasive detection of properties and classification into quality categories. In the past decade and a half, it is among the most widely studied techniques for noninvasive monitoring of quality and ensuring the safety of fruits, vegetables, and food products (Del Fiore et al., 2010; Ekramirad et al., 2016; D. Lorente et al., 2011; Y. Lu et al., 2017; Pu et al., 2015; Rady & Adedeji, 2018; Rady et al., 2017). The result of a sample scanning using the HSI system is a data cube (hypercube), where two (x and y) dimensions represent the spatial coordinates and the third dimension (λ) represents the wavelength coordinate (Lu et al., 2017). The spectral responses can be related to the physical and chemical constituents of different agricultural products.

The main components of an HSI system are a light source in the visible and NIR ranges, a wavelength dispersive device, which is also called a spectrograph, and a camera that is either a charge-coupled device (CCD) or a complementary metal-oxide semiconductor (CMOS). Data acquisition occurs in different scanning modes. Figure 2.3 shows a complete set-up example of the push-broom HSI system (Rady et al., 2017). The most common mode of acquiring data via an HSI system is the line scanning or push-broom mode (Figure 2.4b) (Lu et al., 2017). The other three modes of HSI scanning, point scanning, area scanning, and single shot, are shown in Figure 2.4a, c, d.

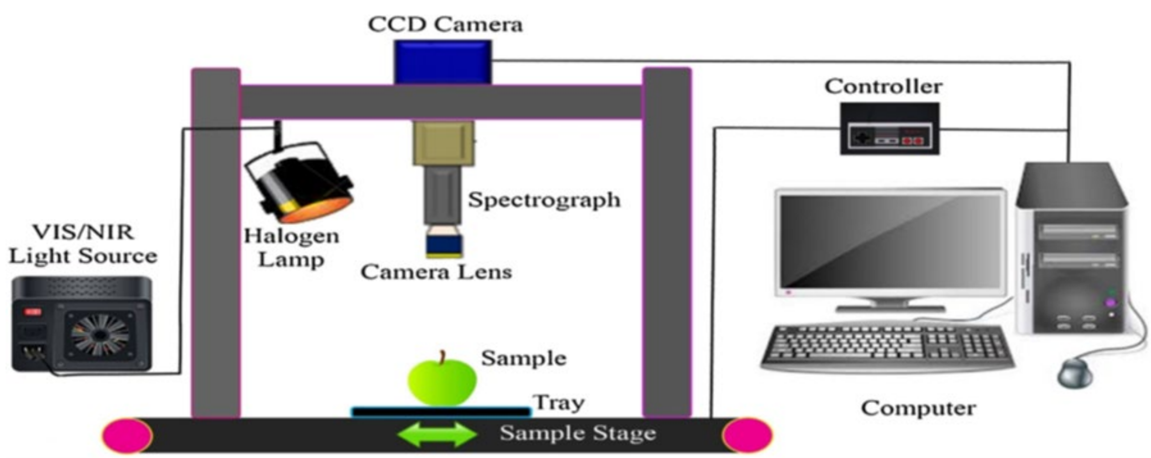

Figure 2.3 The components of a push-broom hyperspectral imaging system (Rady et al., 2017)

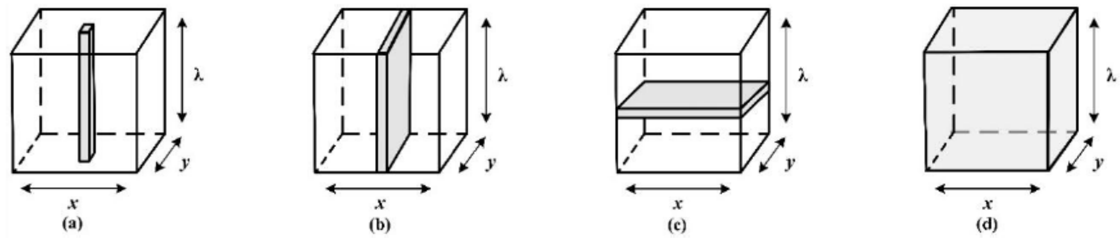

Figure 2.4 The basic hyperspectral imaging scanning modes: (a) point scanning, (b) line scanning, (c) area scanning, (d) single shot. x and y represent the spatial coordinates, λ represents the wavelength (Lu et al., 2017)

In order to normalize reflectance spectra to obtain relative reflectance (equation 2.1), a standard white reference is used to represent maximum reflectance, and by blocking the light source or scanning a complete dark surface, the minimum reflectance is obtained:

$$R_\lambda = \frac{M_\lambda - C_\lambda^0}{C_\lambda^1 - C_\lambda^0} \tag{2.1}$$

where R_λ is the normalized/relative reflectance (%), C^0 is the background (dark) intensity (counts), C^1 is the reference (white) measurement intensity (counts), M is the sample's measured reflectance intensity and λ is a specific wavelength (nm). By normalizing the imaging spectral data, all sample spectral measurements are placed somewhere between the minimum and maximum intensity (Del Fiore et al., 2010; Hamidisepehr et al., 2017). This normalizes the error that may ensue as a result of the change in intensity of the illumination source during scanning.

In order to reduce the dimensionality of hypercube data for a quicker analysis and feedback process, and also to increase the potential application in online/inline settings, certain mathematical approaches, like partial least square (PLS) (Xing et al., 2008), stepwise discrimination analysis (SDA) (Wang et al., 2011), genetic algorithm (GA) (Xing et al., 2008), Bayesian discriminant analysis (Saranwong et al., 2011), sequential forward selection (SFS) and sequential backward selection (SBS) (Rady et al., 2017), and soft independent modeling of class analogy (SIMCA) (Mireei et al., 2017), are applied for feature selection. Determining those wavelength regions allows for building a much simpler model, called a multispectral model. Multispectral imaging systems use the same principle of operation as the HSI systems, with the difference being fewer wavelengths, which accelerates data analysis and decision processes.

The application of HSI systems for detecting fruits and vegetables infested with insects has shown some promising results, even though there are more variations of targeted insects. Table 2.2 shows some of the recent studies where the HSI system was used for detecting insect infestation in fruits and vegetables. Several studies have researched insect infestation of citrus fruits using visible/near-infrared (Vis/NIR) HSI systems. A study conducted by Li et al. (2011) applied an HSI system (400–1000 nm) to detect insect damage in citrus fruits. Principal components analysis (PCA) was used for dimension reduction and the band ratio algorithm was then used for classification. The classification rate was 100% for scale-infested samples.

In other studies, the detection of insect infestations in mango fruits was investigated. Saranwong et al. (2011) studied the application of HSI (400–1000 nm) to assess fruit fly larvae infestation in mango. Reflectance spectra obtained were fed into a discriminant analysis classifier and the classification rate for infested and healthy fruits was up to 99.1% and 94.3%, respectively. It was found that the longer the post-infestation time, the easier the detection and the higher the classification rate, which was attributed to the more visibility and intensity of symptoms of infestation with time. Haff et al. (2013)

also studied the same insect in mango using the same system. These researchers developed an algorithm to identify and mark the infested areas using four steps: background removal, Gaussian blur, thresholding, and particle counting. Discriminant analysis was applied, and the classification rates reached 99% for infested samples.

Table 2.2 Studies on insect infestations detection in fruits and vegetables using HSI

Sensor Type: Wavelength, nm	**Crop**	**Imaging Mode**	**Insect**	**Machine Learning Technique**	**Classification Results**	**Reference**
HSI: 400–900	Apple	Reflectance	Codling moth	DT	Healthy: 81% Infested: 86%	(Rady et al., 2017)
HSI: 400–1000	Citrus: Orange	Reflectance	N/A	PCA and BR	100%	(Li et al., 2011)
HSI: 450–930	Citrus: Red Ruby Grapefruit	Reflectance	Leafminers	SID	95.2%	(Qin et al., 2009)
HSI: 400–720	Jujube	Reflectance	External insect	SDA	Healthy: 98% Infested: 94%	(Wang et al., 2011)
HSI: 900–1700	Jujube	Reflectance	Carposina niponensis walsingham	BR	Healthy: 100 % Infested: 93.1%	(Liu et al., 2015)
HSI: 400–1000	Mango	Reflectance	Fruit fly	DA	Up to 99 %	(Haff et al., 2013)
HSI: 400–1000	Mango	Absorbance	Fruit fly	DA	Up to 99.1 %	(Saranwong et al., 2011)
HSI: 1000–1600	Mung bean	Reflectance	*Callosobru-chus maculatus*	LDA and QDA	Healthy: 93.7% Infested: 75.5–95.7%	(Kaliramesh et al., 2013)
HSI: 740–1000	Pickling cucumbers	Transmittance and Reflectance	Fruit fly	PLS-DA	88–93 %	(Cen et al., 2013)
HSI: 580–980 and 590–1550	Tart cherry	Transmittance and Reflectance	Plum curculio	GA and PLS-DA	Healthy: 81.3% Infested: 95.8%	(Xing et al., 2008)
HSI: 460–800	Tomatoes	Reflectance	Tomato hornworms frass	Detecting algorithm	Healthy: 86–95% Infested: 71–99%	(Yang et al., 2014)
HSI: 400–1100	Tomatoes	Transmittance	*Tuta absoluta* (Meyrick)	ANN	95% Classification accuracy	(Mireei et al., 2017)
HSI: 400–1000	Vegetable soybean	Transmittance	Etiella zinckenella Treitschke (moth)	SVDD	Healthy: 97.3 % Infested: 87.5%	(Huang et al., 2013)
HSI: 400–1000	Vegetable soybean	Transmittance	Pod borer *(Maruca vitrata*)	SVM	Healthy: 100 % Infested: 91.7%	(Ma et al., 2014)

ANN: Artificial Neural Network; BR: Band Ratio; DT: Decision Tree; DA: Discriminant Analysis; LDA: Linear Discriminant Analysis; QDA: Quadratic Discriminant Analysis; PCA: Principal Component Analysis; PLS-DA: Partial Least Square Discriminant Analysis; SID: Spectral Information Divergence; SVDD: Support Vector Data Description; SVM: Support Vector Machine; N/A: Not Available.

The identification of external insect infestation of jujube fruits was investigated by Wang et al. (2011) using the visible range of HSI (400–720 nm). The relative reflectance spectra were extracted for each image and a stepwise discriminant classifier was applied. The classification rates for infested and healthy fruits were 98% and 94%, respectively. On the other hand, Liu et al. (2015) utilized the NIR region of HSI (900–1700) to detect a fruit moth (*Carposina niponensis* Walsingham) infestation in Jujube fruits. Relative reflectance was also determined for each image and the band ratio (BR) algorithm was applied for classification. The rates of classification for healthy and infested fruits were up to 100% and 93.1%, respectively. The most influential wavelengths were found to be 987, 1028, 1160, 1285, and 1464 nm. Huang et al. (2013) used the Vis/NIR HSI (400–1000 nm) in the transmittance mode to detect insect infestation on vegetable soybean (green soybean seed). They applied the support vector data descriptor (SVDD) on the relative transmittance spectra and determined classification rates for healthy and infested samples to be 97.3% and 87.5%, respectively. The work on vegetable soybean was expanded by Ma et al. (2014) to include automatic selection of the region of interest (ROI) based on threshold segmentation. They performed wavelengths selection using a fuzzy-rough set model. The SVDD classifier was applied, and the classification rates boosted to 100% and 91.7% for healthy and infested samples, respectively. The optimal wavelengths were found to be 705 and 943 nm using entropy characteristics, and 692, 743, and 975 nm for both energy and mean characteristics. Rady et al. (2017) applied push-broom reflectance Vis/NIR HSI (400–1000 nm) to detect codling moth larvae in GoldRush apples. They applied several classifiers on the relative reflectance including LDA, partial least square discriminant analysis (PLS-DA), feed forward artificial neural networks (FFNN), decision tree (DT), and K-nearest neighbors (KNN). The highest classification rates were 81% and 86% for healthy and infested fruits, respectively using the DT classifier. Wavelength selection was performed using the sequential forward selection technique that led to the following wavelengths, 434.0, 437.5, 538.3, 582.8, and 914.5 nm to be selected for codling moth infestation detection and classification in GoldRush apples.

The studies profiled provide various levels of accuracy, demonstrating the potential application of HSI as a diagnostic, detection, and classification tool for various types of insects in fruits and vegetables in real-time systems. Because insect infestation happens deep inside the fruit or vegetable, it is challenging to recognize the issue using RGB-based machine vision. The HSI technique is more appropriate. The exploration of this technique is becoming more popular because of continuous price reduction in hardware to build a system, the increasing computing power of systems to handle big datasets, and the nondestructive usefulness in agricultural applications. HSI systems measure the light intensity at several wavelengths from visible to near infrared. Among these many wavelengths, a few of them that are useful are selected for building a model that can predict infestation. These wavelengths are usually figured out using machine learning statistical approaches such as PLS, SDA, GA, and so on. In spite of this promise, HSI technology is still not very rampant in commercial applications with regards to insect infestation detection. One of the limitations of HSI is the accuracy of detection or classification. There are some applications where 100% accuracy is a must—for example, in fruits for the international market where failure can have a far-reaching effect. This challenge is being addressed with some new and more effective analytical approaches, like deep learning, bagging, and boosting, and the potential to further increase the accuracy of HSI measurement is waiting to be further explored (Kubat, 2015; Li et al., 2015; Li et al., 2016; Porkhak et al., 2017). Also, while the major steps (data acquisition, preprocessing, calibration, validation, dimensionality reduction, re-calibration, and re-validation) in developing an HSI solution are well defined, there is no simple way to determine the most effective mathematical-analytical approach needed for some of these. It is mostly trial and error to determine the most effective algorithm or model. There is a need to address this challenge going forward. The appropriate algorithm is determined case-by-case, even though several approaches, such as principal component analysis, used for size reduction, and LDA and artificial neural networks, are often implemented in classification tasks.

2.3.4 X-ray Imaging

The principle of an X-ray imaging system is based on the transmission imaging technique in which an X-ray beam emitted from a source penetrates an object and attenuates based on the density variance of the object. The attenuated energy that passed through the object is detected using a photodetector, a film, or an ionization chamber on the other side. The attenuation coefficients of the object components lead to different contrast between such components (Adedeji, 2011; Adedeji & Ngadi, 2009; Ammari, 2008). Computed Tomography (CT) X-ray imaging is a more recent and advanced technique than plain X-ray technology. The latter technique solves the problem of having overlapping layers of soft tissues or complex bone structures (Ammari, 2008). The source and detector rotate around the object to generate an enormous number of 2-dimensional slices or images, which are used to create a 3-dimensional image called a tomogram (Ammari, 2008; Nicolaï et al., 2014).

X-ray imaging falls within the electromagnetic spectrum with a wavelength range of 0.01 to 10 nm, which corresponds to the frequencies range of 30 to 30,000 Petahertz (Kotwaliwale et al., 2014). It has energy from 0.12 to 12 keV with low penetration power, called soft X-ray, which has been explored as a non-destructive process for internal quality inspection of various agricultural products. Although the onset of the application of X-ray imaging was solely targeted to medical purposes—diagnostic and security inspection areas using the system to detect defects and quality properties in agricultural commodities research commenced around the 1950s (Nylund & Lutz, 1950). Because of the inherent limitations of X-ray (discussed in Section 6), its studies in agricultural products mainly focused on X-ray irradiation quarantine treatments (Follett & Armstrong, 2004) and on dry or lower water-containing materials, e.g., checking seed quality with soft X-ray radiography (Lammertyn et al., 2003) and for detecting hidden infestation of crop plants. Because the grayscale of X-ray images is a function of the density and thickness of the test samples, the relative contrast of infestation spot to the intact region inside a typical fruit will vary. The gray intensity of X-ray images depends on the density and thickness of the test samples, so the relative contrast of the infestation site to the intact region inside a typical fruit varies with its position. In order to accurately determine whether a fruit has signs of insect infestation using an X-ray imaging analysis, an effective adaptive image segmentation algorithm based on the local pixels' intensities and an unsupervised thresholding algorithm is developed.

Soft X-ray emission spectroscopy was also applied by Veena et al. (2015) to detect fruit fly in Mango fruits. Color features were extracted from each image and differentiation between sound and infested fruits was feasible. However, no numerical values of the classification results were provided. Stone fruits—apples and cherries—were scanned for the response of codling moth and western cherry fruit fly respectively, using X-ray imaging by Schatzki et al. (1997). The tests performed included physical inspection of X-ray images by two operators on computers, and the results of both operators were averaged. Real-time sorting was stimulated by scrolling frames containing healthy and defected fruits on the computer screen at different rates, with the operators having the ability to identify the defected fruit on the screen. Classification rates for inspection tests were 0–96%, with the lower rates at the beginning of the infestation. However, such rates were much lower (8–58%) for scrolled frames. Haff and Pearson (2007) utilized X-ray imaging to evaluate olive fruits for fruit fly. An algorithm for feature extraction was developed based on selecting 64 arbitrary features from each image. Iterative discriminant analysis was then used to select the optimal subset of only three features. Results showed that the best classification rates were 50–88%, with the lowest rates associated with fewer infestations. Haff et al. (2015) developed a Bayesian classification algorithm to detect fruit fly on X-ray images of olive fruits. The same 64 features were used for Fruit fly detection in olives and discriminant analysis was applied to select the optimal set of three features. A 90% classification rate was obtained for healthy samples and 50–86% for infested samples. The feasibility of applying X-ray imaging for monitoring saw-toothed beetle in stored dates was studied by Al-Mezeini et al. (2015). The extracted features were 44 in total, based on the histogram and textural characteristics of the images. Linear discriminant analysis (LDA) was then performed along with bootstrapping for classification, and the best rates were 99% and 100% for healthy and infested samples, respectively. However, the infested tissue was not visually clearly differentiable from the healthy tissue, which tends to oppose the application of X-ray imaging in this case compared with other noninvasive systems such as HSI or spectroscopy that base their detection on differences in spectra formed by infested part and a healthy portion. Another major downside of X-ray imaging is the large image dataset that impedes quick feedback time needed for the large quantity of produce often involved. This poses a challenge in online assessment and classification of insect-infested fruits and vegetables. Increasing computing power could significantly reduce the feedback time, then it adds significant cost to the technology. This is the improvement this technique needs.

2.3.5 Magnetic Resonance Imaging (MRI)

MRI is a non-ionizing imaging technique in contrast to X-ray or computed tomography (CT) imaging and was first used for medical applications. The principle of MRI is such that a high-resolution image can be obtained by a strong and uniform magnetic field applied to hydrogen nuclei that are mainly located in water (Ammari, 2008). The image is formed as a result of the different levels of contrast of the object tissues as a response to a vigorous magnetic field and radio frequency waves. Applications of MRI in food quality monitoring is still considerably limited mainly due to the high cost of MRI systems. Torres (2008) studied the application of a low-field MRI system to detect fruit fly in peaches, with classification rates of 58% and 71% for healthy and infested fruits, respectively. Haishi et al. (2011) applied a low-field MRI using a 0.2 Teslaa or T magnet field to track the presence of peach fruit moth on apple fruits by analyzing multi-slice two-dimensional (2D) images. It was shown that the detection of larvae inside the fruit is feasible using a single slice gradient echo method in 6.4 s. Whereas, the multi-slice 2D measurement provided 6 images in 2 min, and these images covered a larger image area in a short time. Although MRI technology has a promising possibility for an effective nondestructive determination of fruits and vegetable defects, several problems still arise, especially when compared to other nondestructive systems such as color vision, hyperspectral and multispectral imaging, and spectroscopic systems. Such problems include the high cost for building, running, and maintenance, and the large volume and heavy weight of the MRI systems (Haishi et al., 2011; Torres, 2006).

2.3.6 Thermal Imaging

Thermal imaging (TI) is a sensing technique that was first illustrated for military applications. Later, TI was extended to agriculture and food process monitoring (Ammari, 2008). A typical TI system consists of a thermal camera that has an infrared detector, a signal processing unit, and an image acquisition unit (O'Donnell et al., 2014). The main idea of forming a TI image is based on the difference in surface temperatures radiated by an object that is linked to the thermal energy values. Such values are translated to electrical pulses which are processed in the signal processing unit to form an image. The same image segmentation approach applied in X-ray imaging to localize the infested ROI is applied to thermal imaging.

Hansen et al. (2008) used an infrared camera that was sensitive to 7.5–15 μm wavelengths to track codling moth in apple fruits. Data analysis was conducted via paired t-test and the results showed a significant difference (at $\alpha = 0.01$) between healthy and infested fruits. In their thermal images, the infested area appeared to be slightly colder than the un-infested tissue. Detecting the infested area was not affected by the storage temperature nor the infestation location. Chen et al. (2018) used an android powered TI system based on an Otsu image processing algorithm to detect maize tumor powdery mildew. Their goal was to use the segmentation result as a reference guide in unmanned aerial vehicles for precision spraying of pesticides. Chen et al. (2018) applied a thermal imaging system to delineate *Callosobruchus maculatus* (F.) (Cowpea seed beetle) infestation in mung bean and reported an accuracy of up to 80% detection using a machine learning approach.

Although TI is a promising non-destructive technique that can be effectively applied for insect detection in fruits and vegetables, either in the field or post- harvest, the sensitivity of a TI system is affected by the weather condition and the relatively high cost required to obtain a high-resolution thermal imaging camera. Combining the TI system with another nondestructive system such as color vision might enhance the sensitivity to weather conditions (Ishimwe et al., 2014).

2.3.7 Acoustic Techniques

Acoustics is the study of sound, which is generated by propagating mechanical waves of energy through an elastic medium by causing particle displacement and vibration. One of the most popular acoustic techniques used in agricultural product processing is ultrasound (Zdunek & Bednarczyk, 2006). Insect pests usually bore deep into vegetable/fruit where other techniques may not be able to detect the infestation. Acoustic detection of insect activities is based on distinct sounds made by the larvae displacement when they are feeding or biochemical reactions in the pest-infested food that creates low-intensity ultrasonic sounds (Li et al., 2018; Soroker et al., 2004). For example, crawling and feeding of two insects *Callosobruchus chinensis* and *Callosobruchus maculatus* in chickpea (*Cicer arietinum*) and mung bean or green gram (*Vigna radiata*) were monitored using a condenser-type microphone probe, with a frequency range of 20–16 KHz, placed inside an acoustic-proof bin (Banga et al., 2019). Their results provided sound signatures for *Callosobruchus chinensis* and *Callosobruchus maculatus* insects as having a sound duration of 59 and 68 ms, and amplitude of 79.32 and 97.65 dB in chickpea and 84.01 and 95.53 dB in green gram, respectively. Moreover, they selected formants, formant bandwidth, frequency, and spectral power as principal features in their analysis for the infestation detection. They concluded that their method can be used for non-destructive early detection of insect infestation in bulk stored foods.

Acoustic emission (AE) is one of the recently evolved areas of acoustics that can detect and monitor hidden insects and their activities in plants (Cox, 2014). AE is the phenomenon where acoustic (elastic) waves are generated and radiated in solids when a material undergoes irreversible changes in its internal structure (Muravin, 2009). Differing from the conventional signaling techniques, AE can detect the physical signals produced from food crops to foodborne bacteria. Yang et al. (2014) established the relationship between AE and crop disease stress, which allowed the detection of diseased crops from healthy ones. A highly sensitive AE device is capable of detecting the signal emitted by *Escherichia coli* and *Lactococcus lactis*, ssp. during their growth phases (Cox, 2014; Meng, 2016). Ghosh et al. (2013) used an AE system to acquire real-time data on *L. lactis*, ssp. metabolic activity and to dynamically monitor phase infection of cells. Application of AE for vegetable and fruit quality and safety assessment, specifically for insect activity detection, has been limited. Some previous studies showed that acoustic devices could be optimized to predict watermelon firmness (Mao et al., 2016), and to classify extruded bread with different water activity (Swietlicka et al., 2015), and a contact AE detector was applied to evaluate apple texture with mechanical destruction of apples (Zdunek et al., 2011). However, most of the studies that applied an AE technique are associated with food quality attributes by mechanically destroying the food. In a recent study, Li et al. (2018) reported that AE detected codling moth activities in infested apples and they obtained a very high classification rate (83%) utilizing 0.5 s of acoustic signal collection.

The use of acoustic technology to replace labor-intensive and less-effective detection and monitoring methods on insect activity started to expand in the last three decades (Mankin et al., 2011). Acoustic technology has successfully detected the presence or absence of target insects (Mankin & Moore, 2010), estimated the population density (Hagstrum et al., 1996), and mapped insect populations (Mankin et al., 2007). The original AE system for detecting fruit fly (*Drosophila*) larvae activity was depicted by Webb et al. (1988). Nowadays, an AE system is usually composed of acoustic sensors, preamplifier, an input-output (I/O) board, and signal preprocessing software (Li et al., 2018). The acoustic sensor (diaphragm) serves as the device for collecting sound signals, and it is placed in direct close contact with the surface of the sample, thus the acoustic signal is propagated from the sample to the sensor (Zdunek & Konstankiewicz, 2004). The sensor sensitivity can vary from 40 Hz to 100 kHz (Mankin et al., 2009; Webb & Slaughter, 1988). A reference sensor can be used to identify background or electrical noise since the sound generated by an insect is of higher energy (Mankin et al., 2011).

A signal triggered by the sensor is amplified through the preamplifier and digitized by the I/O board that serves as an oscilloscope. Signal amplification can range from 40 to 100 dB to minimize noise depending on the signal strength from larvae. Amplifiers can also eliminate extremely low- and high-frequency noises with appropriate filters (Webb & Slaughter, 1988). Much of the background noise can be discarded by high-pass filters to remove long-duration and low-frequency background noises (Mankin et al., 2009). Filters can also help differentiate insect larvae at different development stages. Jalinas et al. (2017b) found that younger larvae have a shorter duration cycle than older (>30 days) larvae. Movements of insects are expected to generate impulses with a broader, higher-frequency spectrum than low-energy movements (Mankin et al., 2010). Signals acquired after amplification have a good signal-to-noise ratio (Mankin et al., 2011). The digital signal is then processed by commercial signal processing software to extract AE features. Common AE features derived from the original signal in previous literature include events and mean amplitude (Zdunek et al., 2010), duration, peak amplitude, rise time, ring down count, and event gap (Omkar & Karanth, 2008), energy rate (Ghosh et al., 2013), and larvae burst rate (Jalinas et al., 2017b). These are time-domain (also called temporal) AE features. Through Fast Fourier Transform (FFT), frequency domain (also called spectral) features such as frequency range (Marzec et al., 2007), frequency centroid, and peak frequency can be obtained (Li et al., 2018).

For data analysis, most researchers applied simple statistical models (analysis of variance (ANOVA), multiple mean comparison) based on acquired AE features (D. Ghosh et al., 2013; Mao et al., 2016). Powerful data analysis methods have been shown to enhance the detection performance of insects. Some advanced statistical and mathematical methods have been used and achieved success in recent years. Pinhas et al. (2008) used Gaussian mixture modeling to obtain a detection ratio as high as 98.9%. Trifa et al. (2008) used hidden Markov models to realize a species recognition rate of 99.5%. Li et al. (2018) applied adaptive boosting to achieve a classification rate of 100%. Novel models for data analysis from insect AE data can be adapted from novel human speech recognition models, such as recurrent and convolutional neural networks (Yu & Li, 2017). It is expected that these advanced and novel models can improve insect acoustic recognition performance.

The promise that AE portend for insect infestation detection is strong, with a high detection rate that needs marginal improvement for industrial deployment, and a short signal collection time for a quick system feedback. However, it is not clear the exact source of sound being detected that allows for differentiation between healthy and infested fruits. The literature has conflicting reports on the source of sound (Appel & Cocroft, 2014; Ghosh et al., 2013; Webb & Slaughter, 1988). Future studies should address the speculation that this is due to insect displacement, or due to biochemical reactions where gas implosion is creating the peculiar sounds being detected.

In summary, the nondestructive methods based on acoustics are among the most important quality evaluation approaches being used for fruit and vegetables in postharvest processes. Especially during the last three decades, there have been a plethora of research on the application of acoustic methods in the quality assessment of agro-products (Fathizadeh et al., 2020). This increasing trend in the implementation of the acoustic methods in agriculture continues to grow by further development in new applications for example in monitoring and detecting insect pests in fruits, vegetables, and grains (Mankin et al., 2021). While nondestructive acoustic methods are inexpensive, fast, environmentally friendly, and easily automated (Adedeji et al., 2020), there are some challenges associated with them like the eliminating of background noise, developing fast signal pre-processing and processing systems, and adapting the method for real-time applications. However, with further development of low-cost modern acoustic equipment, and improved machine learning algorithms this technique will continue to extend its application in the agro-industry.

2.3.8 E-Nose and E-Tongue

Early-stage detection of insect infestation on vegetable/fruit production and logistics is highly desirable to reduce economic loss and to ensure food safety. When vegetable and fruit are under insect attack, the physical, chemical, and biological changes are difficult to determine. Electronic nose (E-nose) and tongue (E-tongue) technologies are effective in determining these changes by applying biosensors to qualify and quantify the changes (Baldwin et al., 2011). E-nose works as artificial olfaction devices that mimic the mammalian olfactory system. Both devices are composed of non-selective or semi-selective sensors interacting with aromatic or tasty compounds to produce electronic signals (Baldwin et al., 2011; Smyth & Cozzolino, 2013). E-noses have been successfully used for the detection of insect-infested fruits and vegetables, and insect population dynamics (Cui et al., 2018). Under different growth conditions, tomato plants infested with spider mites (*Tetranychus urticae* Koch) were correctly classified without a prior knowledge based on the volatile organic compound (VOC) profiles emitted by infested tomato plants (Ghaffari et al., 2011). E-nose has demonstrated the ability to precisely predict the gender and species of stink bugs (Lan et al., 2008; Zhou & Wang, 2011).

One of the most applicable E-noses is based on the phytohormones and VOCs emitted by insects or insect-infested vegetables/fruits. Phytohormones and VOCs are defensive chemical messengers and substances respectively, which will change dramatically when fruits/vegetables are under attack (Alagna et al., 2016). Differential sensor arrays can transform the VOC information into electrical signals. Similarly, insect antenna-based E-nose can be a valuable tool for the detection of pest infestation (Wang et al., 2015). One available commercial E-nose (PEN2) comprising 10 metal-oxide semiconductor (MOS) sensors successfully fingerprinted the VOCs present in insect-damaged samples (Zhang & Wang, 2007). The E-nose systems are manufactured by Win Muster Airsense (WMA) Analytics Inc. of Schwerin Germany (Zhang & Wang, 2007). Despite using commercial E-nose instruments, recently there have been some studies trying to self-design E-nose systems to match case-specific parameters of control and to avoid the costs of using general commercial devices. As an example, Wen et al. (2019) developed a sweeping electronic nose system (SENS), composed of 8 metal-oxide-gas (MOS)-type chemical sensors, combined with PCA and LDA data processing methods to detect the early damage of oriental fruit fly (*Bactrocera dorsalis*) in mandarin (*Citrus reticulate Blanco*) citrus fruit. Their results showed that the SENS could classify the *B. dorsalis*-infested citrus fruits with a recognition accuracy of 98.2%. They concluded that more study is needed to analyze the effects of other pest invasion on VOCs emitted from citrus fruits, and to collect enriched data covering different levels of citrus fruit infested by *B. dorsalis*, different varieties, and ripe stages of citrus fruit.

The studies used E-nose and E-tongue with promising results. The development of intelligent E-nose systems for the specific purpose of detection of insect in fruits and vegetables is the research direction of the future. Specific applications include the discrimination of insect species and gender, insect development stage, insect population dynamics, and damage status of fruits and vegetables. Biosensors are the key to the success of E-nose and E-tongue. Insect odorant receptor based on the sensor is sensitive at ppb levels (Mitsuno et al., 2015). However, fruit and vegetable processing involves high humidity, which shortens the sensor lifetime and deteriorates sensor performance (Cui et al., 2018). Performance of the sensor is important for practical industrial applications, though there is a simple problem: it requires an enduring solution beyond using hydrophobic materials as substrates for the sensor manufacture, which in turn shortens its shelf-life.

2.4 Critical Comparison of Different Nondestructive Methods

Table 2.3 provides an overall comparison of non-invasive methods used for insect infestation detection in fruits and vegetables by summarizing their advantages and disadvantages.

Table 2.3 Critical comparison between different nondestructive methods

	Advantages	**Disadvantages**
Spectroscopy	No sample preparation needed, determining both chemical and physical characteristics, ease of use and suitable for on-line applications (Pasquini, 2003; Wang et al., 2010).	Large amount of samples/data and different chemometrics methods are needed to build accurate models (El-Mesery, Mao, & Abomohra, 2019). Does not provide spatial data.
Visible light sensing	Simple and cost-effective, accurate and suitable for on-line monitoring (Gomes, Leta, & Technology, 2012; Guishan Liu et al., 2015).	Only suitable for detecting external defects, sensitive to external lighting variations.
HSI	Merges the advantage of a color vision system with that of spectroscopic system (Hussain, Pu, Sun, & technology, 2018). Provides both spectral and spatial features for accurate segmentation and identification of ROI, it can detect internal defects (El-Mesery et al., 2019).	HSI data are voluminous, contain huge redundant data that requires tedious analysis to upgrade to multispectral images by selecting useful wavelengths), its hardware is costly, different chemometrics methods are required to extract useful information (El-Mesery et al., 2019).

X-ray imaging	Can detect internal defects causing density differences, such as cavities.	High costs, poor penetration in materials with high water content, and difficulty in effectively differentiating normal and infested tissues with similar densities (Jiang et al., 2008).
MRI	No harmful ionizing radiation, high-resolution visual information of internal structure, it gives quality 2D and 3D images (Pathmanaban, Gnanavel, & Anandan, 2019).	High costs, large dimensions, and heaviness (Haishi et al., 2011; Torres 2006).
Thermal imaging	Easy handling and portability (Pathmanaban et al., 2019).	Sensitivity to the environmental condition and relatively high costs to obtain high-resolution images (Ishimwe et al., 2014).
Acoustic	Sensitive, efficient, and clear detection capabilities of various insects (Alexander Sutin et al., 2019). Inexpensive, automatic, and continuous monitoring (Mankin et al., 2011).	Prone to background noise (Mankin et al., 2011). Incapable of detecting insect eggs.
E- nose and E-tongue	Low-cost, rapid, and environmentally friendly testing (Jia, Liang, Jiang, & Wang, 2019).	Reported detection levels and accuracies are not very high (Jia et al., 2019).

CHAPTER 3. OBJECTIVE ONE

TO IDENTIFY THE SOURCE OF THE DETECTABLE VIBRO-ACOUSTIC SIGNALS COMING FROM CM-INFESTED APPLES

Abstract:

Codling moth (CM) infestation poses a serious threat to agricultural export and import for the apple industry. The detection of infestation often requires destructive testing. Infestation detection is particularly problematic when the larva enters the apple through the calyx without apparent damage on the skin of the fruit. This study considers the use of low frequency (0.4 to 8 Hz) Lead Zirconate Titanate (PZT) sensors to enhance the detection of infestations nondestructively while monitoring larvae activities. This study presents experimental results of a novel approach that correlates the larvae's activities, such as chewing and body movements, with patterns in the vibro-acoustic signal transduced by contact with the PZT sensors. Experiments were performed to correlate various CM activities to specific signals. In these experiments, CM-infested apples were sliced, and a digital camera was used to capture activities while simultaneously registering the signal patterns observed in the PZT signal. The chewing signals show a chewing rate of 1 to 2.3 times a second with internal movement signals showing large transient spikes at irregular intervals above the noise floor. In addition, results from uncut infested apples are also presented showing the occurrence of similar patterns in infested apples. These results suggest that CM activities (chewing and displacement) are mostly responsible for vibro-acoustic signals detected in infested apples. This finding will enhance the use of

acoustic signals in the nondestructive detection of CM in apples. There is a need to expand this test to other varieties of apples and larvae at different stages.

3.1 Introduction:

Codling moth, *Cydia pomonella* L. (Lepidoptera: Tortricide), is the most detrimental internally feeding pest of apples, and at the same time, it is considered as one of the most resistant pests to commonly used chemical insecticides (Jiang et al., 2018; Joshi et al., 2020; Balaško et al. 2020). Moreover, CM has the potential of reducing apple fruit production from 30% up to 50% at different stages (Balaško et al., 2020). As a result, many sensitive markets, especially in Asia, enforce a zero-tolerance policy for this pest. On the other hand, the infestation detection is particularly problematic when larvae enter the apple through the calyx end with no obvious hole on the skin of the fruit. Therefore, there is a need for the development of robust, accurate, and effective nondestructive techniques for early detection of this quarantine pest infestation before export packing and also in import borders to prevent ecological and economical losses.

Insect activities such as movement, feeding and communication generate two-dimensional bending wave vibrations that can propagate relatively long distances in the plant tissue structure (McNett et al., 2007; Mankin et al., 2018). Hence, many attempts have been made by researchers to detect target insect pests inside host plants using mentioned vibrational behaviors (Pinhas et al., 2008; Sutin et al., 2017; Mankin et al., 2018; Li et al., 2018). However, there exist some main challenges such as discriminating insect-induced signals from background noise, variability in specimen structure as well as insect activities, and the presence of other physical causes that affect vibrational signals. Thus, the detailed knowledge of the spectral and temporal acoustic signature of insect pests in their natural hosts can be beneficial in boosting the reliability of real-time detection of insect infestations in the field and industrial applications.

There are a few studies that directly monitored the behavior of insect pests in their natural hosts while recording acoustic signals. For instance, in order to identify the relationship between the feeding behavior of bamboo powder-post beetle *Dinoderus minutus* (Coleoptera: Bostrichidae) larva and adult inside bamboo culms and its acoustic signals, AE method was applied for continuous and nondestructive monitoring and analysis (Watanbe et al., 2016). They used a microscope camera to directly monitor the activities of the pest, while an AE sensor (150 kHz) was attached to the sample to record signals simultaneously. To differentiate various insect activities in the signals, they set a predefined threshold to obtain the AE event rate as an index. They reported that almost all AE hits recorded were the result of chewing movements of the insect mandibles and other activities of the insect were undetectable. In another study, acoustic methods were used to detect and analyze the red palm weevil larvae activities in palms through investigating spectral and temporal patterns in acoustic signals and relating them to physical, physiological, and behavioral effects (Jalinas et al., 2019). To collect the data, they attached AE sensor to the specimen and recorded the signals while monitoring by a microphone to avoid noise incident and only include the known red palm weevil larvae sound addressed by other authors (Mankin 2012; Dosunmu et al., 2014; Jalinas et al., 2014). Their results highlighted two main acoustic patterns as 0.1 to 0.3 s chains of 1 to 10 ms impulses, and 0.2 to 0.3 s squeal with descending bands of loud harmonics resulting from movement and feeding on dry and wet surfaces, respectively. They concluded that these particular spectral features might be advantageous in on-field efficient detection of the target insect where insect and substrate variability existed.

In an introductory work by our team, Li et al. (2018) reported that the AE method detected CM-infested apples with 100% classification rate in relatively long signaling times (5 to 60 min), and the classification rates of 83% for short signaling times (0.5 seconds). Based on their conclusion, the AE method has the potential to be used as a noninvasive technique for the classification of CM-infested apples. They used a novel technique to classify infested fruits, but their classification rate for fast detection required in real-time applications was relatively low. Also, their work did not provide the source of sound detected or the spectral and spatial signature of the larvae activities, to deal with the detection and identification of target event under noisy and variable non-laboratory experiments.

Since most insect signals occur as broadband waves, the detectability of insect acoustic activities is more influenced by the sensor, the substrate, and the interface between the sensor and the substrate, than by the insect itself (Phung et al., 2017). Thus, in this study, in order to find out the most detectable spectral range of CM larvae activities in apples, two different acoustic sensors with varying frequency ranges (high-frequency range 35 to 60 kHz and low-frequency range 0.4 to 8 Hz) were applied and the most detectable range, which was the low-frequency range, was considered for further analysis.

The goal of this study was to determine the source of acoustic signals from CM-infested apples in order to better classify them in apple processing units. To achieve that goal, the CM larvae interactions with an apple were monitored visually while the vibrations were being recorded with the proposed sensor. There is a dearth of information in the literature investigating the CM larvae activities in fruit tissue via direct visual monitoring combined with the vibro-acoustic method. Thus, the particular objective of this study was to detect and characterize the low-frequency sound patterns of CM acoustic activities in apples and to provide an interpretation of their source through visual observation. Finally, in this work, the low-frequency spectral range was chosen for analyzing CM acoustic signals to match the spectral range of larvae activities.

3.2 Materials and Methods

A total of 60 Gala organic apple cultivar was purchased from a commercial market in Lexington, KY, USA, in January 2020 for the experiments. The CM samples were supplied as late instar eggs and early instar larvae in strips of double-sided corrugated paper inside an isolated container containing a specially designed food diet (based on a mix of pinto beans, yeast, agar and proteins) by our collaborator in the Department of Entomology, University of Kentucky, Princeton KY USA. The CM larvae inside the container were kept in the lab at an ambient temperature around 24 ºC to develop into mature larvae for this study. The experiments were conducted in the Audio Signals Laboratory in the Electrical and Computer Engineering Department, University of Kentucky, Lexington, KY, USA.

To carry out each test, an individual mature larva was removed from the container and placed on the apple samples. Two types of apple samples were used in the experiments. For one type, a wedge was cut out of the whole apple for the larva to be placed in so their interactions with the pulp could be visually monitored. For the second type, apples were left intact and one larva was placed on each apple surface so its crawling and entrance through or near the calyx could be visually monitored (Figure 3.1). A digital camera with an adjustable gooseneck fixture was used to monitor and record the activities. Video recordings were made by the Debut video capturing program (NCH Software Co., USA), which can display the computer time on video images on the screen. To perform the vibro-acoustic experiments, the two contact Piezo sensors were attached to two opposite sides of the apple fruit using acoustic gel, and both the video recording and acoustic scanning were performed simultaneously using the same computer clock for reference. Figure 3.1 shows the entire experimental setup consisting of a vibro-acoustic recording system, video monitoring equipment, and a computer with acoustic and video software on it. The vibro-acoustic recording system consisted of two contact Piezo sensors (Buzzer element Std 2.6 kHz 35mm, CUI Devices, USA) with a frequency range of 0.4 to 8 Hz connected to a custom-made instrumentation amplifier, coupled to a data logger (USB 6001 DAQ, National Instrument Co., USA) for sampling the amplifier output at 120 Hz, and connected to the computer with the software on it to record and display the signals. In order to avoid constructional ambient noises, the experimental vibro-acoustic unit was set above an isolated table with acoustic padding to hold the sample.

Different types of larval motion signatures were collected by taking simultaneous video and acoustic data. Thus, by observing a type of motion on the video, the time-scales were synchronized and the sound at a particular time was correlated with the acoustic signature of that type of larval behavior. Then the special larval acoustic signature was segmented manually with four repetitions for each behavior activity. The acoustic signal processing and analysis were performed using MATLAB programming software (Release 2019b, The MathWorks, Inc., Natick, Massachusetts, United States).

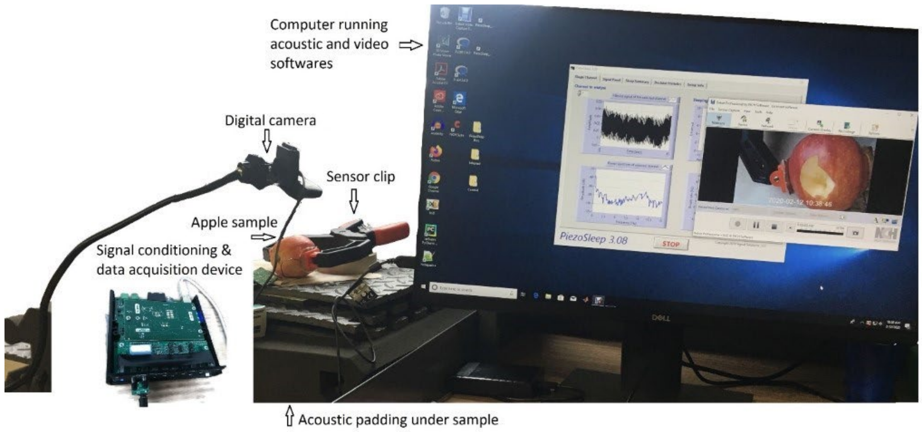

Figure 3.1 The vibro-acoustic and video recording set up

3.3 Results and Discussion

Different larval activities were observed after placing the insect larva in the cut area and on the apple skin. There was no external stimulation process done on the larvae, and typically a few minutes lag time was needed for the larvae to be active. In addition, some of the CM larvae showed a sheltering activity by building a web around themselves before starting to chew the specimen which was visually observed and recorded in the video recordings. In general, three distinct activities of crawling, feeding (chewing), and boring into fruit (feeding and moving inside flesh) were observed and segmented from the data for further analysis. The result of the analysis revealed that the vibro-acoustic patterns related to the mentioned larval activities are clearly different, with feeding signals showing a chewing rate of 1 to 2.3 times a second (Figure 3.2) but crawling signals having a faster rate of 3 to 4 a second with lower amplitudes (Figure 3.3). Also, there existed some large transient spikes at irregular intervals above the noise floor with more broadband spectra relating to the larval internal activities where possibly chewing and sliding along the internal tunnel occur together (Figure 3.4). One interpretation of this could be when the larva had contact with the apple pulp while gliding over juicy surface inside tunnel, high-amplitude impulses are produced. Some other authors have reported such broadband high-amplitude impulses as a result of movement and feeding activity of different larvae inside agricultural products (Dosunmu et al., 2014; Jalinas et al., 2017b; Mankin et al., 2016).

Figures 3.2, 3.3, and 3.4 are plots for 30 s signal segments corresponding to different larval activity phases to provide a visual comparison between the resulting waveform and spectral contents. It can be inferred from Figures 3.2 and 3.3 that the larva crawling on the apple surface generated lower amplitude signals than the chewing signals, and the peak frequency (around 4 Hz) was distinctly different from one for chewing (around 1 Hz). Moreover, as shown in Figure 3.4, the internal activities of CM larva inside apple flesh created a signal signature with higher amplitudes than the chewing signature, but still having their most energy near the 1 Hz spectrum band.

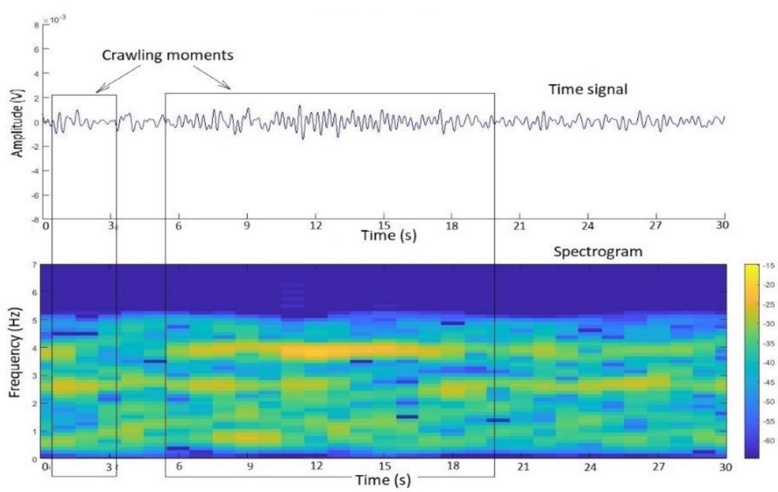

Figure 3.2 Time signal and spectrogram of the crawling moment of CM larva

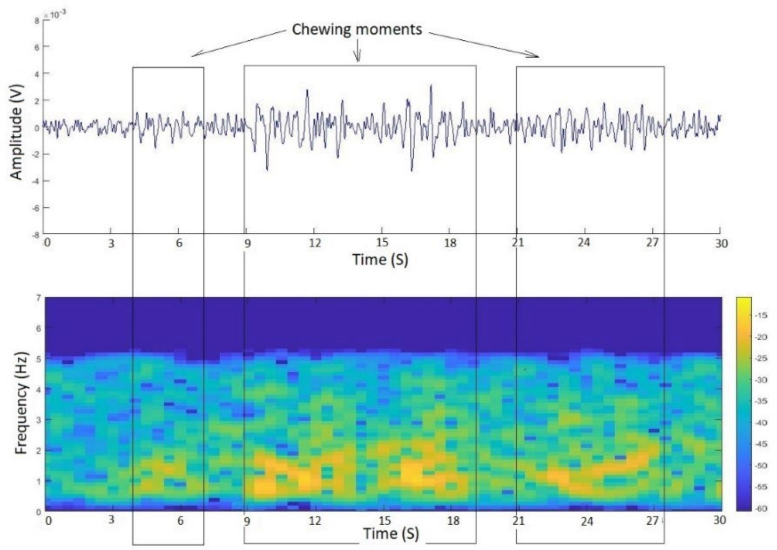

Figure 3.3Time signal and spectrogram of the chewing moment of CM larva

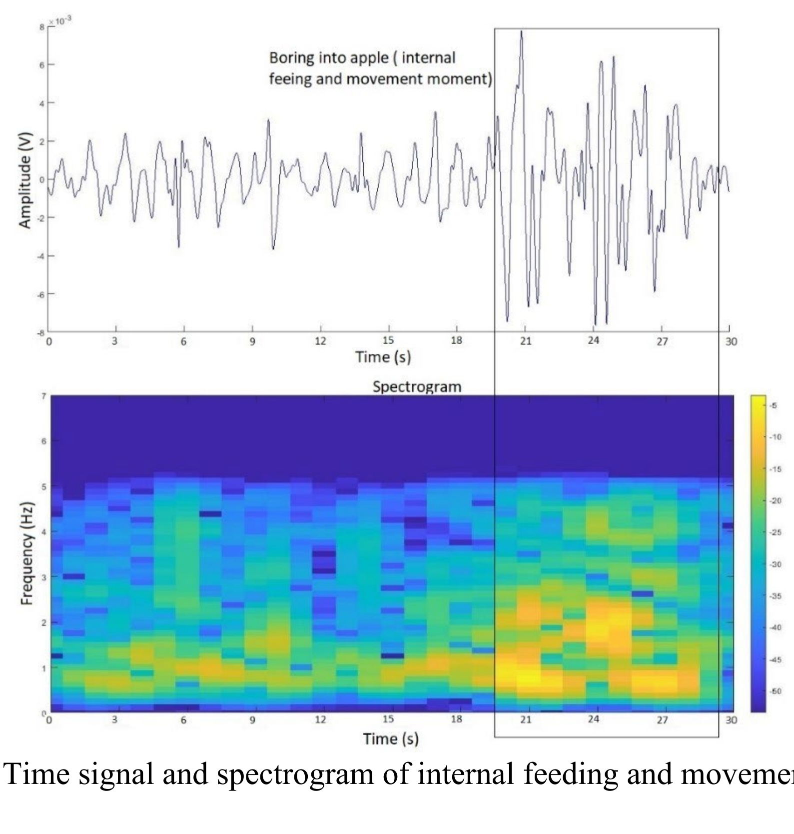

Figure 3.4 Time signal and spectrogram of internal feeding and movement moment of CM larva

Figure 3.5 shows a two-minute time span of a typical CM larva vibro-acoustic signal, in both time and frequency domain, containing all the three phases, starting with crawling on the apple surface followed by chewing the sample and then boring into the fruit. This figure can be matched with Figure 3.6 where a series of successive frames of the video clip is provided displaying the CM larva in crawling, chewing, and boring into apple near the calyx. In frames (a) to (d) the larva gradually approached the calyx, then started chewing the specimen while on apple surface, and then began to bore into the fruit in the last frame. It was found that the most detectable impulses were related to the moments when the larva was boring into the apple (in both the cut or intact apple) with a combination of feeding and locomotion activities.

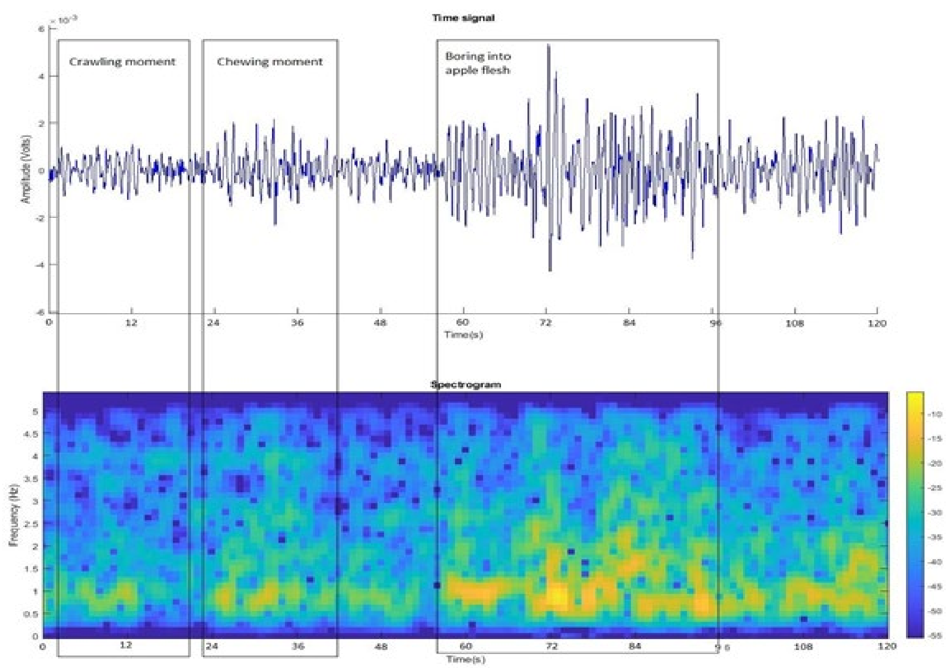

Figure 3.5 Time signal and spectrogram of different moments of CM larva in one example signal

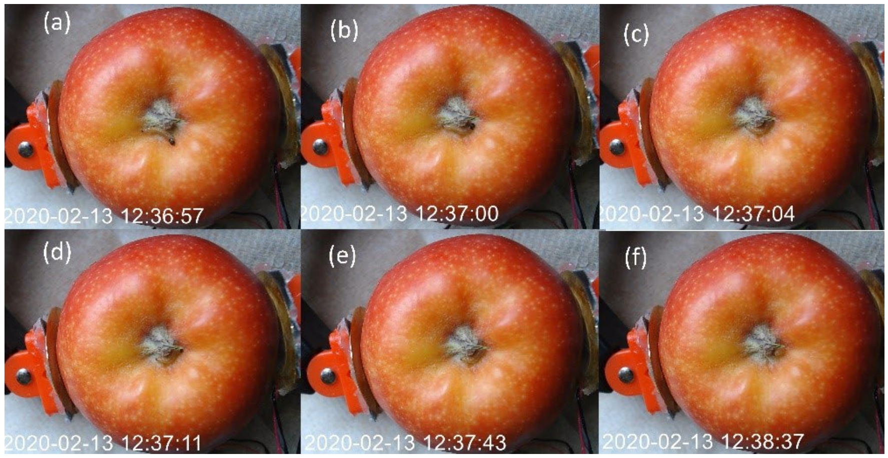

Figure 3.6 An example of successive frames of CM larva on apple; (a), (b) and (c) crawling moments, (d) and (e) chewing moments and (f) boring into apple

To further analyze the CM larval vibro-acoustic patterns, some useful time-domain features were extracted from the vibrational signals. In order to perform these analyses, first, the larval activity vibrational pulses were identified and time-stamped manually via visual observation and matching the video frames to the acoustic signal. Then, to extract pulse duration (Pd) and maximum amplitude (A) features, an amplitude envelope was computed for the signals using Hilbert Transform method (Feldman, 2011). As shown in Figure 3.7, having the Hilbert Transform envelope fitted to the signal, pulse duration was calculated as the time interval between the two adjacent crossings of the envelope with a detection threshold, that was defined as 2.5 times of the envelope median (Sutin et al., 2019).

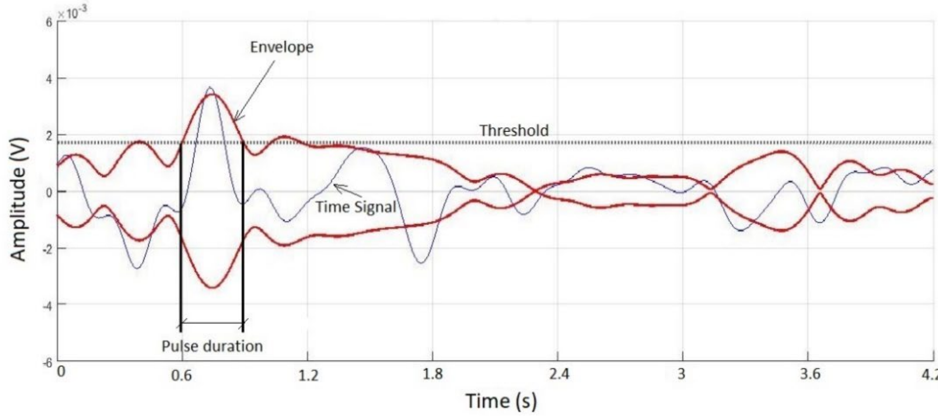

Figure 3.7 An example pulse duration measurement using the Hilbert Transform envelope method

Twenty pulses from each category were identified and selected to extract their time and frequency domain features including; pulse duration Pd, main frequency of pulse f, and maximum amplitude of envelope A. Figure 3.8 illustrates a graphical comparison of a total of 60 pulses for three different activities of CM larva. As shown in Figure 3.8, the combination of the three features can be used to classify the three larval activity pulses.

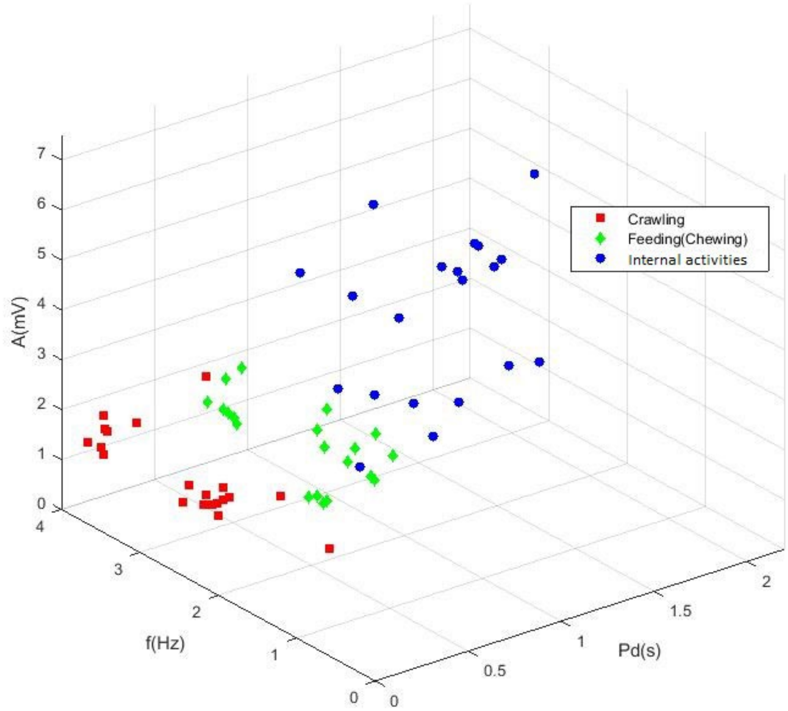

Figure 3.8 Visual comparison between pulse features of three different moments of CM larva activity on apples (A, f and Pd are amplitude, peak frequency and pulse duration, respectively)

In Figure 3.9, a statistical summary for the three features for the three signal groups as box charts are shown. As shown in Figure 3.9, the larva activities inside flesh (feeding and moving inside the apple) generated the highest amplitude and pulse duration with the average values of 5.11 mV and 883 ms, respectively, which were about four times the values for crawling signals. On the other hand, the CM crawling action on the apple surface produced significantly lower amplitude and pulse duration (mean values of 1.38 mV and 209 ms, respectively) than the two other categories. Moreover, the peak frequency of CM crawling pulses had a mean value of 2.94±0.81 Hz, which was significantly higher than the two other signals. In fact, the peak frequency of chewing and boring into flesh moments were not significantly different ($P > 0.05$) and had large overlap, meaning that the chewing frequency appears to be the dominant frequency in the internal activities of CM larva.

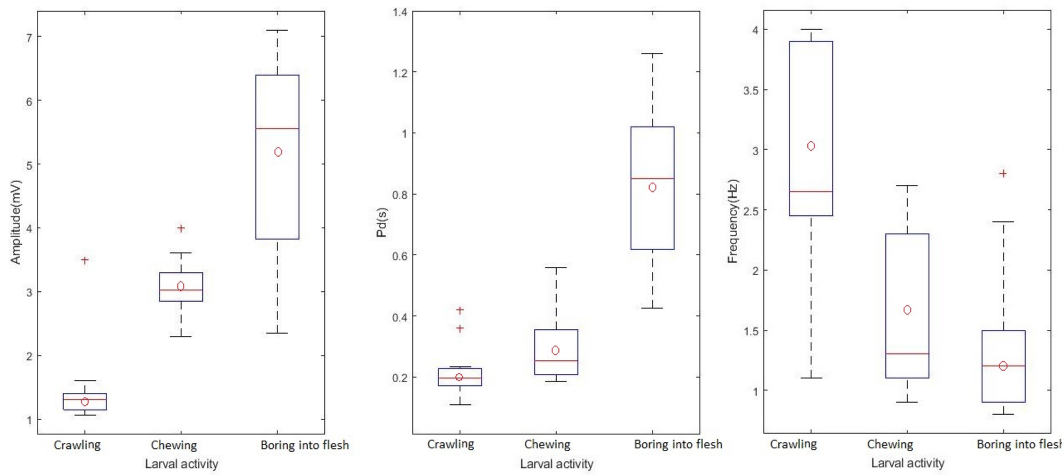

Figure 3.9 Statistical summary of three different moments of CM larva activity on apples with respect to maximum amplitude, peak frequency and pulse duration features

3.4 Conclusion:

In this study, the low-frequency vibro-acoustic signal patterns of CM larvae in apple fruit were detected and characterized. Results showed that among the different patterns identified, the incident of CM boring into the apple and internal feeding and movement had the strongest and the most detectable signal pulses. These low frequency spectral and temporal patterns and features can lead to an effective and reliable assessment of cryptic pest infestations in fruits and vegetables. This was possible with the aid of a portable, easy-to-operate, and low-cost microcontroller platform system used in acoustic devices (Mankin et al., 2015; Jakhete, et al., 2017). These equally proved that these methods have a good potential for application in the monitoring and detection of hidden insect pests in fruits and vegetables for ensuring food safety and profitability in agroindustry. For future work, we combine the use of the unique vibro-acoustic features along with useful features in machine learning techniques to build classifiers for detecting CM infestation in apples.

CONNECTING STATEMENT

In Chapter 3, the signal patterns and spectral signature of CM larval activities in apples were identified and characterized using the low-frequency vibro-acoustic method coupled with real-time video observation. Chapter 4 presents the investigation into the possibility of classifying CM-infested apples based on these characterized vibro-acoustic signals. Additionally, the effect of heat stimulation of infested apples on classification performance was studied. The next chapter is based on our publisher paper: "Nader Ekramirad, Alfadhl Y. Khaled, Chadwick A. Parrish, Kevin D. Donohue, Raul T. Villanueva, Akinbode A. Adedeji, Development of pattern recognition and classification models for the detection of vibro-acoustic emissions from codling moth infested apples, *Postharvest Biology and Technology*, Volume 181, 2021, 111633, ISSN 0925-5214, https://doi.org/10.1016/j.postharvbio.2021.111633".

CHAPTER 4. OBJECTIVE TWO

DEVELOPMENT OF PATTERN RECOGNITION AND CLASSIFICATION MODELS FOR THE DETECTION OF VIBRO-ACOUSTIC EMISSIONS FROM CODLING MOTH INFESTED APPLES

Abstract:

Codling moth (CM) is the most devastating global pest of apples with a huge potential impact on the post-harvest quality and yield of the product. Due to the small size of its larvae and potentially hidden behavior, simple visual inspection is ill-suited for accurate infestation detection. The characteristic vibro-acoustic signals of multiple behaviors of CM larvae such as chewing, and boring were identified in a previous study. In this study, two different approaches were proposed to build on this previous work: multi-domain feature extraction with machine learning to show basic classification potential, and matched filter-aided classification to show the effects of preprocessing using the larval behavior templates. Additionally, low-intensity heat stimulation was applied to improve classification results by increasing the larvae's hidden activity rate. The results indicated that the first approach led to accuracies as high as 97.47% for an acoustic signal duration of 10 s, with heat stimulation improving classification rates to 98.96% for the same interval. Finally, the matched filter-aided classification approach improved upon the heat stimulated results even further to obtain a 100% accuracy on classifying the test set for a signal duration of 5 s. These findings suggest that the vibro-acoustic technique can be an adaptable tool for detecting CM infestation in apples and improve post-harvest classification quality in fruit.

4.1 Introduction:

Apple is one of the fruit with the highest annual production and consumption around the world, with China and the United States being the top two producers (FAO, 2018). One of the biggest burdens to the apple export industry is the possibility of insect infestation, which can incur severe penalties if invasive species somehow are shipped. The main global pest of the apple industry is the codling moth (CM), *Cydia pomonella* (Lepidoptera: Tortricidae) (Jaffe et al., 2018; Witzgall et al., 2008). At a suitable temperature, often over 10 °C, the moths mate and begin laying eggs on apples or nearby leaves (Graf et al., 2018). The eggs will then hatch into larvae and bore into the apple flesh (Unruh et al., 2016). The quality of apples infested with CM larvae is reduced and is unsuitable for sale or human consumption. This leads to a large loss of up to 50% of a harvest (Kadoić Balaško et al., 2020). CM larvae bore their way into the apple interior in whichever way is easiest, often through the apple's calyx. The calyx entry point makes visual inspection difficult because there are no obvious visual markers like when boring is through the side of the apple (Adedeji et al., 2020). Manual detection of CM larvae infestation in apples is a very inefficient and laborious task, so, the industry needs a better solution.

The most common method for infestation detection in apples throughout the years has been a subjective approach of human sensory evaluation (HSE). In HSE, apples are randomly selected manually, examined and if there is a sign of infestation, it is then cut and inspected for evidence of infestation (Mohana et al., 2013). Many factors make HSE insufficient and unsuitable for large volumes, such as being destructive to apples tested, being subjective to the examiners' methods and sight, and the inability to inspect every apple (both due to the destructive nature and relatively high time cost). To solve this problem, several studies have been conducted on the detection and classification of CM in apples to gain more insight into apple's quality in ways that are quicker and nondestructively. The techniques looked at include X-ray imaging (Hansen et al., 2005; Schatzki et al., 1997), infrared (IR) thermal camera imaging (Hansen et al., 2008), hyperspectral imaging (HSI) (Ekramirad et al., 2017; Rady et al., 2017a) and acoustic detection (Ekramirad et al., 2020; Li et al., 2018). Compared to other methods, acoustic detection (acoustic emission (AE) and vibro-acoustic detection) that uses sound produced or attenuated through an apple has shown to be the most promising and efficient classifier for CM infested apple (Li et al., 2018). They had applied an AE methodology using a singular piezoelectric sensor that is based on automatic signal capture and feature extraction in the ultrasonic frequency range (35-100 kHz). From the eleven features obtained, the authors found a test-set classification rate (detection of infested versus healthy apples) of 57-100% using linear discriminant analysis (LDA), and 87-100% using Ensemble adaptive boosting up to 1 s of signal collection. A limitation of this work, however, was that it did not attempt to understand the acoustic patterns detected nor to try to prove how they correlate to the presence of CM activity. Also, the presence of high-frequency signals could not be explained. Since the actual activity of the larva inside the apple is consistent with lower frequencies, a later work by Ekramirad et al. (2020) explored vibro-acoustic techniques (0.4-8 Hz) for picking up the larva activity using dual-channel lead zirconate titanate (PZT) sensors. Sources of the CM larvae sounds were inspected through simultaneous video recording and acoustic signal capture. Using these verifiable methods, significant correlations were found between these signal characteristics and other larvae activities in test apples, including crawling and chewing. An advantage of the lower frequency vibro-acoustic over the higher frequency AE techniques is the significantly lower cost of vibro-acoustic systems and the affinity for sounds produced by larvae displacement (Kabir et al., 2018; Ekramirad et al., 2020). The development of robust detection systems based on this technology could result in a more efficient technology that is easily adaptable to a large-scale apple processing. Thus, there is a need to prove the detection capability and repeatability of a CM infestation detection system, as well as highlight any shortcomings that may need to be addressed either now or in the future.

Signal detection methods differentiate between information-bearing patterns and random patterns that represent noise or other processes that are not relevant (Gao et al., 2017; Sedunov et al., 2016; Wilmshurst, 2017). For example, signal cross-correlations have been used as an acoustic-based leak detection technique in water pipelines to measure the leak noise signals in acoustic/vibration signals (Gao et al., 2017), and in passive acoustic unmanned aerial vehicle detection and tracking (Sedunov et al., 2016). Moreso, matched filters are very common in signal detection and digital communication, due to their ability to obtain the maximum signal-to-noise ratio (SNR) (Zhao et al., 2017) for a simple threshold detector. To use a matched filter receiver, there is a need to know the form(s) of the desired signals to be received, which are stored as templates. Then, the signal will be convolved with a time-reversed conjugate of the template to produce an output analogous to the correlation between the template and the input signal. The increased SNR improves both the sensitivity and reduces the number of false positives. Also, to a direct filtering approach, some classifiers operate on more complex relationships between the signal characteristics. These include k-nearest neighbors (kNN), decision tree, LDA, support vector machines (SVM), Naïve Bayes (NB), and Ensemble (bagged tree). The classifier models are highly recognized in terms of superior performance in the classification of acoustic data because of their ability to map patterns in a high dimensional space, do it efficiently in a cost-effective and accurate manner (Khaled et al., 2018).

The main objective of this study was therefore to investigate the potential of classification of control (healthy) and CM-infested apples based on detecting the recognized vibro-acoustic patterns of larvae activities in the signals from infested samples. To achieve this goal, feature extraction and machine learning were applied for the classification of larvae-infested apples from control ones such that it can be a baseline for the binary classification problem. Finally, the specific objectives in this paper were to study the effects of heat stimulation and matched filter activity labeling on the CM infestation detection capability.

4.2 Material and Methods

4.2.1 Samples Preparation

Gala apple cultivar were procured from a local grocery market in Princeton, Kentucky in the US around June 2020. Samples were manually inspected to ensure they were defect-free and were selected based on similar physical appearances (shape, color, and size). The samples were then washed in a 0.5% (v/v) sodium hypochlorite solution according to Louzeiro et al. (2020) for fungal and bacterial disinfection. They were rinsed with distilled water and dried at ambient conditions in the lab (Department of Entomology, University of Kentucky, USA). The apples were then artificially infested by placing neonate larva near the calyx end of each apple. After 24 h, each infested apple was placed into a tapered plastic cup (8 cm bottom diameter, 10 cm top diameter, 10 cm high) with a plastic lid. Two groups of 60 infested and 30 control (healthy) apple samples were stored at ambient storage conditions (21 °C and 75% relative humidity) for three weeks and acoustic scanning was carried out daily. Four infested and two control apples were randomly selected for each day's tests. After the first set of acoustic experiments were performed at ambient conditions, half of the apples were then treated with heat stimulation. The heat stimulation was carried out in a laboratory-scale drying unit at 30 °C for one hour before the apples were taken out for acoustic scanning.

4.2.2 Vibro-acoustic Data Acquisition

The data acquisition system consisted of eight channels connected to contact piezoelectric (PZT) sensors (Buzzer element Std 2.6 kHz 35 mm, CUI Devices, Lake Oswego, OR, USA) with a frequency range of 0.4 to 8 Hz. The PZT sensors were connected to a custom-made instrumentation amplifier, coupled to a data logger (USB 6001 DAQ, National Instrument Co., USA) for sampling the amplifier output at 120 Hz and connected to the computer with the software on it to record and display the signals. In order to preclude background ambient noise, the vibro-acoustic experimental unit was set above an isolated table that had a 15 cm layer of sand, topped with a 5 cm slab of granite with acoustic padding sitting in a room with a concrete padded floor built on 20 cm of gravel above the loam soil bed in a lab at Biosystems and Agricultural Engineering Department, University of Kentucky, Lexington, KY, USA. The vibro-acoustic recordings were carried out inside an insulated chamber set on the table (Figure 4.1). To carry out the tests, three apples were placed inside the chamber with each one in contact with two PZT sensors. Two remaining sensors were used as a reference without contact with any apple sample to collect background noise that is applicable in the noise correction during data analysis. Signals were recorded for a time span of 10 min. Additionally, for monitoring and recording larval activities a digital camera with an adjustable gooseneck fixture was utilized. Video recordings were made by Debut video capturing program (NCH Software Co., USA), which can display the local computer time on video images on the screen. To obtain the template signals for each of the observed larvae activities (crawling, chewing, and boring), both the video recording and acoustic scanning were performed simultaneously using the same computer clock for reference (Ekramirad et al., 2020).

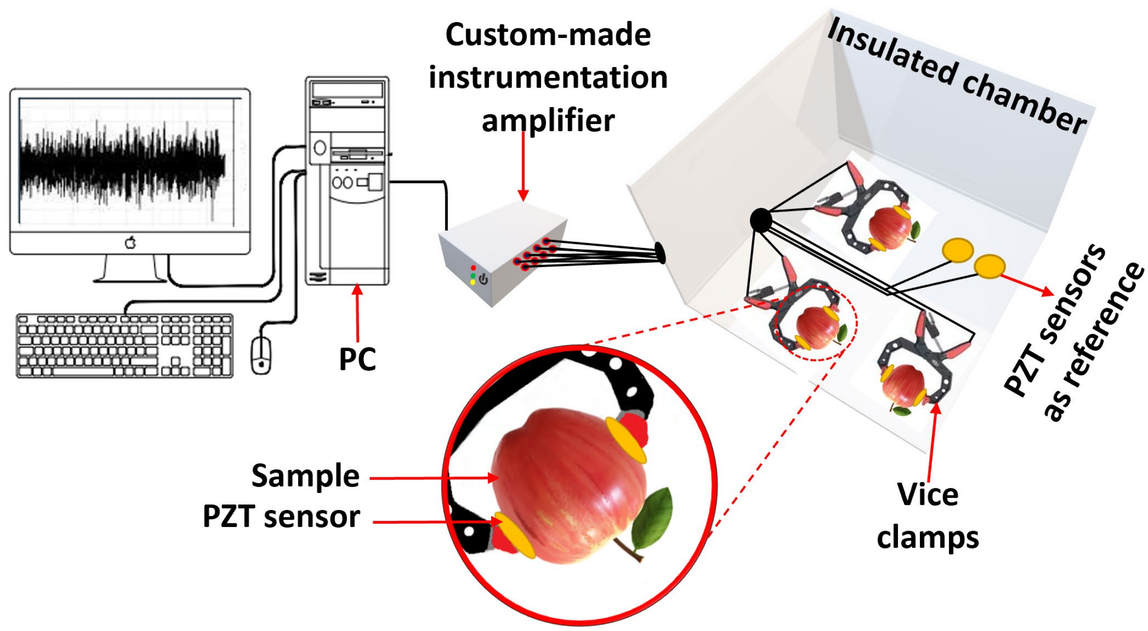

Figure 4.1 Experimental setup for vibro-acoustic data acquisition of apple samples (PZT: Lead Zirconate Titanate).

4.2.3 Data Pre-processing

Before analysis, all vibro-acoustic data were preprocessed with a band-pass filter from 0.4 – 8 Hz. Then time segmentation was applied to the vibro-acoustic data to determine how well the larva activity could be detected over short time intervals. After collecting the 10 min signals, the initial 1 min of data were removed at the beginning and end to eliminate any residual background noise from human activities or any other background conditions that occurred at the start/end of recording equipment. From these 8 min signals, further sub-segmentation was considered to evaluate detection capabilities at smaller intervals (2 min, 1 min, 30 s, 10 s, and 5 s).

A set of 22 time and frequency domain features were extracted for all the segmented signals. Due to the possibility of the larvae being inactive during any capture window and the likelihood of being inactive in at least one capture window, there is the possibility that an infested signal will have no indication of being infested and will be labeled as control. Therefore, it is desirable to determine if any of these moments exist and try to point them out through clustering. For further analysis, Gaussian mixture modeling (GMM) was used as the clustering technique to group the input signal samples into either of the two classes, which provide more accurate labels for each input signal. Steps for using cluster as a new feature in classification are as follows: fit a GMM with your training data, use this fitted GMM to get cluster labels for both your training and test data, append the cluster labels as a new feature in both datasets, and fit the classifier with this "enhanced" training data. Figure 4.2 shows the flowchart of the methodology of vibro-acoustic data processing.

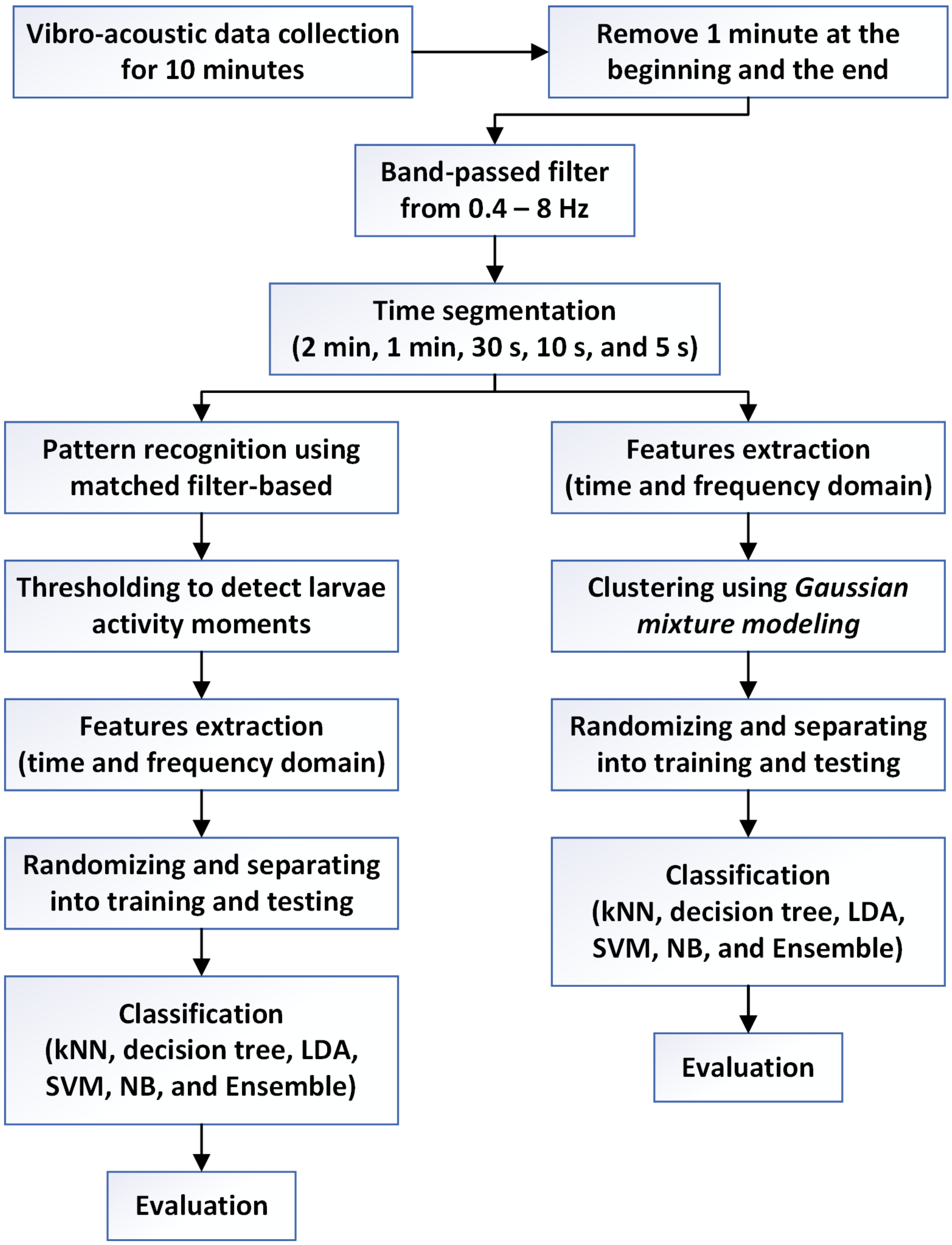

Figure 4.2 The flowchart for sequence of steps for vibro-acoustic data acquisition and processing (kNN: k-nearest neighbors, LDA: linear discriminant analysis, SVM: support vector machine, NB: Naïve Bayes).

4.2.4 Machine Learning Classification

Two different machine learning procedures were developed to evaluate infested apple classification from sound signals collected at a low frequency range. In the first approach, all the signal segments from infested samples were labeled as infested signals. Different classification algorithms were applied to classify apples from the low frequency vibro-acoustic signals of control (healthy) and CM infested apples. These classification models include kNN, decision tree, LDA, SVM, NB, and Ensemble. Several studies have used these algorithms for various classification applications (Khaled et al., 2018; Liaghat et al., 2014). The best model was selected according to accuracy although further metrics such as low false positives (healthy samples classified as CM infected) and low false negatives (CM infected samples found as healthy) were also considered. Prior to classification, 70% of the data were allocated for model development and training, and the remaining 30% were used for evaluation and testing. Ten-fold cross-validation was used in the training process to avoid overfitting and to obtain a good generalization of model performance. Then, each classification model was tested using the test set and the test performance measures were reported.

In the second approach, a matched filter-based pre-processing method was used to detect the larval activity segments in order to label them as infested signals. The main objective of this section was to introduce a promising pattern recognition technique called matched filter aided classification. The template used for this task was from larval boring that was determined in the previous study (Ekramirad et al., 2020). By thresholding the output of the matched filter receiver, only the signal segments that originated from the activity of larvae were labeled as infested in the machine learning model. After labeling, four features of the peak value, centroid, equivalent width and mean square abscissa were extracted for usage in the classification models (Chandaka et al., 2009).

In both machine learning methods applied in this study, the prediction success of the classifiers was evaluated by examining the confusion matrix. Accuracy, sensitivity (true positive ratio), specificity (true negative ratio), and precision were computed to understand the classifier performance. All the classification algorithms were developed and performed using MATLAB R2020b (The MathWorks, Inc., Natick, Massachusetts, United States).

4.3 Results and Discussions

4.3.1 Vibro-acoustic Signal Patterns in Apples

The identification of the signal associated with larvae activity is important because it can be used to study how external stimuli like heat or sound impact the activity rate. Vibro-acoustic signal patterns related to specific activities in CM-infested apples are shown in Figure 4.3 as the vibration waveform and associated spectrograms. Patterns of different larval activities, such as crawling, feeding (chewing), boring into fruit (feeding and moving inside flesh), were obtained by placing the CM larvae on the apples, at the same time, video recording of the larval behavior was captured to correlate the vibro-acoustic signals being collected. The results illustrated that the signals from infested samples are clearly different from the ones from non-infested samples as shown in Figures 3A-C and 3D, respectively. For example, feeding signals shows a chewing rate of 1 to 2.3 times per second (Figure 4.3 B) while crawling signals have a faster rate of 3 to 4 times per second with lower amplitudes (Figure 4.3 A). It was observed that the boring moment has the highest signal strength compared to the crawling and chewing. This can be

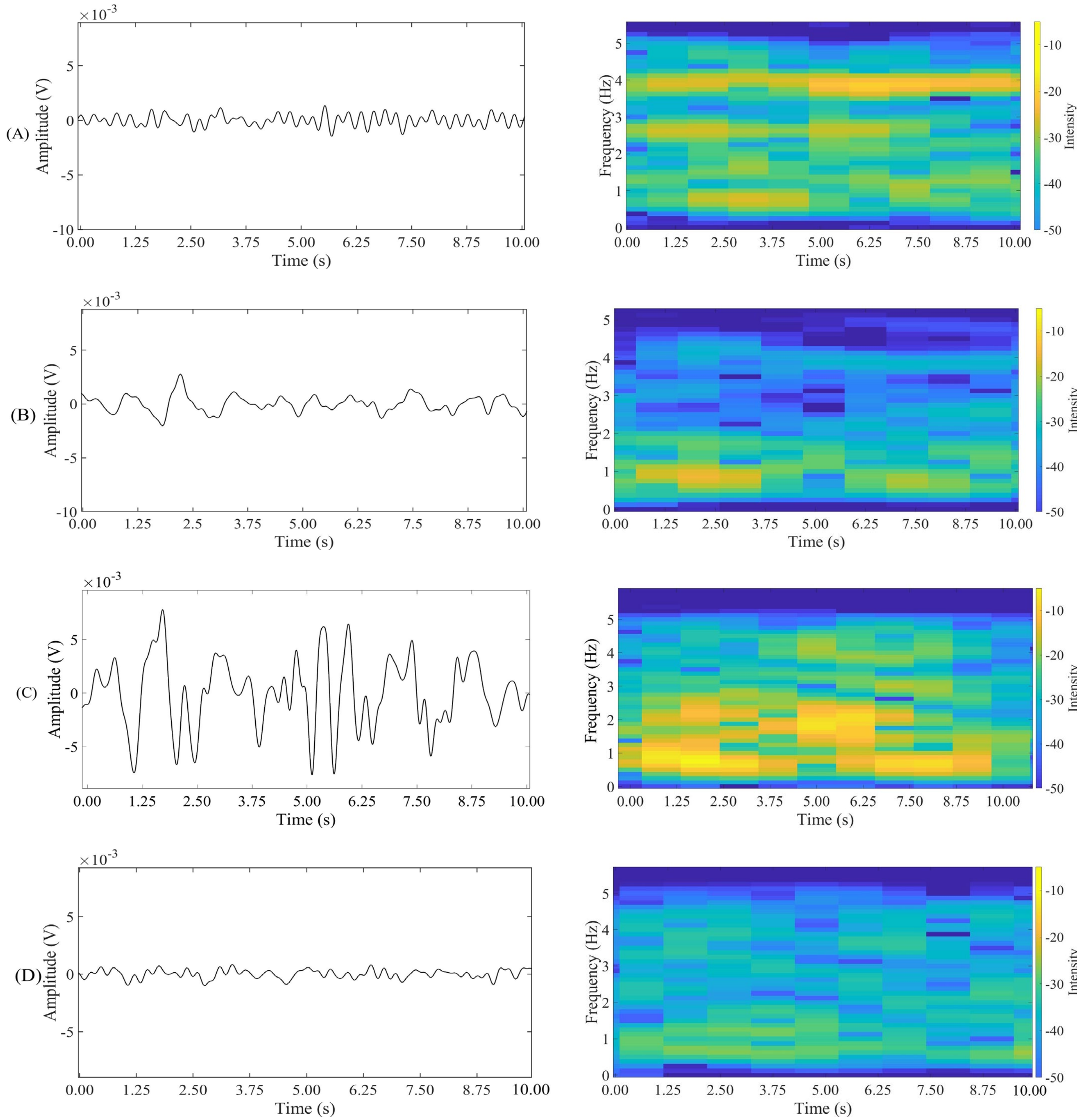

Figure 4.3 Time signals and spectrograms of different moments of CM larva activities: (A) crawling, (B) chewing, (C) boring, and (D) control samples.

attributed to the direct contact of larva with the apple pulp while gliding over the juicy surface inside the bored tunnel. These results agree with findings from the previous studies (Ekramirad et al., 2020 Dosunmu et al., 2014; Jalinas et al., 2017; Mankin et al., 2016), which showed high-amplitude broadband impulses as a result of movement and feeding activity of different larvae inside agricultural products.

Figure 4.4 provides a statistical summary for the amplitude, pulse duration, and peak frequency for the three signal types from larval activities (crawling, chewing and boring) in the apple. The CM larval boring into apple pulp (internal activity) generated the highest amplitude and pulse duration with the average values of 5.11 mV and 883 ms, respectively. On the other hand, the larvae crawling action on the apple surface produced significantly lower amplitude and pulse duration (mean values of 1.38 mV and 209 ms, respectively) than the two other categories. In addition, the peak frequency of larval crawling pulses had a mean value of 2.94±0.81 Hz, which were significantly higher than the other two signals. In fact, the peak frequency of chewing and boring into flesh moments were not significantly different and had a large overlap, meaning that the chewing frequency is the dominant frequency in the internal activities of CM larva.

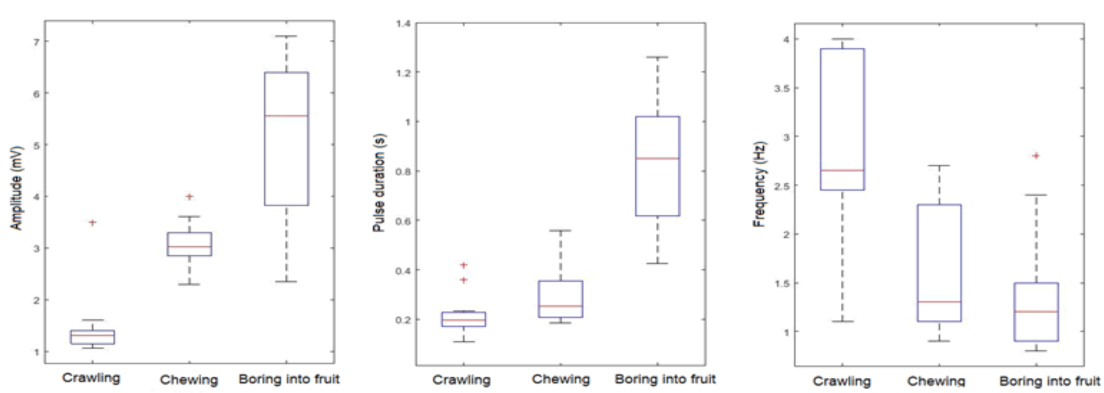

Figure 4.4 A comparison of signal amplitude, pulse duration, and frequency for different larval moments

4.3.2 Classification of Vibro-acoustic Signals

Table 4.1 summarize the overall recognition accuracy in identifying CM infestation in apples using various classifiers (kNN, decision tree, LDA, SVM, NB and Ensemble). The classifications were performed in five signal segments or window sizes, namely 2 min, 1 min, 30 s, 10 s and 5 s, where the whole 10 min signal was segmented according to the time frames listed after removing the initial and final 1 min because of noise. The detection window size is important because this vibro-acoustic signal is non-stationary with rapidly varying characteristics over time. Therefore, the segmentation window should be selected based on the duration of larvae activity. Moreover, the signal collection time is desired to be as short as possible such that it could be used in an industrial facility without much delay. However, if the capture time is too short a larval activity could be missed or the larvae could be inactive within the window, resulting in false negative readings (infested apples classified as healthy). Table 4.1 presents the classification test accuracy obtained with the different window sizes for all classifiers. Overall, the shorter signal segments provided better classification than the longer signals, except for LDA and kNN, which showed a decrease in classification accuracy from 76.19% in 2 min to 65.82% in 1 min, and from 90.48% in 2 min to 79.75% in 1 min, respectively. The results indicate that there is an improvement trend in the classification accuracy as the window size is shortened from 2 min to 10 s followed by a slight decrease in the classification accuracy from 10 s to 5 s. The improvement in classification accuracy can be attributed to the shorter signal that matches the active moments of the larvae leading to maximizing the percentage of the larvae activities in the window. On the other hand, additional noise may exist in the longer signals in the form of non-active moments of the larvae, which increases the variance among the evaluated features. Furthermore, the response time of the system should be as low as possible; thus, the 5 s signals are suitable for feature extraction and classification in this application. Similarly, Nanda et al. (2019) reported that the average duration of termite larvae activities, such as feeding, is 4.02 s and they suggested 4 s window size for practical purposes.

Looking at the performance of the classifiers (Table 4.1), it is obvious that LDA and NB had performed poorly with accuracy only up to 76.42% and 77.26%, respectively. The LDA outcome can be attributed to the limitation of linear plane that separates feature samples between classes. While the features have some direct proportionality to the presence of larvae, there are other relationships between features that more complex classifiers can characterize as evidenced by the increase in performance when using these models. The kNN and Ensemble classifiers performed better than others across time frame. The accuracy reached was 97.47% when using Bagged Tree in the 10 s signal data set. Overall, the Ensemble was more successful than all other classifiers at correctly classifying the vibro-acoustic signals based on the classification accuracy, sensitivity, specificity, and precision (Table 4.1). The best classifier was the Ensemble - GentleBoost algorithm, which was trained with Bayesian optimizer by using a weighted combination of several classifier models using 10 s signal data. From this optimized process, the accuracy, sensitivity, specificity, and precision were 97.47%, 96.98%, 98.31%, and 98.97%, respectively.

Table 4.1 Classification performance for unstimulated data set.

Signal length	**Classifier**	**Test accuracy (%)**	**Sensitivity (%)**	**Specificity (%)**	**Precision (%)**
2 min	kNN	90.48	91.67	88.89	91.67
	Decision tree	71.43	70.83	72.22	77.27
	LDA	76.19	79.17	72.22	79.17
	SVM (Quadratic)	73.81	70.83	77.78	80.95
	NB	52.38	58.33	44.44	58.33
	Ensemble (Bagged Tree)	80.95	87.50	72.22	80.77
1 min	kNN	79.75	91.30	63.64	77.78
	Decision tree	83.54	89.13	75.76	83.67
	LDA	65.82	76.09	51.52	68.63
	SVM (Cubic)	74.68	80.43	66.67	77.08
	NB	73.42	84.78	57.58	73.58
	Ensemble (Boosted trees)	87.34	93.48	78.79	86.00
30 s	kNN	85.62	93.94	72.13	84.55
	Decision tree	90.00	92.93	85.25	91.09
	LDA	73.75	79.80	63.93	78.22
	SVM (Cubic)	84.38	83.84	85.25	90.22
	NB	75.62	70.71	83.61	87.50
	Ensemble (GentleBoost)	90.00	89.90	90.16	93.68
10 s	kNN	93.89	96.64	89.27	93.81
	Decision tree	90.11	93.96	83.62	90.61
	LDA	76.42	79.19	71.75	82.52
	SVM (Gaussian)	95.16	96.64	92.66	95.68
	NB	77.26	77.52	76.84	84.93
	Ensemble (Bagged trees)	**97.47**	**96.98**	**98.31**	**98.97**
5 s	kNN	91.66	91.22	92.37	95.15
	Decision tree	91.12	90.19	92.66	95.27
	LDA	74.12	76.42	70.34	80.87
	SVM (Gaussian)	93.16	94.15	91.53	94.80
	NB	72.41	68.33	79.10	84.29
	Ensemble (GentleBoost)	95.94	96.39	95.20	97.05

kNN: k-nearest neighbors, LDA: linear discriminant analysis, SVM: support vector machine, NB: Naïve Bayes, The classification results for the heat-stimulated test data set are summarized in Table 4.2. The aim here was to improve the detection and classification of CM infested apples by instigating external stimulation of the larvae as a treatment to generate sustained vibro-acoustic signals. As shown in Table 4.2 and Figure 4.5, while the classification accuracies increased with heat stimulation in comparison to unstimulated data for all classifiers, the ANOVA results were not significantly different from each other ($P > 0.05$ level significant). Figure 4.5 shows the average accuracies of all the classifiers used in this study for unstimulated and heat-stimulated data sets derived from all signals. The best result was achieved by Ensemble for heat-stimulated signals with an average accuracy of above 96.29%. Specifically, the 10 s heat-stimulated signals had the highest amount of classification accuracy, sensitivity, specificity, and precision (98.96%, 97.77%, 96.48%, and 98.86%, respectively). The underlying motivation behind the heat stimulation is that it will spur the larvae into a state of increased activity, which increases the likelihood of the signal used for classification being present in the analysis window. Several reports have shown the influence of heat stimulation on increased acoustic activities of larvae in different agricultural and wood commodities (Hagstrum et al., 1998; Hagstrum & Flinn, 1993; Nanda et al., 2019a; Nanda et al., 2019b; Nowakowska et al., 2017). For instance, Hagstrum and Flinn (1993) studied the Acoustic detection of five species of adult stored-product insects in wheat at different temparatures. They reported that there was an increase in the acoustic signal hits recorded as the temperature increased from 17.5 to 35 °C, following a decrease at higher temperatures. Moreover, the locomotive behavior of *Tribolium castaneum* (Herbst) adults over a temperature range of 22-36 °C in wheat was recorded over a 20 h period using an array of 8 acoustic sensors (Hagstrum et al., 1998).

Their result showed that both male and female adults favoured temperatures higher than 30 °C. In another study, Nanda et al. (2019a) found that the maximum activity tempareture for termite was around 26 °C, which is obtained by metabolic process of the insect inside the wood. As another example, the results of a study by Lewis et al. (2013) suggested that pellets and active drywood termite infestation detection could be enhanced by heating the wood to 25 °C before acoustic inspection to stimulate larval foraging and feeding.

Table 4.2 Classification performance for heat stimulated data set.

Signal length	Classifier	Test accuracy (%)	Sensitivity (%)	Specificity (%)	Precision (%)
2 min	KNN	85.50	92.31	66.67	92.31
	Decision tree	81.25	84.62	66.67	91.67
	LDA	77.08	87.18	33.33	85.00
	SVM (Quadratic)	83.33	97.44	22.22	84.44
	NB	83.33	87.17	66.67	91.89
	Ensemble (AdaBoost)	91.67	97.44	66.67	92.68
1 min	KNN	91.67	94.59	81.82	94.59
	Decision tree	81.25	89.19	54.55	86.84
	LDA	82.29	93.24	45.45	85.19
	SVM (Quadratic)	83.33	90.54	59.09	88.16
	NB	80.21	87.84	54.55	86.67
	Ensemble (GentleBoost)	97.92	100	90.91	97.37
30 s	KNN	93.23	96.45	84.31	94.44
	Decision tree	87.50	92.20	74.51	90.91
	LDA	74.48	87.94	37.25	79.49
	SVM (Gaussian)	90.10	96.45	72.55	90.67
	NB	79.17	87.94	54.90	84.35
	Ensemble (GentleBoost)	98.96	99.29	98.04	98.04
10 s	KNN	93.75	94.70	90.85	96.93
	Decision tree	94.97	96.31	90.85	96.98
	LDA	77.43	87.10	47.89	83.63
	SVM (Cubic)	91.15	93.32	84.51	94.85

	NB	75.17	82.95	51.41	83.92
	Ensemble (GentleBoost)	**98.96**	**97.77**	**96.48**	**98.86**
5 s	KNN	91.71	96.03	81.37	92.51
	Decision tree	90.26	93.02	83.65	93.16
	LDA	68.87	91.43	14.08	72.00
	SVM (Gaussian)	89.14	92.54	80.99	92.10
	NB	76.48	74.76	80.61	90.23
	Ensemble (Bagged tree)	93.95	95.87	89.35	95.57

kNN: k-nearest neighbors, LDA: linear discriminant analysis, SVM: support vector machine, NB: Naïve Bayes. Bolded data indicate the best result.

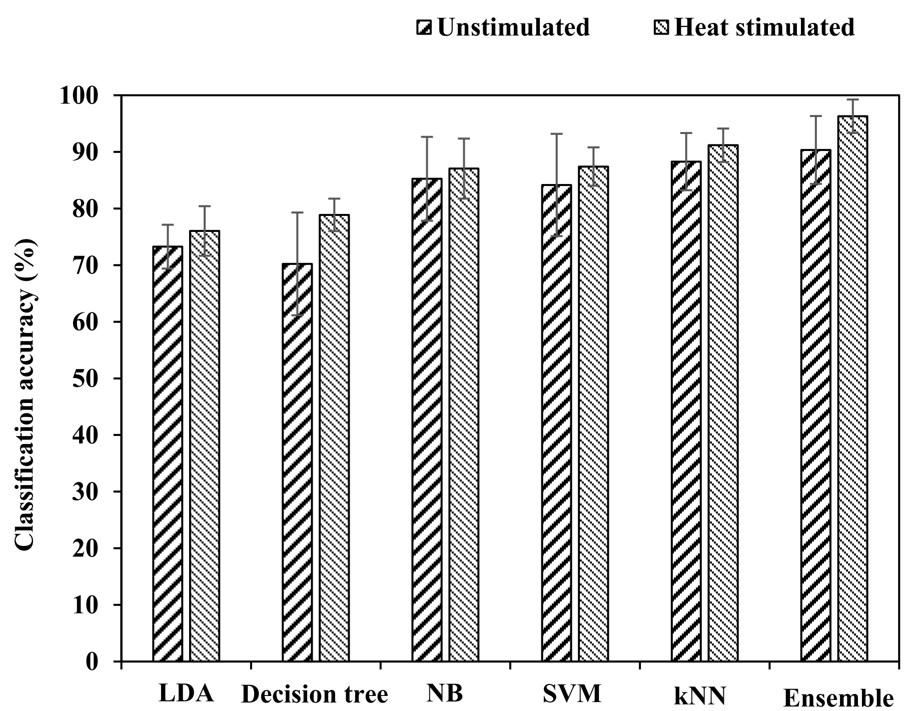

Figure 4.5 Classification accuracies using different types of classifiers for unstimulated and heat-stimulated signals across all data sets. (LDA: linear discriminant analysis, NB: Naïve Bayes, SVM: support vector machine, kNN: k-nearest neighbors).

Figure 4.6 shows the confusion matrix for the best classification model using the testing data set. This model attempts to predict the target class (i.e., infested and control apples) based on vibro-acoustic signals. The rate of incorrectly detected healthy apples (false positive = 7%) is greater than the percentage of incorrectly classified infested apples (false negative = 1%).

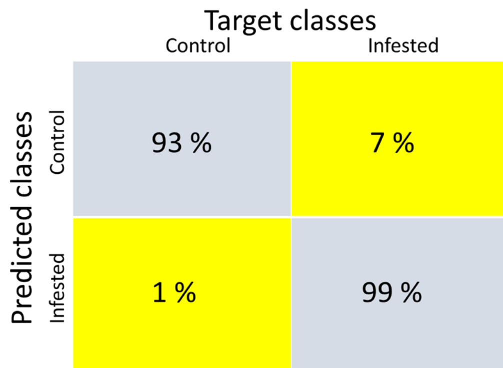

Figure 4.6 Confusion matrix for the best classification model.

4.3.3 Vibro-acoustic Signal Pattern Recognition

Following the recognition of the signal patterns for different activities of CM larvae in section 4.3.1, the similarity and repeatability of these patterns within the vibro-acoustic signals for "reference" (sensors without contact with apples), "control" (healthy apples) and "infested" samples (apples with live larvae inside them) were evaluated using matched filter analysis. In Figure 4.7 a cross correlograms is shown for a typical signal from reference, control, and infested samples correlated with a typical short pattern of larvae activity moment obtained by video observation in section 4.3.1. As illustrated in Figure 4.7 is the correlation between larval activity moment and the signals from infested apples with active larvae inside.

(A)

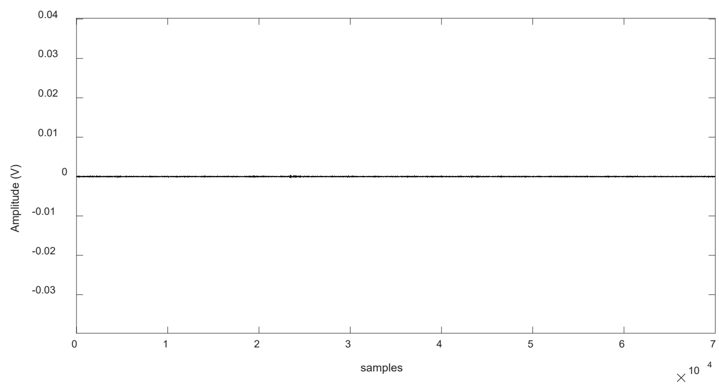

(B)

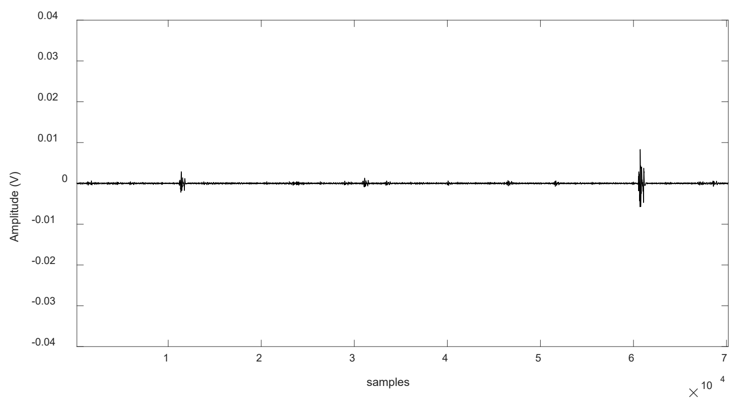

(C)

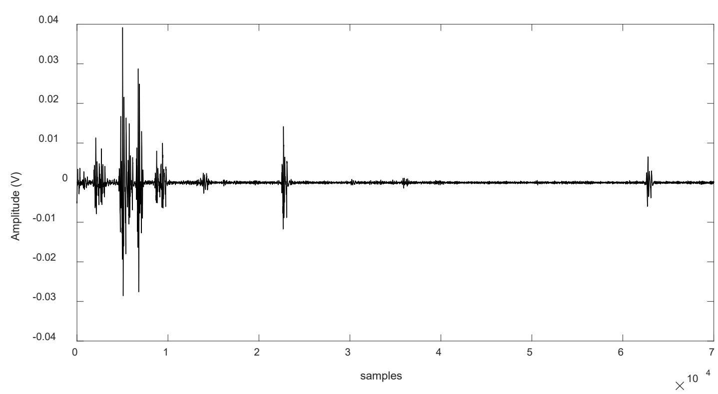

Figure 4.7 Matched filter output for the reference (A) – no sample, control apple (B) and infested (C) apples.

Table 4.3 Classification performance for heat-stimulated data set using matched filtering labeling.

Classifier	Test accuracy	Sensitivity	Specificity	Precision
	(%)			
kNN	98.06	71.43	100	100
Decision tree	100	100	100	100
LDA	96.12	57.14	98.96	80.00
SVM (Cubic)	99.03	85.71	100	100
NB	96.12	85.71	96.88	66.67
Ensemble (RUSBoost)	**100**	**100**	**100**	**100**

kNN: k-nearest neighbors, LDA: linear discriminant analysis, SVM: support vector machine, NB: Naïve Bayes

Table 4.3 represents the test performance of classifying the 5 s heat-stimulated signals by different classifiers, using the matched filtering preprocessing. This approach produced a better classification accuracy (up to 100%) compared to the classification method in the previous section where the signals from infested samples did not have larvae activity in them due to inactive moments and were thus mislabeled. Furthermore, in the matched filtering approach only three features (the peak value, centroid, equivalent width and mean square abscissa) were selected to use as inputs in classification phase, which reduced the complexity and computation time of the model. No literature was found on the use of matched filter detection in vibro-acoustic signals of insects, but the results in this study are similar to that of comparable studies in the automatic detection of epileptic spikes in electroencephalogram (EEG) using matched filter in combination with machine learning. For example, Mera-Gaona et al. (2020) achieved a sensitivity of 99.96% and specificity of 99.26% in the detection of epileptic spikes in EEG records using match filter. Their automatic detection of epileptic spikes was based on the implementation of an

Artificial Neural Network to verify detections made by a matched filter which used a template that represents a waveform of an epileptic spike pattern.

4.4 Conclusion

Based on the vibro-acoustic signals generated during CM larvae activities in and on apples, such as feeding, crawling, and boring into apple fruit, a vibro-acoustic signal monitoring system was proposed in this study to noninvasively detect CM in apples. The results showed that there were significant differences in vibro-acoustic features between control and infested samples, which was enhanced by heat-stimulation treatment. Various machine learning algorithms were developed to recognize vibro-acoustic signals from CM infested apples, and the Ensemble method showed better performance, with overall test accuracy of 98.96%. Also, matched filtering approach for pattern recognition further improved the classification results. The result was further improved by employing an Ensemble classification to classify the apple as healthy or infested based on whether or not segments were labeled as infested. Moreover, the combination of matched filtering approach with the Ensemble method achieved the best classification accuracy of 100% for the test data set. The proposed CM infestation detection system is a new approach that employs an artificial intelligent classification strategy for recognizing CM insects' acoustic signals. The advantages of this system include low cost, rapid response, noninvasiveness, and flexibility. It also serves as a baseline in terms of the potentials of using vibro-acoustic approach for non-destructive classification of CM infested apples in online post-harvest apple processing that targets local and international apple supply chain.

CONNECTING STATEMENT

In chapters 3 and 4, low-frequency vibro-acoustic method was used to detect and classify CM-infested apples based on the activities of CM larva. In chapter 5, high-frequency acoustic impulse response method will be investigated as an active acoustic method for nondestructive detection of CM-infested apples based on CM damage.

CHAPTER 5. OBJECTIVE THREE

HIGH-FREQUENCY ACOUSTIC IMPULSE RESPONSE TEST AS A NOVEL NONDESTRUCTIVE METHOD FOR DETECTION OF CM-INFESTED APPLES

Abstract

Codling moth (CM) infestation causes physical and chemical changes in the tissue of apples. These changes could be associated with biochemical reactions (microbial and enzymatic) resulting in alterations in the mechanical and acoustic parameters of the infested samples. Also, it is expected that the acoustic response of an infested apple with internal damage and possibly cavity is different from the acoustic response of a normal apple with healthy internal quality. In this study, CM infestation and the subsequent physicochemical changes occurring in apples were correlated to the high-frequency acoustic impulse response signals from apples. To achieve this, a novel approach was designed to measure the vibrational-acoustic response of infested apple fruit to a pre-defined impulse in a knocking test. Then the acoustic response signal of CM-infested sample was characterized in a controlled environment by obtaining its power spectral density (PSD) to compare it with that of healthy samples. The result showed that there is an significant difference between the spectral properties of the impulse signals coming from CM-infested and healthy apples. Moreover, the machine learning classification of the CM-infested and healthy apples was performed based on the features extracted from the acoustic impulse signals. A high accuracy of 97% and a short data collecting time per sample between 60-80 ms (not counting setup/transition time) were obtained. These

findings make the acoustic impulse response test a promising method for the detection of CM infestation post-harvest apple.

5.1 Introduction

Fresh fruits can undergo physical and chemical changes as a result of some internal and external factors including breaching of the structural integrity of the surface (e.g. bruising and pitting) alterations in metabolic reactions and physiological systems (Chapman et al., 1991; Elbashir & Abu-Goukh, 2003), environmental conditions such as temperature and relative humidity (Ueda et al., 2000), and diseases and insect damages (Umeh et al., 2004). As an example, Louzeiro et al. (2020) found that the infestation of fruit flies led to significant changes in firmness, total acidity, total soluble solid (TSS) and weight loss in apples, and mango. Their results showed a remarkable loss of fresh fruit quality after four days of fruit fly infestation. They concluded these changes were due to specific responses to stress caused by puncture, oviposition, and feeding of the larvae.

For apples, the relationship between induced biochemical responses by the fruit to CM larvae attack is not known (Landolt et al., 2000). However, it has been proved that infested apples contain significantly greater amounts of the larval attractant odorant (*E,E*)-α-farnesene, compared to healthy apples (Landolt et al., 2000). Thus, in this study, we tested the hypothesis that the biochemical changes in apples induced by CM larvae cause differences in acoustic parameters of apples which could enhance infestation detection. It is well proven that the mechanical properties of biological tissues~~,~~ depend on the molecular and cellular structure and their physicochemical interactions will change because of insect infestation (Jackman et al., 2007; Waldron et al., 1997). Since the vibrational and acoustic properties of apple fruit depend on the mechanical properties of its tissue, it was taken that the vibrational/acoustic traits of the fruit will change due to the CM infestation damage. Also, the texture of fruits has been reported to be dependent on cellular structure and the way it responds to applied external forces (Costa et al., 2011). Therefore, in this study, a novel test was designed to assess the knock-generated vibration/acoustic signals of the CM-infested apples in response to a pre-defined impulse and this response was compared to the ones from healthy samples. It was expected that the mechanical vibration created by the knocking impulse will attenuate differently through infested texture in comparison to the healthy one. This can lead to the establishment of a relationship between CM infestation in apples and the knock-generated vibration/acoustic response.

In the acoustic impulse response method, the excitation impact generates vibrational acoustic waves which propagate through the sample providing some internal structural information. Most of the works which applied acoustic techniques in agriculture have used the impulse response method for evaluating the quality characteristics of produce and plants such as firmness evaluation and ripeness detection. There are several studies that used the impulse acoustic response method for the detection of internal defects and damage in agricultural commodities (Armstrong et al., 1997; Diezma-Iglesias et al., 2004; Elbatawi, 2008; Rao et al., 2004; Stone et al., 1996). Elbatawi (2008) studied the potential of acoustic impact test to detect and classify hollow heart disorder in potatoes using linear discriminate analysis (LDA) classifier based on the features extracted from the acoustic signal. The peak frequency of hollow potatoes was significantly lower than that of healthy ones. They reported a high classification rate of 98% for detecting the tubers with a hollow heart. In another study, Su et al. (2008) developed a fast method for sorting internal defects in apples using the acoustic impulse response technique. They found a high correlation between the acoustic attributes of the fruit and the decayed area of the defected apples with an R^2 value of 0.99 for Red Fuji and 0.87 for Golden Delicious apples. Impulse response method is reported to have the advantage of simplicity and low equipment cost as well as short detection time, which makes it suitable for fast inline/online applications (Zhang et al., 2018).

Therefore, the objective of the study in this section was to evaluate the potential of the acoustic impulse test for the classification of CM-infested apples by characterizing the high-frequency response signals from the infested and healthy samples.

5.2 Material and Methods

5.2.1 Sample Preparation

Freshly harvested organic Gala apple cultivar were purchased from a commercial market in Princeton, KY, USA in October 2020. Samples were manually inspected to ensure they were defect-free and almost of the same size. The samples were disinfected against fungal and bacterial decay using sodium hypochlorite solution (0.5% v/v) according to Louzeiro et al. (2020). The samples were then rinsed in distilled water and dried naturally in the lab in the Department of Entomology, University of Kentucky, Princeton, KY, USA. To artificially infest the apples, one first instar CM larva was placed near the calyx end of each apple in an isolated cup (8 cm bottom diameter, 10 cm top diameter, 10 cm high) with a porous plastic lid for respiration. The two groups of 60 infested and 30 control samples were stored at ambient storage condition (21 °C± 2 °C and 75 % relative humidity) for three weeks and the acoustic impulse response tests were carried out daily. Four infested and two control apples were randomly selected for each day's tests.

5.2.2 Experimental Set-up and Signal Recordings

A schematic of the acoustic impulse response test is shown in Figure 5.1. It consisted of two main parts: the acoustic recording unit and the impulse or knocking unit. The impulse or knocking test unit consisted of two major components: an impulse generator, and a mechanical support structure (retort stand) to securely hold the apple, impulse generator, and a sensor in repeatable relative positions (Figure 5.1). The support structure was constructed from standard lab metalware. The structure was supported on a single ring-stand with a cast-iron base to minimize resonance (American Educational 7-G15-A). Three-prong gripper was hung from the stand using a 90° bosshead. The outer two grippers are 0-30 mm rubber coated Zinc alloy flask clamps (from Dtacke), which hold the solenoid used to generate the impulse in the bottom gripper and the sensor pickup in the top gripper. The apple is held between them with 10-90 mm rubber-coated three-prong grips as shown in Figure 5.1.

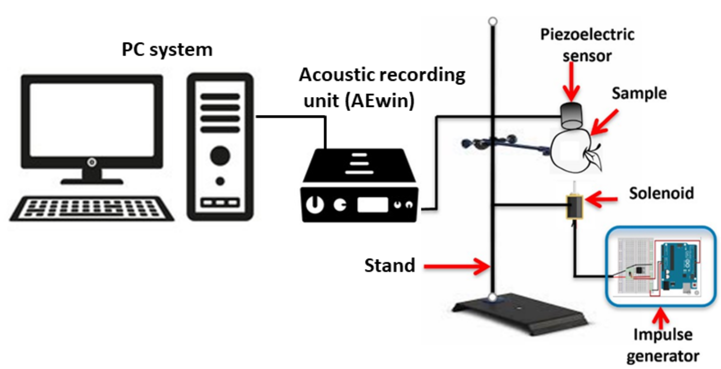

Figure 5.1 Schematic of the acoustic impulse system for data acquisition from apple

To collect data, the apple to be tested was placed between the large central three-prong gripper and secured with its actuating screw. The other two grippers were then adjusted vertically on the rod and laterally in their bosses such that they make firm contact with the top and bottom of the apple. A spacer attached to the end of the solenoid was used so its head could be placed at a consistent distance from the surface of the apple such that the same portion of the stroke was in contact with the apple for each test. This configuration gave the necessary degrees of freedom to consistently accommodate apples with a variety of sizes and shapes while still firmly securing them during the test.

The impulse generator was a solenoid precisely driven by a microcontroller (Apex AGM32F103CB, RobotDyn, Arduino) through an amplifying transistor. The solenoid used was a Guardian Electric model A420-067074-01 (Guardian Electric Manufacturing, Woodstock, Illinois, USA). The solenoid delivered impact through a 6.35 mm radius nose on the armature. The impulse was triggered by a simple push-button, pressed by the experimenter after data capture had been initiated. The input button was connected to the microcontroller and pulled up through the internal resistor. The microcontroller tying the system together is an Apex AGM32F103CB in a “Black Pill” breakout board from RobotDyn, running the Arduino bootloader. It was configured with a simple circuit to make it act as a one-shot pulse generator producing a single 50 μs output pulse on each button press with hold-off to filter any potential switch bounce. The charge 50 μs was chosen as it was adequate to reliably “bottom out” the solenoid's pin to maximum extension against gravity at 9 V. The pulse output from the microcontroller was then driven into the base of a TIP-31c NPN transistor through a 130 Ω resistor, to handle the large current requirement and EMF kick of the solenoid. The solenoid was lower side switched by the transistor. Power for the system was supplied by a commodity 9 V DC “wall wart” power adapter.

The acoustic recording unit was a custom-designed system to record the high-frequency acoustic response signals from apples generated by the impulse/knocking test. This system consisted of a contact piezoelectric sensor (R6α-SNAD 52, Physical Acoustics Corporation, New Jersey, USA) with a frequency range of 35 to 100 kHz, a preamplifier (model1220A, Physical Acoustics Corp., Princeton Junction, N.J.), an I/O board (PCI-2, Physical Acoustics Corp.), and signal processing software (AEwin by MISTRAS).

To reduce the ambient noise, the acoustic impulse response experimental unit was set above an isolated table that had a 15 cm layer of sand, topped with a 5 cm slab of granite with acoustic padding. This unit was in a room with a concrete padded floor built on a 20 cm of gravel above the loam soil bed in an isolated room in Food Engineering lab at the Biosystems and Agricultural Engineering Department, University of Kentucky, Lexington, KY, USA. To carry out each test, an apple was placed between the sensor and the impulse generator (solenoid). Signal recording for each test was performed for 10 seconds with two impulses for each apple sample where the first impulse was generated in 5th second and the second impulse in the 10th second. The acoustic signals derived from the knocking impulse on apples were collected and processed by different signal processing methods and then the correlation between time-domain and frequency-domain features of vibration acoustic signals and sample infestation and quality was established.

5.2.3 Signal Processing and Characterizing

First, all the acoustic impulse signals were preprocessed by manually segmenting the piece of signal which corresponded to the actual impulse response with a length of 60 ms to 80 ms in MATLAB (R2020b, The MathWorks, Inc., Natick, Massachusetts, United States). To characterize and compare the impulse signals from CM-infested and healthy apples, Welch method was used to calculate the power spectral density (PSD) for each impulse signal. Welch's PSD method provides an estimate of the power of a signal at different frequencies as a modified periodogram by first segmenting the signal, calculating the PSD of each segment, and then averaging the spectral densities to reduce the variability. In our implementation, the sampling rate was 100 kHz and the signals had different durations (around 2,000 samples each). To obtain Welch's overlapped segment averaging, the PSD estimate of the signal used a segment length of 2000 samples with 1000 overlapped samples and a hamming window of 4000.

5.2.4 Data Processing and Machine Learning Modeling

After manually segmenting the actual impulse moment from the entire signal, 21 important time and frequency domain features were extracted for the segmented impulse signals as shown in Table 5.1 using a code (APPENDIX) created in MATLAB. Having these features as the variables (columns) for all the sample (as rows), the dataset was built to be used for the machine learning classification. To measure the performance of the classification models, ten-fold cross-validation was used to calculate the average value of accuracy, sensitivity, and the precision for the hold-out datasets.

Table 5.1 Selected time and frequency domain features

No.	Feature Name	Domain Type	Explanation
1	Average signal level	Time	A signal processing technique applied to increase the strength of a signal relative to noise that is obscuring it.
2	Variance	Time	The expectation of the squared deviation of a random variable from its mean.
3	Kurtosis	Time	A measure of the "tiredness" of the probability distribution of a real-valued random variable.
4	Skewness	Time	Distortion or asymmetry in a symmetrical bell curve, or normal distribution, in a set of data.
5	Mean absolute deviation	Time	The average distance between each data point and the mean.
6	Root mean square	Time	The square root of the mean square
7	Entropy	Time	A measure of signal spectral power distribution.
8	Mean rise time	Time	The mean time taken by a signal to change from a specified low value to a specified high value.
9	Absolute energy	Time	The summation of square of signal values.
10	Area under curve	Time	The summation signal values.
11	Signal strength	Time	A measure of the power of signal.
12	Average number of peaks	Time	The mean number of maximum amplitudes.
13	Number zero crossing	Time	the instantaneous point at which there is no frequency present.
14	Number of peaks	Time	The number of maximum amplitudes.
15	Energy spectral density	Frequency	The distribution of the energy of the signal in the frequency domain.
16	Maximum power spectral density	Frequency	The maximum power present in the signal as a function of frequency.
17	Centroid	Frequency	The arithmetic mean position of all the points in the signal.
18	Peak frequency	Frequency	The frequency of maximum power.
19	Power bandwidth	Frequency	The power difference between the upper and lower frequencies in a continuous band of frequencies.
20	Maximum spectral entropy	Frequency	A method of spectral density estimation.
21	Fast Fourier transform mean coefficients	Frequency	The mean of signal values in the frequency domain.

5.3 Results and Discussion

5.3.1 Impulse Response Signal Characterization

The magnitude of PSD for the CM-infested and control apple samples presented as the average over the two classes is shown in Figure 5.2. From the figure, differences between the two classes (CM-infested and control) at specific frequencies can be seen in the peaks of PSD for the samples, which occurred at the initial frequency of 10-50 kHz, then 60 kHz, and 88 kHz. The other less severe peaks are at about 5-10 kHz. However, for all the remaining frequencies, the two classes show no difference. These differences between the control and infested classes proves that CM-infested apples can be detected using the acoustic impulse response test combined with machine learning models.

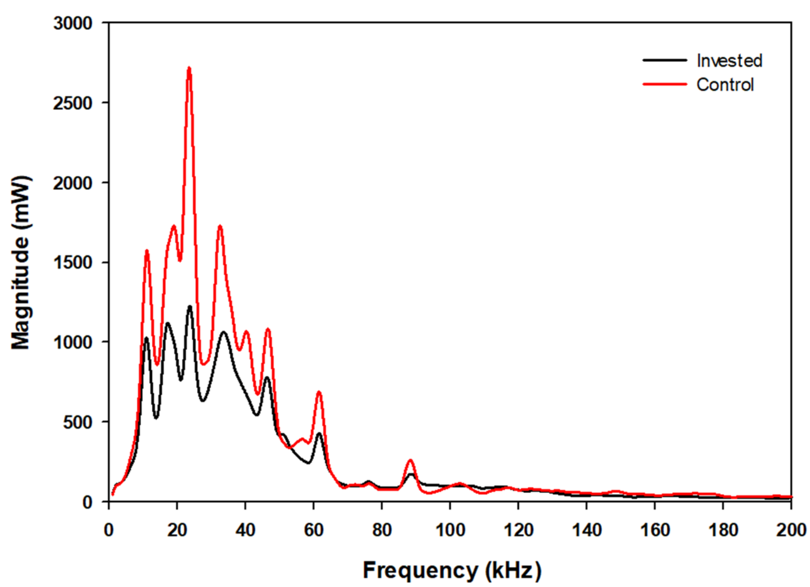

Figure 5.2 PSD of healthy and CM-infested apples

5.3.2 Classification of Impulse Response Signals

Table 5.2 shows the performance of the classifiers for the classification of CM-infested and control apples based on the impulse response signals. As shown in Table 5.2, the highest classification rates were found using AdaBoost ensemble model with 97%, 1%, 96%, 97%, and 97% for accuracy, SD, precision, recall, and F1-score, respectively. Li et al. (2018) reported the same classifier (AdaBoost) for obtaining the best accuracy under a similar set-up. They had applied acoustic emission (AE) method and machine learning to detect CM infestation in apples. The authors collected passive high-frequency (35-100 kHz) data using an ultrasonic contact sensor and performed automatic feature extraction using a commercial signal processing software. From the 11 features obtained, the authors obtained a test-set classification rate of 57-100% using LDA, and 87-100% using ensemble AdaBoosting up to 1 s of signal collection time. The higher classification results achieved by Li et al. (2018) compared to this study could be due to the longer signal length. However, with their shortest signal length (0.5 s), Li et al. (2018) reported an accuracy of 87% which is less than the classification rates (> 90%) achieved in this study in a much shorter signal length (60-80 ms). While a long signal length would likely contain more activities and information, long scanning time is undesirable for industrial applications. Thus, this study offers high improvement as compared to our group's previous study (Li et al., 2018) in terms of shorter scan time which makes the impulse method more amenable to industrial application.

Table 5.2 Classification performance of models based on impulse response signals for classifying control and CM-infested apples

Classifier Model	Accuracy	Standard Deviation	Precision	Recall	F1-score

SVM	64	11	64	65	60
RF	96	2	96	96	96
kNN	68	5	63	62	62
DT	96	2	96	97	97
LDA	96	3	96	93	94
NB	62	10	67	68	62
Ridge	96	3	96	95	96
GB	96	3	96	97	97
QDA	74	5	75	79	73
ET	96	2	96	96	96
AB	97	1	96	97	97

SVM: Support Vector Machine, RF: Random Forest, kNN: k-Nearest Neighbors, DT: decision trees, LDA: Linear Discriminant Analysis, NB: Naïve Bayes, GB: Gradient Boosting, QDA: Quadratic Discriminant Analysis, ET: Extra Trees, AB: Ada Boost, SD

5.4 Conclusion

In this study, the feasibility of using the acoustic impulse response test in the detection and characterization of the high-frequency signals from the CM-infested apples was investigated. Overall, the signal analysis revealed a strong correlation between the CM infestation in apples and the acoustic properties and affirmed the potential for real application in nondestructive sorting of apples. Significant differences between the CM-infested and control apples were shown using the magnitude of PSD. This proved the feasibility of CM infestation detection using the impulse response method. Moreover, some machine learning classifiers were built based on the extracted features from the impulse response signals to classify the CM-infested apples. All classifiers used performed well for the dataset generated using acoustic impulse response signals, except Naïve bayes, and SVM. While the accuracies were higher than 90% in most cases, the best classifier was AdaBoost with an accuracy of 97%. The outcome of this study proved the potential of applying acoustic impulse method for nondestructive detection of CM-infested apples.

CONNECTING STATEMENT

In previous Chapters, the vibro-acoustic and acoustic impulse methods were used for the nondestructive detection and classification of CM-infested apples. While the acoustic methods used in this study were promising in the problem of detection of CM-infested apples, there are some situations where these methods cannot provide desired information. For example, the external symptoms like CM frass and eggs, and the color (chemical) changes in apple tissue due to the infestation cannot be detected using the acoustic methods. Therefore, in chapter 6, the HSI method will be investigated and discussed for the nondestructive detection of CM infestation in apples. For this purpose, two techniques of the mean spectra extraction for the whole fruit and the pixel-based classification of the CM infestation on apples will be evaluated and compared. Chapter 6 is based on our published paper as "Ekramirad N, Khaled AY, Doyle LE, Loeb JR, Donohue KD, Villanueva RT, Adedeji AA. Nondestructive Detection of Codling Moth Infestation in Apples Using Pixel-Based NIR Hyperspectral Imaging with Machine Learning and Feature Selection. Foods. 2022; 11(1): 8. https://doi.org/10.3390/foods11010008".

CHAPTER 6. OBJECTIVE FOUR

NONDESTRUCTIVE DETECTION OF CODLING MOTH INFESTATION IN APPLES USING PIXEL-BASED NIR HYPERSPECTRAL IMAGING WITH MACHINE LEARNING AND FEATURE EXTRACTION

Abstract:

Codling moth (CM) (*Cydia pomonella* (L.)), a devastating pest, creates a serious issue for apple production and marketing in apple-producing countries. Therefore, effective nondestructive early detection of external and internal defects in CM-infested apples could remarkably prevent postharvest losses and improve the quality of the final product. In this study, near-infrared (NIR) hyperspectral reflectance imaging in the wavelength range of 900–1700 nm was applied to detect CM infestation at the pixel level for Gala, Fuji and Granny Smith organic apple cultivars. An effective region of interest (ROI) acquisition procedure along with different machine learning and data processing methods were used to build robust and high accuracy classification models. Optimal wavelength selection was implemented using sequential stepwise selection methods to build multispectral imaging models for fast and effective classification purposes. The results showed that the infested and healthy samples were classified at pixel level with up to 97.4% total accuracy for validation dataset using a gradient tree boosting (GTB) ensemble classifier, among others. The feature selection algorithm obtained a maximum accuracy of 91.6% with only 22 selected wavelengths. These findings indicate the high

potential of NIR hyperspectral imaging (HSI) in detecting and classifying latent CM infestation in apples of different cultivars.

6.1 Introduction

Apples are a very important fruit in the global produce market and industry. The United States of America is the second largest producer of apples, producing about 4.5 million tons of apples in 2020 (Economic Research Center USDA, 2020), exporting 1 out of 3 apples grown, and averaging $1 billion annually on apple exports (USApple association, 2018). Additionally, apples are the most consumed fruit in the US, with the market value of about $5 billion in 2018 (USApple association, 2018). Because apple marketing is such a big business worldwide, preserving their quality to meet the ever increasing demands of consumers is essential. Codling moth (CM) *Cydia pomonella* (Lepidoptera: Tortricidae) is known to be the most devastating pest that infects apples (Kadoić Balaško et al., 2020; Pajač et al., 2011). It causes direct damage to the fruit's skin and pulp. CM is known to infest pome fruits, with a special preference for apples in almost every country the fruit is grown (Kadoić Balaško et al., 2020). This larva enters the apple by feeding through the skin of the fruit, burrowing into the fruit's core to cause major damage (Pajač et al., 2011). If untreated, CM can result in up to a 50% loss in pre- and post-harvest apples (Kadoić Balaško et al., 2020). Furthermore, production will only tolerate 1% of affected fruit (Pajač et al., 2011), where if any apple infestation is found in some of the US' top importing countries, the whole shipment is rejected (Walker et al., 2013). Detection of infestation, therefore, is very critical but the current manual random methods are inefficient.

Presently, apple quality assessment, including testing for possible insect infestation, is done at random, manually, and in a destructive manner. When assessing apples for packaging, inspectors visually examine the external qualities, scoring the apple surface to comply with certain specifications and tolerances for defects. To determine the internal quality, apples are cut in half to visually inspect their cross-sectional areas (Lu, 2017). After testing, the used apples are discarded, wasting about three percent of the product (2017 USDA Annual Report). In this way, detection of infestation is time-consuming, costly, subjective, and laborious, and yet does not assure that the batch will be pest free. Currently, machine vision has been implemented to monitor the outside of the apple at low-cost and rapid speed, but issues arise in interference of the sample's color and the presence of stem and calyx (Fan et al., 2020), coupled with the inability to inspect the internal qualities of the apple where most pest infestation damage resides. To correct this issue and increase detection efficiency, a better method is needed to identify both internal and external damages to apples by a pest such as CM.

Whereas current techniques are very wasteful, nondestructive techniques preserve the fruit, give a definitive result, and can easily look at the whole batch to ensure no bad apple gets through to the supply chain. Using forms of nondestructive testing to assess certain qualities of apples is not new. Some of the nondestructive techniques used on apples include hyperspectral imaging (HSI) (Tian et al., 2020; Zhang et al., 2019), vibro-acoustic signaling (Ekramirad et al., 2020; Fathizadeh et al., 2020), ultrasonic acoustic detection (Vasighi-Shojae et al., 2018), delta absorbance meter (Cocetta et al., 2017), machine vision (Gongal et al., 2016; Silwal et al., 2014), and spectroscopy (Ma et al., 2021; Tian et al., 2020). Each technique has its advantages and disadvantages; however, the one that stands out is HSI because of the unique method of application and degree of accuracy.

While some of these techniques have been used to detect and classify infested apples, such as the work done with acoustic emissions (Li et al., 2018) and vibro-acoustic signaling (Ekramirad et al., 2020), HSI is ideal because it conveys additional useful information for nondestructive applications. HSI combines the capability of spectroscopy and machine vision techniques. Spectroscopy is used to create a spectrum of data based on light absorbance at different wavelengths (Qu et al., 2015; Sun, 2010). This is useful in finding specific chemical components but lacks a sense of location or direction since the device scans at a single point (Craig et al., 2013; Li & Church, 2014). Additionally, machine vision converts photographic scanning of 3D objects into 2D images by capturing and documenting the reflected light into grayscale and RGB color (Sonka et al., 2014). Machine vision is great at scanning objects quickly and acquiring a sense of location, allowing for analysis of spatial qualities such as size, shape, and color (Delia Lorente et al., 2012; J. Ma et al., 2016). However, it only looks at the surface of the object in primary color (Sun, 2010). HSI uses the best parts of both techniques, looking at the reflectance at every point of the image showing a spectrum of reflectance for each pixel in the spatial image while still retaining the analytical benefits of the two techniques (Baohua Zhang et al., 2015). Each hyperspectral image is a three-dimensional data cube (3D hypercube) with X and Y coordinates as the spatial information and λ as the spectral data. HSI not only has the capability to detect infestation on and in the sample under test, but also is used to find the exact location of infestation due to the spatial information and the ability to evaluate the different levels of pixels in the images (Peerbhay et al., 2015; Wu et al., 2016).

HSI has been investigated as a rapid and relatively low-cost nondestructive technique in the quality assessment of apples. This application mainly falls into three categories including external quality, internal quality, and pest detection (Ekramirad et al., 2021). Regarding external quality of apples, HSI was used to evaluate defects (e.g., surface defects and bruising) because of its ability to penetrate beneath the apple's skin. For example, bruises on apples are detectable in the range of shortwave-near-infrared (SNIR), particularly around 675 nm and 960 nm, which represent the region for carotenoids, chlorophyll pigments, sugar, and water content (ElMasry et al., 2008). This reveals that the bruise on the apple causes large imbibition of water and total sugar contents at the early stage of bruising, and then causes assimilation of chlorophyll pigments and carotenoids in the subsequent stage (Wang et al., 2007). Thus, the application of HSI to detect bruises on apples can reduce or prevent further losses from cross-contamination of others by damaged apples. HSI also has been used for nondestructive prediction of internal quality of apples such as the nutritional value, texture, and flavor components, and in estimating physiochemical parameters such as vitamin and sugar content (Lu et al., 2017). Additionally, HSI has been tested for safety assurance of apples through effective detection of pests (Ekramirad et al., 2021; Rady et al., 2017). In 2021, Ekramirad et al. (2021) determined the best classification result for CM detection in apples using NIR HSI and the mean spectra extraction method on dataset consisting of three apple orientations (calyx, sides and bottom). Applying partial least squares-discriminant analysis (PLS-DA) classifier, they obtained an overall validation accuracy of 81.04%. While the calyx and side orientations had similar classification rates of about 80%, the stem orientation gave the lowest classification accuracies. These results are better than the findings of Rady et al. (2017) who achieved a maximum classification rate of 74% using the side orientation of apples, using all the spectral wavelengths in the Vis-NIR range. However, they reported that by reducing the data dimensions using the sequential forward selection method, their classification accuracy was enhanced to 82%. In the same study conducted by Ekramirad et al. (2021), they applied a second pixel-wise method instead of the mean spectra extraction and found an accuracy as high as 98.2% in classifying the infested and healthy pixels using the random forest (RF) classifier. However, they had manually segmented a rectangular ROI around the calyx end of the apple sample to extract pixels data by spectra for infested and healthy, which is a cumbersome subjective task that increases the processing time. Hence there is a need to develop a new method for automatic extraction of target pixels. Additionally challenges to be considered in developing an automatic algorithm based on HSI for the classification of CM-infested apples include the following. First, since the shape and size of ROI in HSI affect the measurement performance (Guo et al., 2014), a proper geometry should be selected for the ROI. Second, the infested region should be well localized for accurate labeling as an infested class. Therefore, to address these issues a special procedure was developed in this study to automatically extract pixel-wise ROI around the calyx of the apples, which is the usual point of entry for the CM larvae.

Normally, HSI technique produces large spectral data and for this, its analysis is associated with the utilization of mathematical or statistical methods to make it readable and to discover useful information about the data. However, such analyses are time consuming because of the large size of the datasets. In computational intelligence methods, dimension reduction is often used to optimize data processing time, reduce dimensionality, and enhance data generalization (Khaled et al., 2021; Khaled et al., 2018). Principal component analysis (PCA) is the main dimensional reduction step used for hyperspectral data to transform its spectra into some independent features. Moreover, some approaches have been developed to optimize the HSI to perform real-time hyperspectral data reduction using the extraction of predefined features (Firtha, 2007; Firtha et al., 2008). This is carried out by real-time multiplication of the acquired spectral data by a feature extraction operator (vector-to-scaler) consisting of the desired features (less than ten as opposed to >100 spectral features in the hypercube) predefined by experiment. The optimal feature extraction operators are usually obtained by mathematical and statistical methods, such as that applied in PCA. Some of the most frequently used classification methods include k-nearest neighbor (kNN), Linear discriminant analysis (LDA), Quadratic discriminant analysis (QDA), and Naïve Bayes (NB) (Khaled et al., 2018). In addition, PLS-DA has been proven in many studies to be a powerful classification method for HSI data analysis with high-dimensional data (Feng & Sun, 2012). Additionally, the ensemble methods such as RF and gradient tree boosting (GTB) can integrate weak classifiers to achieve powerful anti-noise classifiers (Che et al., 2018).

While HSI has been widely applied for quality assessment of agricultural products, there is no report on the application of NIR hyperspectral imaging combined with feature selection algorithm and various machine learning algorithms to detect CM latent infestation in apples. The infestation of plant tissue by pests can induce different defense mechanisms, such as hypersensitive reactions, production of metabolites and proteins, and altered plant tissue structure, leading to various reflectance spectral signatures that can be measured and localized by spectral imaging methods (Žibrat et al., 2021). Thus, the main objective of the current work was to develop and validate a robust model for the accurate detection of latent CM infestation in apples based on the NIR HSI technique. The specific objectives were to: (1) develop an automatic procedure for pixel-based extraction of infestation region on apple to address the issues related to manual segmentation of the infested area, (2) compare the results of the classification method for three major apple cultivars: Fuji, Gala, and Granny Smith, and (3) select some optimal wavebands for reducing the dimensions of the large scale HSI data leading to a multispectral imaging system.

6.2 Materials and Methods

6.2.1 Sample Preparation

The apple samples used in the experiment were USDA-certified organic Gala, Fuji, and Granny Smith cultivars purchased from a commercial market in Princeton, KY, USA in October 2020. After careful inspection, 60 sample apples similar in size, diameter, and shape, and without infestation or mechanical damage, were chosen from each cultivar. The apples were then disinfected against fungal and bacterial decay by washing in a 0.5% (*v*/*v*) sodium hypochlorite solution (Louzeiro et al., 2020). The samples were rinsed with distilled water and dried in open air at ambient conditions in the laboratory (Department of Entomology, University of Kentucky, Princeton, KY, USA). To artificially infest the apples, newly hatched neonate of CM larva was placed near the calyx end of each apple in an isolated cup (8 cm bottom diameter, 10 cm top diameter, 10 cm high) with a plastic lid. Apples of each cultivar were divided into 20 control and 40 infested groups and stored in an environmental control chamber at 27 °C and 85% relative humidity for three weeks to cause infestation to occur. The hyperspectral data acquisition was carried out in the Food

Engineering lab at Biosystems and Agricultural Engineering Department, University of Kentucky, Lexington, KY, USA.

6.2.2. HSI System and Image Acquisition

A HSI system based on shortwave near-infrared (NIR) bands was used to acquire the hyperspectral data of all apple samples—control and infested (Figure 6.1). The HSI system consisted of a NIR spectrograph with a wavelength range from 900 nm to 1700 nm and a spectral resolution of 3 nm (N17E, Specim, Oulu, Finland), a moving stage driven by a stepping motor (MRC-999-031, Middleton Spectral Vision, Middleton, WI, USA), a 150 W halogen lamp (A20800, Schott, Southbridge, MA, USA), an InGaAs camera (Goldeye infrared camera: G-032, Allied Vision, Stradtroda, Germany) mounted perpendicular to the sample stage and a computer with data acquisition and analysis software (FastFrame™ Acquisition Software, Middleton Spectral Vision com., Middleton, WI, USA). Three scanning orientations of the stem, calyx, and side of each apple were captured during hyperspectral image acquisition. To acquire clear images, the parameters of the sample stage speed, the exposure time of the camera, the halogen lamp angle, and the vertical distance between the lens and the sample were set to 10 mms^{-1}, 40 ms. 45°, and 25 cm, respectively. Samples were placed on the sample stage and captured in a line scanning or pushbroom mode. The acquired hyperspectral images contained 256 wavelength bands stored as "*.raw" file along with a header file as "*.hdr".

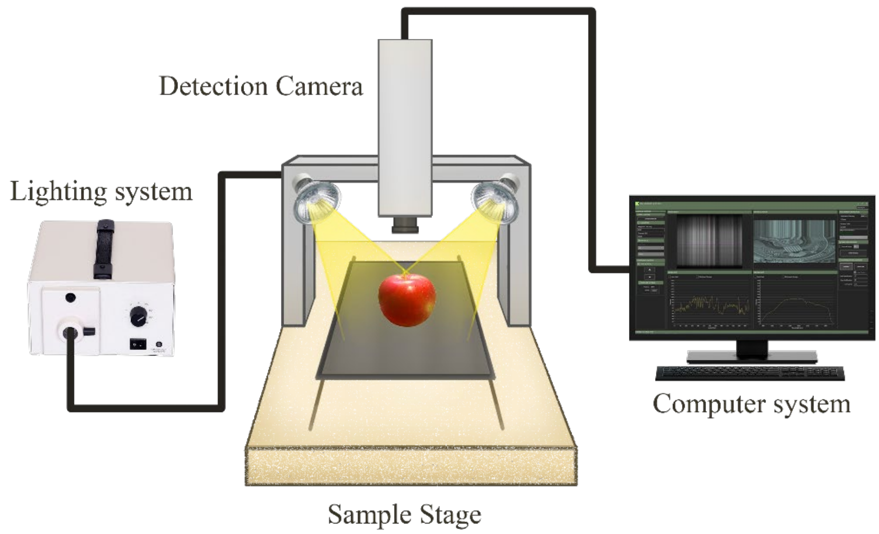

Figure 6.1 Schematic of the hyperspectral imaging system (Ekramirad et al., 2022).

6.2.3. Preprocessing of Hyperspectral Images

6.2.3.1. Image Calibration

Image callibration is needed to correct the acquired raw images with the white and dark reference images to eliminate the influence of illumination and dark current of the camera. The reference image data were obtained after the samples were scanned every day. The dark reference images were obtained by completely covering the lens of the HSI system while turning off the lights. The white reference images were acquired using a polytetrafluoroethylene (PTFE) Teflon plate of 99% reflectivity and 10 mm thickness placed on the black sample stage. The calibration was done based on the following equation:

$$R = \frac{R_0 - R_d}{R_w - R_d} \tag{6.1}$$

where R_0 is the raw hyperspectral image, R_d is the dark image, and R_w is the white reflectance image (Sun et al., 2018).

6.2.3.2. Infestation Region Acquisition

After the acquisition and correction of the hyperspectral images, the spectral information of the infested and healthy tissue was automatically extracted from ROIs using the algorithm described in Figure 6.2. Since the CM larvae, especially the first generation, mostly enter apples from the calyx end (Susič et al., 2020) and the initial results by Ekramirad et al. (2021) showed that the highest infestation classification accuracy was achieved in images from the calyx view, the ROI to extract infested pixels was segmented around the calyx end. This novel method can select the complete infested region, with pixels in the healthy region as few as possible, to obtain a precise infested region for subsequent classification. To do this, first the background and calyx end were segmented out using the image at 1084 nm wavelength to obtain a masked image in a binary image format using a binary thresholding method. To obtain a solid area around the calyx, the morphological image processing of erosion operation was applied. Then, the center of the calyx area was localized using mathematical operations to calculate the centroid of the eroded area. Finally, having the orientations of the center of the calyx area, a circular region with 50 pixels diameter was drawn as a mask binary region. The circular ROI fits with the spherical shape of apple fruit and it has been shown that a round ROI gave higher accuracy and predictive capability than square ROI in HSI on apples (Khaled et al., 2020). Then, the circular masked image was applied on each image of the hypercube (i.e., all the 256 wavebands) to obtain the calyx area with other pixels equal to zero. The spectrum for each pixel in the circular ROI was then extracted and unfolded and labeled for building the dataset to develop machine learning models.

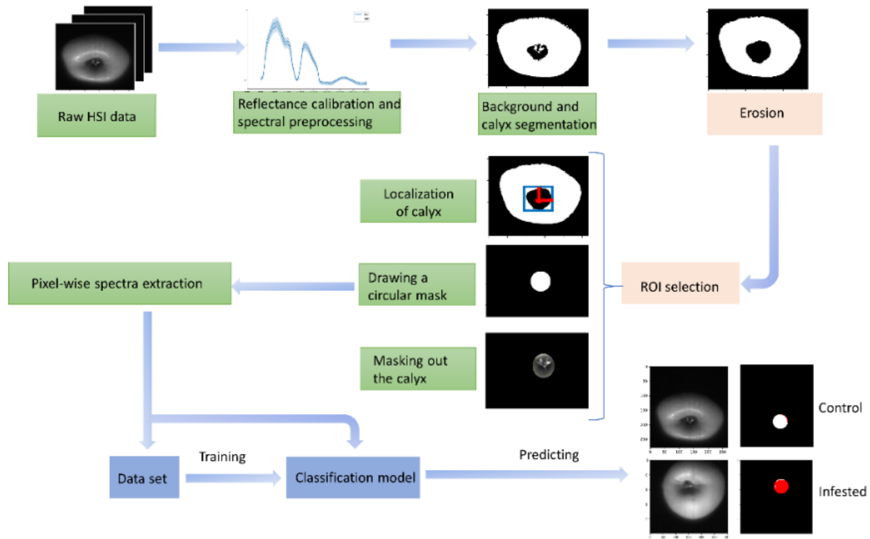

Figure 6.2 Flowchart of apple infestation area acquisition around calyx end for building the classification model (Ekramirad et al., 2022).

6.2.3.3. Spectral Extraction and Preprocessing

To obtain the spectral characteristics of apples, the spectrum for each pixel inside the ROI was extracted in the form of reflectance intensity versus wavelength and then labeled as either infested or healthy spectral signature. After spectral data extraction, pre-processing was carried out by wavelength trimming, maximum normalization, a Savitzky-Golay smoothing filter, and mean centering to remove the noisy wavelengths at the edges of each spectrum, to get all data to the same scale, to account for particle size scattering and path length difference effects, and to keep only significant features, respectively. The maximum normalization was carried out by dividing each spectrum by the maximum value (Keresztes et al., 2016). The Savitzky-Golay method involves the application of the second-order polynomial and the filter window length of 31.

6.2.3.4. Dimensionality Reduction

With respect to data architecture in HSI, high dimensional images with fixed training sample size can result in overfitting problems leading to degraded classification rates. It is usually the case when the size of training samples is limited in comparison to the feature space size resulting in low generalization of the results and overfitting problems (Plaza et al., 2009). The higher the dimensionality of the model, the higher the likelihood of over-fitting. Therefore, hyperspectral data size compression, especially spectral dimensionality reduction, is usually required to achieve better data visualization, save storage space, eliminate redundant data, and avoid model over-fitting. Principal component analysis (PCA) was used in this study as the dimensionality reduction technique. PCA is a transformation of the data through an axis rotation, in the direction of maximum variance. Successive principal components (PCs) are the linear combinations of the variables with maximum variance, which are orthogonal to the previously computed components. The total variance can be represented in a significantly small number of components (extracted features). The PCs are the eigenvectors of the covariance matrix of the data, and the associated variance is represented in the corresponding eigenvalues. The PCs are orthogonal and have successively ordered variances. PCA transforms multivariate data into a new coordinate system to produce new uncorrelated orthogonal variables which are called PCs or loadings. These PCs are arranged according to their eigenvalues, with the 1st PC having the highest variance, the 2nd PC containing the highest residual variance, and so on (Abdi & Williams, 2010). As most of the information is included in the first PCs, eliminating PCs with a small variance will remove unnecessary information. The advantages of this technique over nonlinear dimensionality reduction techniques include being easy to apply, invertible, and volume-preserving transformation.

6.2.3.5. Spectral Variable Selection

Acquired data from HSI systems usually have high dimensions both spatially and in spectral form. These data contain highly correlated continuous wavelengths with a lot of redundancy resulting in high complexity and computation costs. Feature selection methods through selecting optimal wavelengths can provide the informative wavelengths to build fast and simpler multispectral imaging models. In this study, the optimal wavelength selection was conducted using the sequential stepwise selection method. In this method, which is a wrapper method, a specific machine learning classifier is fitted to the dataset. It acts as a greedy search approach through evaluating all the possible combinations of features against the evaluation criterionsuch as accuracy, precision, sensitivity, etc. Finally, it selects the combination of optimum features that gives the best results for the specified machine learning algorithm.

6.2.4. Development of Machine Learning Classifiers

Having the spectral data for healthy and infested pixels from all the samples, the labeled dataset was built by organizing pixels (observations) as rows, and the features (spectral data) as columns. The predictor variables (features) are the spectral data while the dependent variables are the classes, namely control and infested. After building the dataset, Kennard & Stones algorithm was implemented to split 70% of the data as the training and 30% as the validation datasets. The Kennard & Stones method has been widely used in chemometrics and spectroscopy, and it has been proven to give good performance in separating spectral data into training and test sets (Nawar & Mouazen, 2018). Different machine learning classification algorithms including Linear discriminant analysis (LDA), k-Nearest Neighbors (kNN), PLS-DA, and two ensemble methods, namely Random forest (RF) and GTB, were performed and compared for their classification accuracies. For evaluating the performance of the various models in this study, five-fold cross-validation was used. The metrics used for assessing the classification performance of the models included precision, recall, and the F1-score. Precision is the positive predicted value and quantifies the correctly classified pixels as infested (the fraction of true positives out of all positive predictions whether true positive or false positive). While precision gives a quantitative measure of how exact the classifier's prediction is, recall (or sensitivity) helps avoid missing any undetected infested samples. Recall is the true positive rate that relates to the number of pixels belonging to the infested area that were predicted as positive (true positive) and those that the model incorrectly does not capture as infested (false negative). F1-score is the harmonic mean of recall (R) and precision (P), calculated as: $F1 = 2RP/(R + P)$, reflecting the balance between the classifier's precision and recall (Garillos-Manliguez & Chiang, 2021). The F1-score can be used to evaluate the entire model, considering both the precision and recall, making it a sensitive metric to changes in the data distribution and ratios.

All algorithms used in this study for pre-processing and data analysis and post-processing were performed on Python 3.7 (Python Software Foundation, https://www.python.org/ (accessed on 15/10/2021)) platform and in Jupyter Editor Notebook. The open-source libraries of spectral, Numpy, Scikit-learning, and Matplotlib were used in this work.

6.3 Results and Discussion

6.3.1. Spectral Analysis

Figure 6.3 shows the typical mean spectra for healthy and infested apple samples as normalized reflectance versus wavelength. While the average spectra of the control and the infested samples have a similar trend and curve variation tendency, the reflectance of the healthy samples is remarkably higher than the one for the infested samples (or the absorbance of the infested samples are higher than the healthy ones). Thus, this NIR reflectance difference for healthy and infested samples shows the potential to be applied for the binary classification. As reported by several authors (Munera et al., 2021; Zhang et al., 2015), the absorbance of defective samples was higher than the healthy ones due to the cellular structure difference. As a result of plant tissue infestation, there will be biochemical, tissue structure, and pigment composition changes leading to the different spectral signatures (Susič et al., 2020).

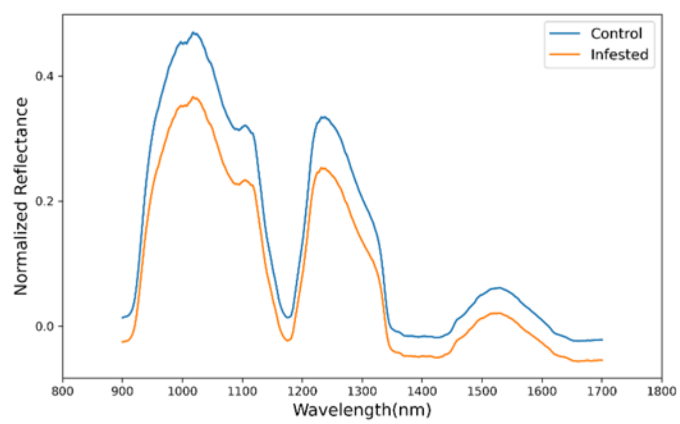

Figure 6.3 Mean reflectance spectra of control and CM-infested samples acquired by NIR HSI.

As shown in Figure 6.3, there are some distinct absorption valleys around 950, 1200, and 1400 nm in the mean spectra of both sample classes. The absorption at about

950 and 1200 nm relates to the first overtones of O-H band in water molecules (Ghosh & Jaya, 2009). The absorption at around 1400 nm is attributed to the combination of the second overtone of C-H and the first overtone of O-H (Zhang et al., 2019). The spectral curve of samples in this study agrees with the finding of other studies on apples in the same spectral range (Zhang et al., 2019).

6.3.2. Pre-processing and Feature Extraction Results

For classification of infested samples of the three different cultivars of apples, PCA was performed on the preprocessed spectra before building the classification models. Results showed that the sum of the variance explained by the first three PCs for all the cultivars was more than 98% of the total variance. It means the sum of the accumulative contribution rate of the first three PCs represents 98% of the total variability of the spectral data, so it could be a reasonable way to recognize patterns in the tested samples using these limited number of PCs. As shown in Figure 6.4, the control and infested samples were well clustered with some minor overlaps between them. Moreover, PCA score values for infested apples were tightly clustered over the two first PCs space, while scores for control fruits were more widely scattered. Therefore, the machine learning models for classification of apples were built using the extracted PCs as features. Moscetti et al. (2015) reported similar PCA score plot trends for non-infested and infested olive fruits using the NIR spectroscopy for the mean spectra of the whole fruit where the first two PCs accounted for 98.3% of the total variance. They used the pre-processing steps of multiplicative scatter correction, a Savitzky-Golay smoothing filter, and mean centering followed by PCA dimensionally reduction and LDA, QDA, and kNN classification. Additionally, the results of Keresztes et al. (2016) for pixel-based apple bruise detection using shortwave infrared HSI showed that the three first PCs represented 98.36%, 1.24%, and 0.15% of the total variance in the data. They also used the pre-processing methods of multiplicative scatter correction, Savitzky-Golay smoothing, and mean centering before PCA dimensionally reduction followed by PLS-DA classification.

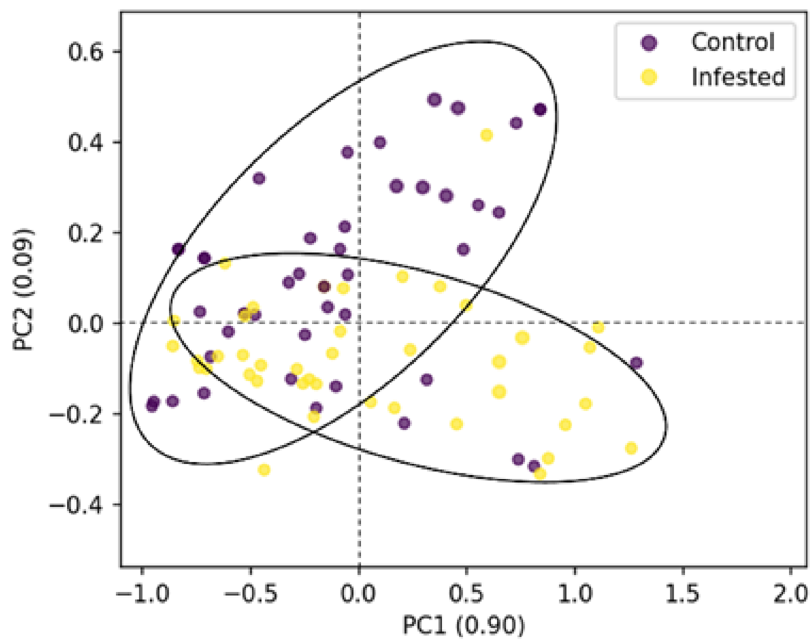

Figure 6.4 Principal component analysis of two types of apple sample tissues for Fuji cultivar computed from the mean spectral of the whole fruit.

Table 6.1 Results of the PCA-based classification of control and infested samples for training and validation sets based on mean spectra for each sample.

Sample Orientation	Classifier [1]	Training Set (%)			Validation Set (%)		
		Precision	Recall	Total Accuracy	Precision	Recall	Total Accuracy
Stem	LDA	95.00	94.00	94.70	57.00	58.00	62.50
	kNN	58.00	57.00	57.90	36.00	42.00	62.50
	RF	**100**	**100**	**100**	**83.00**	**92.00**	**87.50**
	AdaBoost	95.00	95.00	94.70	75.00	83.00	75.00
	PLS-DA	**100**	**100**	**100**	**83.00**	**92.00**	**87.50**
Calyx	LDA	90.00	90.00	90.50	78.00	78.00	77.80
	kNN	63.00	61.00	61.90	68.00	68.00	67.00
	RF	100	100	100	88.00	83.00	83.30
	AdaBoost	**100**	**100**	**100**	**92.00**	**88.00**	**88.90**
	PLS-DA	90.00	90.00	90.50	78.00	78.00	78.00
Side	LDA	100	100	100	83.00	80.00	77.80
	kNN	86.00	80.00	80.00	75.00	60.00	55.60
	RF	100	100	100	83.00	80.00	77.80
	AdaBoost	100	100	100	83.00	80.00	77.80
	PLS-DA	**100**	**100**	**100**	**90.00**	**90.00**	**88.90**
All	LDA	80.00	80.00	79.00	71.00	73.00	72.00
	kNN	76.00	76.00	76.30	70.00	71.00	72.00
	RF	100	100	100	91.00	94.00	92.00
	AdaBoost	100	100	100	88.00	91.00	88.00
	PLS-DA	**98.00**	**98.00**	**98.00**	**91.00**	**94.00**	**92.00**

1 LDA: Linear Discriminant Analysis, kNN: k-Nearest Neighbors, RF: Random Forest, **PLS-DA**: Partial Least Squares-Discriminant Analysis. Bolded line indicates the best result.

6.3.3. Results of Machine Learning Classification

In order to compare the results of different approaches for classification of apple samples, classification results of the three approaches are presented in this section. Table 6.1 provides the classification results of infested and healthy Fuji apples using the mean spectra extraction method and for three orientations of stem, calyx, and side of apple along with the data for all the orientations together. In this method the reflectance spectrum for each pixel was extracted and then the average of all the pixels were calculated as the mean reflectance spectra for that sample. As shown in Table 6.1, the best classification result for the mean spectra extraction method was achieved using the data for all the orientations of apples and by PLS-DA and RF classifiers, with a validation accuracy of 92%. While the calyx and side orientations had similar classification rates of 88.9%, the stem orientation gave the lowest classification accuracies. These results are better than the findings of Rady et al. (2017) who achieved a maximum classification rate of 74% using the mean reflectance spectra from Vis-NIR hyperspectral images of the side views of apples.

In the second approach, pixels from infested apples were localized and segmented manually using a 10 × 10 rectangular ROI around calyx end of samples. To do this, the ROI were selected in the images and the spectrum of each pixel in the ROI was extracted. Thus, a total of 100 spectra for each infested or control apple were extracted and labeled to build the classification dataset. Table 6.2 shows the classification results for the control and infested pixels in apples using the manual ROI selection method. The result gave a good performance with the accuracy of up to 99.24% for the ensemble classifiers. These findings are in good agreement with those of Munera et al. (2020) who reported an overall accuracy of up to 97.5% in classifying the healthy and defective pixels in hyperspectral images of loquat fruits using the manual ROI selection method.

Table 6.2 Results of the PCA-based classification of control and infested samples for training and validation data sets based on manually selected ROI.

Classifier [1]	Training Set (%)			Validation Set (%)		
	Precision	Recall	Total Accuracy	Precision	Recall	Total Accuracy
LDA	72.20	79.20	75.24	71.60	78.40	74.64
kNN	100	99.20	99.52	99.60	98.80	99.06
RF	100	100	100	99.20	99.60	99.24
AdaBoost	100	100	100	98.00	98.4	98.20
PLS-DA	84.60	88.80	86.40	80.60	82.60	80.18

1 LDA: Linear Discriminant Analysis, kNN: k-Nearest Neighbors, RF: Random Forest, PLS-DA: Partial Least Squares- Discriminant Analysis.

6.3.4. Performance of Classification Models Based on Apple Cultivar

The detailed performance of different models for classification of CM-infested and healthy samples of Gala, Fuji, and Granny Smith apple cultivars using the automatic pixel-based method developed and implemented in this study is shown in Table 6.3. All the classifiers gave higher results using the PCs as the input variables except for LDA and PLS-DA, which gave slightly better classification rates using raw data without dimensionality reduction. The GTB ensemble method yielded the highest classification rates for all three cultivars, reaching as high as 97.4% accuracy of the validation set for Fuji apples. Similar classification rates were achieved by Saranwong et al. (2011) using HSI in the range of 400–1000 nm in reflectance mode to assess fruit fly larvae infestation in mango. Using a discriminant analysis classifier, they obtained a validation classification rate of up to 99.1% and 94.3% for infested and healthy fruits, respectively. Haff et al. (2013) also researched the same insect in mango using the same method and the classification rates reached 99% for infested samples. While they achieved a high classification rate in both studies, they artificially created pores on the fruit in a grid pattern to expose the fruit to the pest insects to have a priori knowledge of the locations of infestation. Then they extracted the spectra from the pore locations and compared them with the spectra from healthy areas to identify the spots generated in hyperspectral images of mangoes infested with fruit fly larvae. They reported that classifying the samples that were deliberately infested following a predefined pattern, and the algorithm relying on that pattern in the images would be useless in real-world applications. In a similar study to our current research, Rady et al. (2017) studied the ability of Vis-NIR HSI (400–900 nm) in the reflectance mode for the detection and classification of CM infestation in GoldRush apples. Their best classification rates were obtained using decision trees at five selected wavelengths with an overall classification rate of 82%. Their relatively low classification rate can be related to the limited spectral range used to detect internal and invisible defects in samples. Moreover, they used the traditional image processing-based method combined with the mean spectral extraction for the whole sample. Thus, the broader spectral range as well as the pixel-based method for extracting the spectral signature of infested regions could be the reason behind the higher classification rates in the current study. In another study on apples for a different application, Che et al. (2018) used pixel-based Vis-NIR HSI to classify bruised Fuji fruits. They also reached their best accuracy of 99.90% with the ensemble method.

Table 6.3 Classification accuracy (%) for validation data set based on automatically selected pixels for three apple cultivars.

Classifier	Raw Data (no Dimensionality Reduction)				PCA-Based			
	Gala	**Granny Smith**	**Fuji**	**All**	**Gala**	**Granny Smith**	**Fuji**	**All**
LDA	65.38 ± 0.62	72.24 ± 0.23	70.46 ± 0.72	69.22 ± 0.10	65.38 ± 0.62	70.38 ± 0.17	66.94 ± 0.33	68.70 ± 0.14
SVM	80.18 ± 0.06	76.42 ± 0.17	81.40 ± 0.44	72.54 ± 0.36	82.60 ± 0.70	77.20 ± 0.18	81.62 ± 0.33	73.84 ± 0.39
kNN	93.72 ± 0.19	93.26 ± 0.15	95.46 ± 0.32	89.12 ± 0.12	93.80 ± 0.15	93.30 ± 0.07	95.69 ± 0.26	88.84 ± 0.11
RF	89.66 ± 0.19	89.04 ± 0.18	91.52 ± 0.27	82.82 ± 0.14	94.28 ± 0.31	93.22 ± 0.25	96.62 ± 0.13	89.74 ± 0.13
GTB	92.32 ± 0.37	91.00 ± 0.25	94.68 ± 0.39	84.66 ± 0.18	94.76 ± 0.16	93.66 ± 0.18	97.36 ± 0.28	90.00 ± 0.23
PLS-DA	62.76 ± 0.66	71.64 ± 0.24	68.56 ± 0.15	69.14 ± 0.15	62.76 ± 0.66	71.34 ± 0.16	66.92 ± 0.35	68.72 ± 0.16

PCA: principal component analysis, LDA: Linear Discriminant Analysis, SVM: support vector machine, kNN: k-Nearest Neighbors, RF: Random Forest, GTB: Gradient tree boosting, PLS-DA: Partial Least Squares- Discriminant Analysis.

Table 6.4 summarizes some important performance evaluation indices for the best classifier (GTB) for the three apple cultivars. The most important metric for the detection of a pest of concern such as CM is recall or sensitivity which reflects the amount of incorrectly classified infested samples (false negative) or the truly infested samples that were not detected as infested and were classified as healthy. As shown in Table 6.4, the recall values for infested samples were higher than the precision values for all the cultivars reaching as high as 0.98 (98%).

Table 6.4 Classification performance of gradient tree boosting for control and infested samples for three apple cultivars based on automatically selected pixels for three apple cultivars.

Cultivars	Classes	Precision	Recall	F1-score	Overall Accuracy (%)
Fuji	Control	0.98	0.96	0.97	97.36
	Infested	0.97	0.98	0.97	
Gala	Control	0.93	0.93	0.93	94.76
	Infested	0.95	0.96	0.95	
Granny Smith	Control	0.91	0.90	0.91	93.46
	Infested	0.95	0.95	0.95	

6.3.5. Optimal Wavelength Selection

As mentioned above, the optimal wavelengths were selected from the whole spectra by the sequential forward selection (SFS) method to minimize variable collinearity and select the most informative variables. This algorithm started with one wavelength and then added a new one in each iteration process, and a specified number of wavelengths were selected at the end. The selections of optimal wavebands are shown in Figure 6.5 and Table

6.5. The results in Figure 6.5, obtained by applying SFS, illustrate a graph of classification accuracy changing with increasing the number of selected wavelengths. As shown, when 22 wavelengths variables were selected, the classification performance rate approached an asymptote while the number of selected variables was significantly less than the raw spectral data (356 wavebands). Therefore, the optimal variable wavelength subset, which consists of 977.2, 983.9,1050.9, 1064.3, 1081.0, 1151.28, 1184.6, 1228.0, 1248.1, 1288.1, 1351.4, 1447.9, 1530.9, 1554.2, 1574.1, 1590.7, 1627.1, 1647.0, 1653.7, 1657.0,1663.6, and 1680.2 nm, was determined for classifying the CM infestation on Fuji apples, while the corresponding number of sampled variables was 22. The first 22 wavelengths for apples are mainly distributed around 1000, 1200, 1550, and 1650 nm.

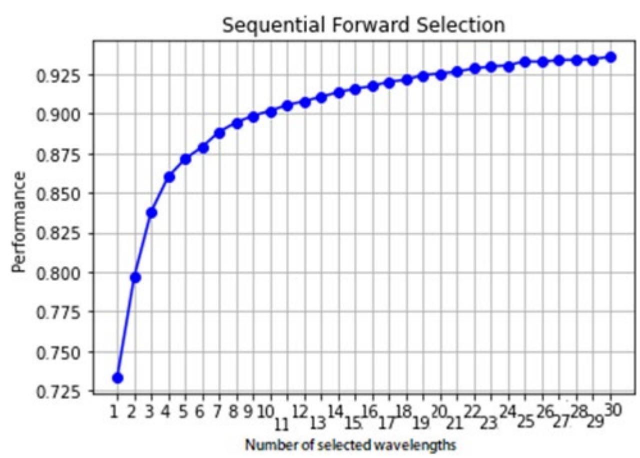

Figure 6.5 Classification performance (accuracy) as a function of the number of wavelengths.

After selecting optimal wavelengths by SFS, the selected optimal wavelengths carrying the most valuable information in the spectra were considered as the input variables to build the ensemble classifier model. Additionally, to further evaluate the representativeness of the chosen optimal size of the validation set, the classification results of the ensemble model based on the different number of optimal wavelengths for each of the three cultivars were compared (Table 6.5).

The classification accuracy of 91.6% for the validation set, which is very close to the maximum classification accuracy obtained with the whole range of wavelengths (97.4%), further validated the representativeness of the chosen optimal size of the data set. While this result is better than the results of Rady et al. (2017) who achieved an accuracy of 82% in classification of CM-infested apples using Vis-NIR HSI, their best classification accuracy was obtained using only five selected wavelengths. It is worth noting that the number of wavelengths in current study reduced from 356 to 22, which only accounts for 6.17% of the total wavelengths, making the simplified model better than the model developed using the full spectra. Overall, results indicate that this is an effective way to select optimal wavelengths to build discriminant models by SFS, with a potential reduction in computational cost and relatively satisfying model performance.

Table 6.5 Classification performance of selected optimal wavelengths

No. of Wavelengths	Gala		Granny Smith		Fuji	
	Selected Wavelengths (nm)	Classification Accuracy	Selected Wavelengths (nm)	Classification Accuracy	Selected Wavelengths (nm)	Classification Accuracy
30	900.1, 903.5,920.3, 970.6, 997.4, 100.7, 1014.1, 1071.0, 1077.7, 1261.4, 1278.1, 1281.4, 1298.1, 1324.7, 1328.1, 1361.4, 1384.7, 1408.0,1447.9, 1464.5, 1447.8, 1477.8, 1627.1, 1647.0, 1653.7, 1657.0,	88.5%	900.1, 916.9, 977.2, 1010.7, 1020.8, 1030.8, 1047.6, 1074.3, 1178.0, 1181.3, 1204.7, 1274.7, 1284.7, 1294.7, 1298.1, 1304.7, 1308.1, 1371.4, 1414.6, 1471.1, 1481.1, 1494.4, 1653.7, 1660.3,	87.7%	977.2, 980.6, 1044.2, 1074.3, 1077.7, 1081.0, 1137.9, 1147.9, 1151.2, 1211.3, 1264.7, 1294.7, 1314.7, 1344.7, 1348.0, 1381.3, 1421.3, 1507.7, 1530.9, 1544.2, 1560.8, 1580.7, 1623.8, 1630.5,	92.4%

	1663.6, 1666.9, 1676.8, 1693.4		1666.9, 1673.5, 1680.2, 1683.5,1686.8, 1693.4		1647.0, 1650.3, 1653.7, 1657.0, 1663.6, 1673.5	
22	923.6, 973.9, 1000.7, 1067.6, 1081.0, 1084.4, 1127.8, 1268.1, 1281.4, 1308.1, 1351.4, 1401.3, 1411.3, 1461.2, 1491.1, 1607.3, 1643.7, 1663.6, 1670.2, 1676.8, 1690.1, 1693.4	87.8%	903.5, 916.9, 987.3, 1047.6, 1081.0, 1131.2, 1141.2,1181.3, 1204.7, 1274.7, 1288.1, 1304.7, 1371.4,1467.8, 1471.1, 1481.1, 1643.7, 1673.5, 1680.2, 1683.5, 1686.8, 1693.4	87.5%	977.2, 983.9, 1050.9, 1064.3, 1081.0, 1151.28, 1184.6, 1228.0, 1248.1, 1288.1, 1351.4, 1447.9, 1530.9, 1554.2, 1574.1, 1590.7, 1627.1, 1647.0, 1653.7, 1657.0, 1663.6, 1680.2	91.6%
15	903.5, 990.6, 997.3, 1071.0, 1084.4, 1281.4, 1294.7, 1371.4, 1384.7, 1447.9, 1477.8, 1663.6, 1673.5, 1680.2, 1690.1	86.2%	1010.7, 1081.0, 1131.2, 1181.3, 1184.6, 1281.4, 1298.1, 1491.1, 1657.0, 1663.6, 1670.2, 1680.2, 1683.5, 1686.8, 1693.4	86.3%	977.2, 983.9, 1050.9, 1074.3, 1081.0, 1311.4, 1381.3, 1401.3, 1447.9, 1507.7, 1627.1, 1637.1, 1647.0, 1653.7, 1673.5	91.0%
5	997.3, 1084.4, 1281.4, 1663.6, 1693.4	81.5%	1014.1, 1274.7, 1494.4, 1683.5, 1693.4	80.7%	983.9, 1050.9, 1311.4, 1653.7, 1663.6	86.2%

6.4 Conclusions

In this study, machine learning models were developed to perform classification of CM infestation in apples using pixel-level NIR hyperspectral image data. Combined NIR HSI, machine learning and image processing methods were applied to discriminate healthy and infested tissues in three apple cultivars. The results of three approaches were provided; the first approach was based on using image-level mean spectra extraction for the whole sample analysis, and the second and third approaches were conducted at the pixel level using manual and automatic ROI segmentation around the infested area of the sample, respectively. Furthermore, the optimal wavelengths were selected using SFS algorithm to develop multispectral models. The total classification accuracy for the infested and healthy samples are as high as 97.4% for the validation dataset using GTB ensemble classifier among others. The feature selection algorithm obtained a maximum validation accuracy of 91.6% with only 22 selected wavelengths. Therefore, the NIR HSI method for infestation detection demonstrated the capacity to detect CM infestation in apples of different varieties with potential in post-harvest inline apple sorting applications. Overall, the good results obtained in this study represent a promising step forward for sorting technologies employed in the apple processing units especially in packinghouses and export/import inspections. Moreover, the proposed NIR HSI could be useful as a remote monitoring tool for quality control and for studying CM incidence directly in the orchard; for example, through UAV-based HSI. Finally, future research could include evaluating the computational costs and processing speed, improving hardware, and applying other machine learning methods such as deep learning, as these could improve the accuracy and the robustness of the HSI detection system.

CONNECTING STATEMENT

In chapter 6, HSI was used for the classification of CM-infested and control apples. In the next chapter, we are interested in finding out if HSI can be used to predict some important quality attributes of apples. Does CM-infestation affect the quality attributes of apples during storage? How about CM effect on predicting quality of apples using HSI?

CHAPTER 7. OBJECTIVE FIVE

NON-DESTRUCTIVE DETERMINATION AND PREDICTION OF PHYSICOCHEMICAL QUALITY ATTRIBUTES OF APPLES DURING STORAGE USING HYPERSPECTRAL IMAGING

Abstract:

The year-round demand for high quality apples, as one of the top three most popular fruits in the world, continues to increase. Therefore, monitoring of quantitative and qualitative postharvest losses of apples against invasive pests during long-time storage remains a critical issue in the apple industry. In this chapter, the effect of codling moth (CM) (*Cydia pomonella* (L.)), as one of the most detrimental pests of apples, on the quality of the fruit was investigated under different storage conditions. Specifically Gala apples were evaluated for qualities such as firmness, pH, moisture content (MC), and soluble solids content (SSC). Near-infrared hyperspectral imaging (HSI) was implemented to build machine learning models for predicting the quality attributes of apples during a 20-week storage using partial least squares (PLS) and support vector regression (SVR). Data were pre-processed using Savitzky-Golay smoothing filter and standard normal variate (SNV) followed by removing outliers by Monte Carlo sampling method. Functional analysis of variance (FANOVA) was used to interpret the variance in the spectra with respect to the infestation effect. FANOVA results showed that the effects of infestation on the NIR spectra was significant at $P < 0.05$. Initial results showed that the quality prediction

models for the apples during cold storage at three different temperatures (0 ℃, 4 ℃ and 10 ℃) were very high with a maximum correlation coefficient of prediction (Rp) of 0.92 for SSC, 0.95 for firmness, 0.97 for pH, and 0.91 for MC. Furthermore, the competitive adaptive reweighted sampling (CARS) method was employed to extract effective wavelengths to develop multispectral models for fast real-time prediction of the quality characteristics of apples. Model analysis showed that the multispectral models have better performance than the corresponding full wavelengths HSI models. The results of this study can help in developing nondestructive monitoring and evaluation systems for apple quality under different storage conditions.

7.1 Introduction

Apples are considered one of the most important fruits that are a source of nutrients like vitamins, minerals, and bioactive compounds, providing so many health benefits (Salehi & Aghajanzadeh, 2020). However, apples, like other fruits, are highly perishable goods that require proper preservation to reduce the degradation of macro and micro-nutrients and to extend their shelf life (Liu et al., 2022). For this, apples are typically packaged and kept in a low temperature environment at 0 °C to 4 °C using different refrigeration systems during the transportation and postharvest processes. Generally, this process reduces and delays microbial growth and enzymatic reaction, thereby improving overall apple quality, reducing mass loss, and extending shelf-life (Onwude et al., 2020). Codling moth (CM), (*Cydia pomonella* L.) is the most problematic pest to the apple industry in the United States that can have large economic effects if uncontrolled (Ekramirad et al., 2021). Researchers have been studying methods to nondestructively detect and sort CM-infested apples with high accuracy (Li et al., 2018; Rady et al., 2017). There is greater interest in this approach due to zero-tolerance for the occurrence of CM in most international destinations, particularly Asia, for U.S. apples where there may be import ban if a pest like CM is entrained in a shipment. Cold storage is one of the system approaches used to reduce the risk of possible pest infestation. To meet the severe phytosanitary regulations for apples, cold storage treatment has been already used against the apple maggot and the oriental fruit moth pests (Breth, 2002; Hong et al., 2019). Normally, the CM begins to reproduce by laying eggs on apples and the surrounding leaves at temperatures above 10 °C; however, when they are exposed to temperatures below 1 °C, the physiological condition of the CM larvae undergo preconditioning for diapause, an inactive state that allows the larvae to last through the winter season within their cocoons (Rozsypal et al., 2013). Diapausing larvae do not feed and are freeze-tolerant (Rozsypal et al., 2013). Cold storage may not eliminate CM in apple during shipment to foreign markets and can cause some physiochemical change to apples if it falls below certain threshold that can cause physiological damage like chilling injury. While it is known that cold storage will slow down the CM activities, a better understanding of the impact of cold storage conditions on quality attributes of healthy and infested apples is desired in this study.

Inefficient apple storage in terms of temperature and humidity can change the fruit external and internal quality (Mditshwa et al., 2018). In terms of external quality, apples are typically evaluated based on physical appearance including shape, color, size, and the presence or absence of surface defects. These attributes affect the pricing of horticultural products in the market. The internal quality of apples refers to the nutritional value, texture, and flavor. The internal quality features cannot be evaluated using visual inspection and they often require destructive physicochemical analysis such as Brix refractometer to test the soluble solids content (SSC) or the Magness-Taylor test for firmness. Firmness is the primary textural attribute of horticultural products. The sensory properties such as bitterness, sweetness, and sourness, as well as various volatile compounds form the characteristic flavor (Fathizadeh et al., 2021). Thus, there is a need to study the effect of cold storage on the important quality attributes of apples and to develop quality predicting models using nondestructive evaluation methods. Evaluation of internal qualities has been a key theme in nondestructive quality assessment of horticultural products (Nturambirwe & Opara, 2020). Different techniques have been explored by researchers for nondestructive evaluation of apple quality features. These techniques include machine vision (Cárdenas-Pérez et al., 2017), Vis/NIR spectroscopy (Ma et al., 2021), and computed tomography (CT) (Du et al., 2017). Most of these techniques have limitations that include long setup processes, high-cost and being sensitive to the changes in environmental conditions.

Hyperspectral imaging (HSI) has emerged as a promising tool in detecting apple quality as it combines imaging and spectroscopy technologies for providing spatial and spectral information of the sample simultaneously. By this integration, HSI can detect the external and internal quality characteristics of a sample (Shi et al., 2019). HSI technique, which is based on the relation between light scattering, and the structural and textural properties of biological tissues, uses a highly focused light beam to generate scattering images to enhance its assessment of fruit qualities. Lu (2007) applied Vis/NIR HSI to evaluate SSC and firmness of two types of apple varieties, namely golden delicious and red delicious. The author used an artificial neural network (ANN) model to analyze the data and found that R^2 for SSC prediction were 0.79 and 0.76 for golden delicious and red delicious apples, respectively. It was concluded that the relatively poor predictions for red delicious apples might be attributed to their irregular fruit shape, which could have negatively affected the scattering measurements. Relatively poor predictions of SSC using Vis/NIR HSI compared to point Vis/NIR spectroscopy could be attributed to the lower signal-to-noise ratio and the fact that the light scattering technique tends to be more suitable in predicting structural features such as firmness than SSC. In addition, using NIR HSI in comparison to Vis/NIR system will insure full coverage of the spectral absorption bands such as water (1150, 1450, and 1900 nm), lipids (1040, 1200, 1400, and 1700 nm), and collagen (near 1200 and 1500 nm) at the longer wavelength range (Ma et al. 2018). For example, Ma et al. (2018) applied near-infrared HSI in 913 to 2519 nm to predict the SSC in Fuji apples and obtained a higher R^2 of 0.89 using PLS regression.

Vis-NIR HSI has been widely used for quality assessment of fruits because of lower cost than that of longer wavelength range NIR; however, the absorption of chemical components of tissue such as water, lipids, and collagen at the longer wavelength range are much more conspicuous than the features observed in the Vis-NIR range. Thus, the longer wavelength NIR HSI has the potential to provide enhanced sensitivity compared to the Vis-NIR range (Ma et al., 2018). In addition, there is no study that investigates the cold storage effect on CM infested apples in term of the quality of apples as well as prediction of the quality of the fruit using the spectral information from HSI method. Since any biological variability will affect the prediction of the quality parameters and also the developed models (Peirs et al., 2003), it is needed to study the CM infestation variability in the measured spectra. This gap in knowledge indicates a need to understand the influence of cold storage on CM infestation and the ability of using HSI approach to predict physicochemical changes in healthy apples under different storage conditions. The main objectives of this study were to study the effect of storage conditions (temperature and time) on the quality changes of apples as well as the ability to predict the quality characteristics of apples using HSI combined with machine learning regression models. The specific objectives were to: (1) to investigate the effect of the CM infestation as a sources of variability on the measured HSI spectra and to evaluate its impact on the performance of the models for predicting the quality characteristics of apples, (2) to select optimal wavebands to develop a multispectral imaging system for nondestructive quality prediction of apples.

7.2 Material and Methods

A total of 180 organic Gala apple samples, with a diameter ranging from 60 to 75 mm, with no sign of pest attack, diseases, or damage, were purchased from a local market in Lexington, KY, U.S.A. in February 2021. The apple samples were divided into two groups: 60 samples as a control, and 120 samples as the infested group. The samples of the infested group were artificially infested by placing first instar larvae on each apple and isolating it in a plastic container with a removable lid. The samples were further divided randomly into three groups of 60 apples (20 control and 40 infested) to put in three different storage conditions of 0 °C, 4 °C and 10 °C at a relative humidity of 85–90%. The physiological quality attributes of the apples were measured on the first day and after being refrigerated for 4, 8, 12, 16, and 20 weeks. The hyperspectral data acquisition and measurement of quality characteristics of apples were carried out in the Food Engineering lab at the Biosystems and Agricultural Engineering Department, University of Kentucky, Lexington, KY, USA.

The shortwave near-infrared (SWNIR) HSI system used in this study consisted of a NIR spectrograph with a wavelength range from 900 to 1700 nm and a spectral resolution of 3 nm (N17E, Specim, Oulu, Finland), a moving stage driven by a stepping motor (MRC-999-031, Middleton Spectral Vision, Middleton, WI, USA), a 150 W halogen lamp (A20800, Schott, Southbridge, MA, USA), an InGaAs camera (Goldeye infrared camera: G-032, Allied Vision, Stradtroda, Germany) mounted perpendicular to the sample stage and a computer with data acquisition and analysis software (FastFrame™ Acquisition Software, Middleton Spectral Vision com, Middleton, WI, USA) (Figure 7.1). The parameters of the sample stage speed, the exposure time of the camera, the halogen lamp angle, and the vertical distance between the lens and the sample were adjusted to 10 mm/s, 40 ms, 45°, and 25 cm, respectively, in order to acquire clear images. The size of each acquired hyperspectral image was 266×320×256 (X, Y, λ) which was saved as "*.raw" file along with a header file as "*.hdr".

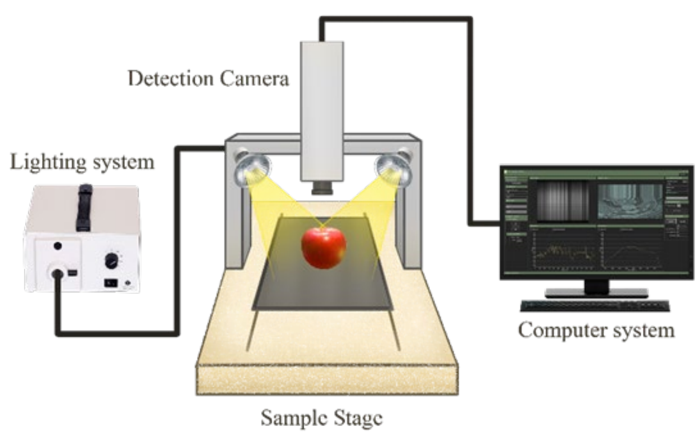

Figure 7.1 Schematic diagram of the hyperspectral imaging system

After the image acquisition, it was necessary to calibrate the raw hyperspectral images with white and dark reference images to compensate for the effect of illumination as well as the dark current of the detector. A whiteboard with reflectance of 99% from a polytetrafluoroethylene (PTFE) Teflon plate was used to acquire the white reference image. Then lights were turned off and the camera lens was covered completely with a cap to acquire the dark reference image. Then the hyperspectral images were corrected with the white and dark reference according to the following equation (Tian et al., 2019):

$$R = \frac{R_0 - R_d}{R_w - R_d}$$

where R is the corrected image, R_o is the raw hyperspectral image, R_d is the dark image, and R_w is the white reflectance image.

After HSI image acquisition, destructive tests were carried out immediately. The apple firmness measurement was carried out at three locations around the equatorial region of each apple, using a texture analyzer (TA. XT express, Stable Micro Systems Ltd., UK), with a 6-mm flat probe, a puncture depth of 5 mm, and a puncture speed of 25 mm/min. From the force–displacement curve, the peak force was used as the firmness value in N. The average of the three measurements was calculated to represent the firmness of a sample. The soluble solids content (SSC), which is considered as an index for evaluating the sweetness of apples, was determined in °Brix using a portable refractometer (PAL-BX/ ACID5, ATAGO Co. Ltd., Japan). Apple pulp from each tested position was cut out to extract the juice to place on the refractometer sample glass for the measurement (Tian et al., 2019). Also, the extracted juice was used to determine pH by means of a digital pH-meter (Sartorius PB-10, Germany) under room temperature at 25±2 °C. Finally, to measure of the moisture content of the apple slices, 20 g of each sample was weighed using a digital balance with an accuracy of 0.001 grams and dried in an oven at 105°C for 24 h. Afterwards, the wet basis moisture content was calculated by dividing the final weight by the initial weight.

After the acquisition and correction of the hyperspectral images, to acquire spectral data, three regions of interest (ROIs) as rectangles with 10×10 pixels were segmented near the equatorial area of each apple in the images. The average spectral information of all the pixels within each ROI was extracted and represented as the spectral data of the sample in the form of reflectance intensity versus wavelength.

After spectral data extraction, the pre-processing steps of wavelength trimming, maximum normalization, Savitzky-Golay smoothing (with the moving window width of 27, and the second-order polynomial), and standard normal variable (SNV) were performed to remove the noisy wavelengths at the edges of each spectrum, to scale data, and to compensate the particle size scattering and path length difference effects, respectively. Also, the Monte Carlo sampling approach was used to detect the outliers before building the regression models.

To analyze the variance in the spectra with respect to the storage time and infestation effects, functional analysis of variance (FANOVA) was used. This method adapts the traditional analysis of variance by representing each observation (spectrum) as a function. Many authors have shown that the functional approach in chemometrics has some advantages in building predictive models and analyzing the sources of variance in spectroscopic data (Saeys et al., 2008). In this method, the spectrum of a sample is the result of the reflection and absorption peaks for different chemical components where the spectral information is represented by the overall mean and the main effects (Saeys et al., 2008). In this study, the storage time and CM infestation effects were considered the main effects. For each main effect, the group effect was considered to be significant if $P \leq 0.05$.

This study applied partial least squares regression (PLSR) and support vector regression (SVR) to build the regression models using the mean spectrum of the ROI as the independent variables (X) and the measured quality values as the dependent variables (Y). PLSR is particularly useful in spectral analysis for constructing a linear model when the amount of sample data used for modeling is small. The data used for modeling were divided into the training (80%) and prediction (20%) sets using the Kennard-Stone sample selection algorithm.

The performance of the training and prediction models were evaluated by the correlation coefficient of training (Rc) and its root mean square error (RMSEC), and the correlation coefficient of prediction model (Rp) and its mean square error (RMSEP). All algorithms used in this study for pre-processing and data analysis were performed on the Python 3.10 (Python Software Foundation, https://www.python.org) platform and in Jupyter Editor Notebook. Open-source libraries of Spectral, Numpy, Sklearn, Scikit-fda and Matplotlib were used in this work.

Wavelength selection is an important part of spectral data analysis. Its function is to eliminate the redundant information contained in the spectrum, retain the data information related to the current task, and then reduce the data dimension. In this paper, competitive adaptive reweighted sampling (CARS) was applied for selecting useful wavelengths.

7.3 Results and Discussion

7.3.1 Quality Change of Control and Infested Apples During Storage

Changes in quality attributes of apples, namely SSC, pH, moisture content and firmness measured during cold storage at three different temperatures are presented in Figure 7.2. The results of analysis of variance (ANOVA) showed that there was a significant ($P < 0.05$) change in pH and firmness of apples with storage time. However, SSC and moisture content did not show a significant change during storage. The pH values of apples tended to decrease at first, then increase during cold storage. It declined from 3.81 ± 0.02, 3.79 ± 0.02, and 3.70 ± 0.09 to 3.53 ± 0.24, 3.62 ± 0.11, and 3.51 ± 0.23 during the first two months for samples at 0 °C, 4 °C and 10 °C, respectively. The increase in pH towards the end of the storage is related to metabolism activities, especially respiration which consumes organic acid, as the main factor in pH of the fruit (Jan et al., 2012). There was no significant ($P < 0.05$) difference in pH values for apples stored at different temperatures and they showed a similar trend during storage. In addition, the results of ANOVA showed that there was a significant difference in pH of control and infested apple fruits

For SSC, no significant change was observed with time or temperature. This is because the apples used in this study were fully mature. The results are in agreement with the findings of (Ghafir et al., 2009) who show that the value of SSC undergo the highest changes in low-maturity apples by nearly 13% in comparison to only 2% for fully mature apples. This is because of the lower initial starch content in low maturity apples, which converts into sugar as apple fruits mature causing the change in the SSC value during storage (Blažek et al., 2003). Since the apples used in the current study were at high maturity level, the change in the SSC value was minimum. (Ghafir et al., 2009) presented a result that shows no significant change in total soluble solid, SSC and starch concentration in mature Gala apples during 180 days of storage at 0 °C. In Figure 7.2, the values of SSC of apples at 4 °C and 10 °C tended to increase at first, peaking around two months of storage, then decreased until the end. This changing trend agrees with the results of (Zhang et al., 2021) who reported an increase in the SSC of fully mature apples in the first two months of storage at 1 °C followed by a decrease towards the end of the 6-month cold storage.

As shown in Figure 7.2, the firmness of apples significantly ($P < 0.05$) decreased with storage time for samples stored at 4 °C and 10 °C, but the apples at 0 °C did not change significantly over time. This decrease in firmness during storage has been related to the water loss in cells, the cell walls becoming thinner, and the degradation of the cell wall materials and the pectin (Johnston et al., 2002; Szymańska-Chargot et al., 2016). Also, the results showed that temperature had a significant effect on apple firmness with the higher temperatures having less firmness values.

The ANOVA showed that the effect of time and temperature on the moisture content of stored apples were not significant ($P > 0.05$). This could be as a result of keeping the relative humidity of the controlled environment chamber at a high level, around 90% to minimize water loss in apples during storage.

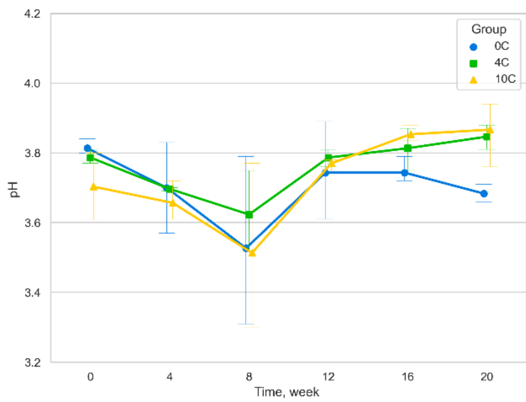

(A)

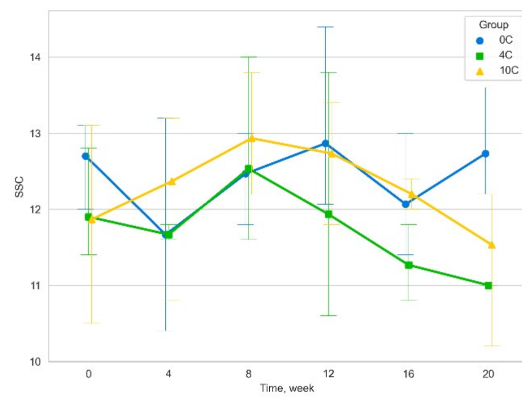

(B)

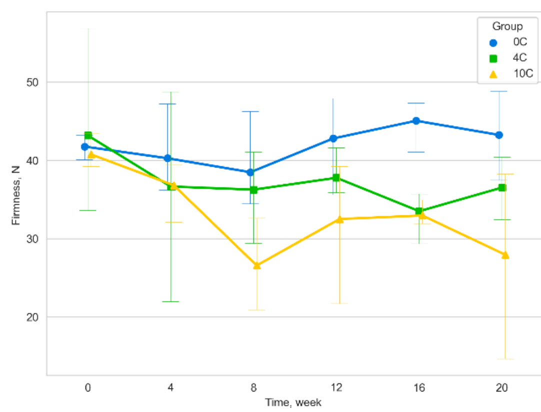

(C)

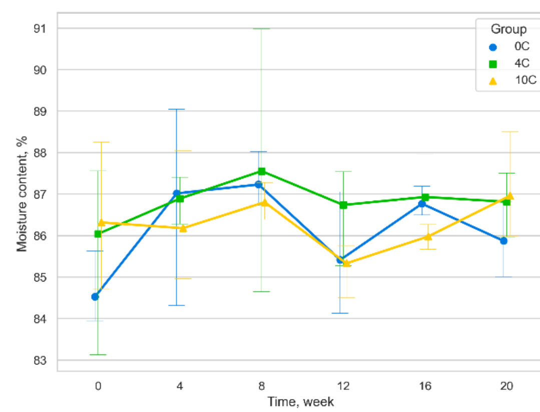

(D)

Figure 7.2 Changes during cold storage in the pH (A), SSC (B), firmness (C) and moisture content (D) of control apples at different temperatures.

7.3.2 Reflectance Spectra

Figure 7.3 shows the measured reflectance spectra of all measured apples in the region between 900 and 1700 nm in the raw spectra form and after pre-processing by Savitzky-Golay smoothing and SNV. There are some distinct absorption valleys in the spectra around 950, 1200, and 1400 nm. The absorption at about 950 and 1200 nm relates to the first overtones of O-H band in water molecules (Kuchenberg et al., 2008). The absorption around 1400 nm is attributed to the combination of the second overtone of C-H and the first overtone of O-H (Cortés et al., 2019) . Similar spectra were also reported for apples by Peirs et al. (2005), and Nicolaï et al. (2007).

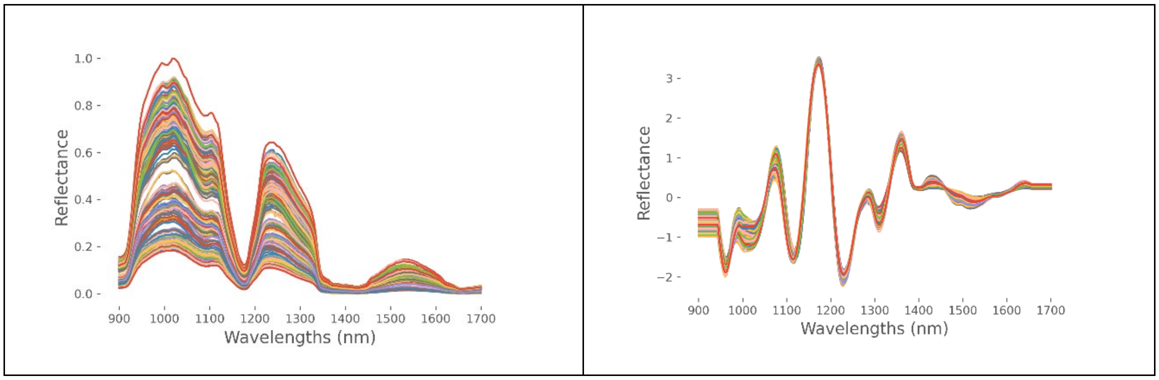

Figure 7.3 Spectral curves obtained by the mean spectra for the control and infested samples over the storage period (left), and Savitzky-Golay combined with SNV pre-treatment (right)

7.3.3 Predicting the Quality of Control and Infested Apples During Storage

To study the effect of biological variability on the spectra, one-way FANOVA was applied to analyze the effect of CM infestation on the spectra. The results showed that CM infestation effect on the spectra was significant with a $P \leq 0.05$.

Overall, it can be seen from Figure 7.4 that the CM infested apples had more absorption, especially at peak points. The higher absorbance by the infested apples can be explained by a combination of chemical and textural changes due to the infestation (Susič et al., 2020).

While all spectra have a very similar shape and trend (Figure 7.4), there is a significant difference between the mean spectral for the control and infested apples. This variability affects the performance of predictive models. It should be noted that although all spectra have a very similar shape, there is a large variability in absorbance at certain wavebands of each class.

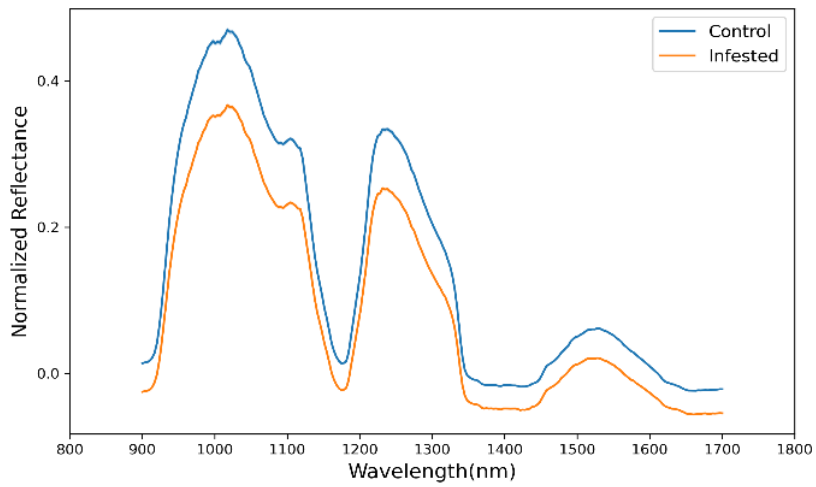

Figure 7.4 The mean spectra of the raw data for CM-infested and control apples

Tables 7.1 and 7.2 show the performance of the PLSR and SVR regression methods in predicting SSC, pH, moisture content and firmness of the apples. The spectral data with the full spectrum (900 - 1700 nm) were used to establish PLSR and SVR models for the quality parameters. In order to get an efficient and reliable model, the optimal number of latent variables (LVs) were first selected (in the range of 1 to 20) as the inputs of the training model through calculating the RMSECV using a 10-fold cross-validation. In Table 7.1 the regression models for predicting pH were established separately for the control, infested and combined samples. This is because the ANOVA results showed a significant difference between control and infested samples in terms of pH value. While the model for pH prediction in the control samples gave a high correlation coefficient of prediction (up to 0.97), the accuracies for the infested and combined models are not satisfactory, possibly because of the large variations in the spectra as well as the differences in chemical characteristics and cell structure of infested apples versus healthy ones. It has been shown

Table 7.1 The prediction performance of regression models for pH during the storage time and across three temperatures

Samples condition	Regression model	R_C	RMSEC	R_P	RMSEP
Control	PLSR	**0.94**	**0.17**	**0.97**	**0.25**
	SVR	0.93	0.19	0.93	0.30
Infested	PLSR	0.97	0.13	0.71	0.24
	SVR	0.65	0.24	0.44	0.24
Combination	PLSR	0.85	0.24	0.54	0.33
	SVR	0.89	0.22	0.49	0.34

Rc: correlation coefficient of calibration, Rp: correlation coefficient of prediction, RMSEC: root mean square error of calibration, RMSEP: root mean square error of prediction

that any source of biological variability such as cultivar, harvest season, and origin as well as maturity and shelf-life, will greatly affect the fruit quality properties and also the accuracy and robustness of the models for the prediction of those properties (Bobelyn et al., 2010). Thus, the poor predictive models for the combination of control and infested samples may be due to not accounting for these variabilities. This is mainly because of significantly different spectra coming from control and infested samples for which the predictions were poor. When this source of variability was excluded from the data by separating control and infested samples, there were considerable improvements in the results (from R_P=0.54, RMSEP=0.33 to R_P = 0.97, RMSEP= 0.25). Thus, for the purpose of predicting the quality attributes of apples, only the control samples will be considered to establish accurate and robust models. In addition, PLSR gave higher accuracies than SVR in predicting apple's pH values. These results are comparable to the results of Guo et al. (2014) who established PLS model based on shortwave infrared hyperspectral imaging (1,000–2,500 nm) for the pH of Fuji apple with the best Rp of 0.847 and RMSEP of 0.0398.

The training and prediction performances of PLSR and SVR models for determining firmness, SSC, and MC of control apples stored at 0 °C, 4 °C and 10 °C are shown in Tables 7.2, 7.3 and 7.4, respectively. As shown in Table 7.2, the best results for pH was achieved using PLSR, however, SVR model had the highest R_P and the lowest RMSEP for firmness, SSC and MC prediction. For firmness, PLSR gave 0.96, 0.95, 1.21, and 1.45 for R_C, R_P, RMSEC, and RMSEP, respectively. In addition, Table 7.2 shows that the R_C and R_P of all models for the samples stored at 0 °C exceeded 0.84, indicating the efficiency of PLSR and SVR models to predict the internal quality attributes of apples in long term cold storage.

Table 7.4 shows that the predictive models for the samples stored at 10 °C had a high performance for all the attributes except from SSC. In a similar work, Dong & Guo (2015) used NIR hyperspectral reflectance imaging in the range of 900–1700 nm to predict SSC, firmness, MC, and pH values of Fuji apples by PLS regression, least squares support vector machine (LSSVM), and back-propagation network modeling during a 13-week storage period. They reported that while all their models failed to predict firmness, the LSSVM model gave better accuracy in predicting SSC, MC, and pH with R_P of 0.961, 0.984, and 0.882, respectively.

Table 7.2 Prediction performance of regression models for the control samples at 0 °C

Quality attributes	Samples condition	Regression model	R_C	RMSEC	R_P	RMSEP
pH	Control, stored at 0 °C	PLSR	**0.94**	**0.17**	**0.97**	**0.25**
		SVR	0.93	0.19	0.93	0.30
Firmness	Control, stored at 0 °C	PLSR	0.95	1.26	0.93	1.62
		SVR	**0.96**	**1.21**	**0.95**	**1.45**

SSC	Control, stored at 0 °C	PLSR	0.95	0.53	0.90	0.81
		SVR	**0.95**	**0.56**	**0.92**	**0.89**
MC	Control, stored at 0 °C	PLSR	0.85	0.81	0.88	0.88
		SVR	**0.84**	**0.82**	**0.91**	**0.82**

SSC: soluble solids content, MC: moisture content, Rc: correlation coefficient of calibration, Rp: correlation coefficient of prediction, RMSEC: root mean square error of calibration, RMSEP: root mean square error of prediction

Table 7.3 Prediction performance of regression models for the control samples at 4 °C

Quality attributes	Samples condition	Regression model	R_C	RMSEC	R_P	RMSEP
pH	Control, stored at 4°C	PLSR	**0.92**	**0.29**	**0.89**	**0.51**
		SVR	0.95	0.25	0.76	0.90
Firmness	Control, stored at 4 °C	PLSR	**0.95**	**1.37**	**0.74**	**3.19**
		SVR	0.67	2.20	0.54	2.54
SSC	Control, stored at 4 °C	PLSR	0.88	0.68	0.58	0.91
		SVR	0.99	0.36	0.77	0.80
MC	Control, stored at 4 °C	PLSR	0.98	0.39	0.66	1.08
		SVR	**0.96**	**0.58**	**0.95**	**0.87**

SSC: soluble solids content, MC: moisture content, Rc: correlation coefficient of calibration, Rp: correlation coefficient of prediction, RMSEC: root mean square error of calibration, RMSEP: root mean square error of prediction

Table 7.4 Performance of regression models for the control samples at 10 °C

Quality attributes	Samples condition	Regression model	R_C	RMSEC	R_P	RMSEP
pH	Control, stored at 10 °C	PLSR	0.97	0.18	0.94	0.40
		SVR	**0.97**	**0.20**	**0.96**	**0.35**
Firmness	Control, stored at 10 °C	PLSR	0.98	0.98	0.95	0.97
		SVR	**0.99**	**0.10**	**0.98**	**1.77**
SSC	Control, stored at 10 °C	PLSR	0.92	0.65	0.73	1.03
		SVR	0.71	0.92	0.56	1.19
MC	Control, stored at 10 °C	PLSR	**0.97**	**0.53**	**0.94**	**1.31**
		SVR	0.99	0.10	0.80	1.16

SSC: soluble solids content, MC: moisture content, Rc: correlation coefficient of calibration, Rp: correlation coefficient of prediction, RMSEC: root mean square error of calibration, RMSEP: root mean square error of prediction

In Figure 7.5 the values of pH, SSC, firmness, and MC in the training, and prediction sets predicted by the PLSR model are plotted against the actual values. These results indicate that these apple quality parameters can be accurately predicted from NIR reflectance HSI using PLSR.

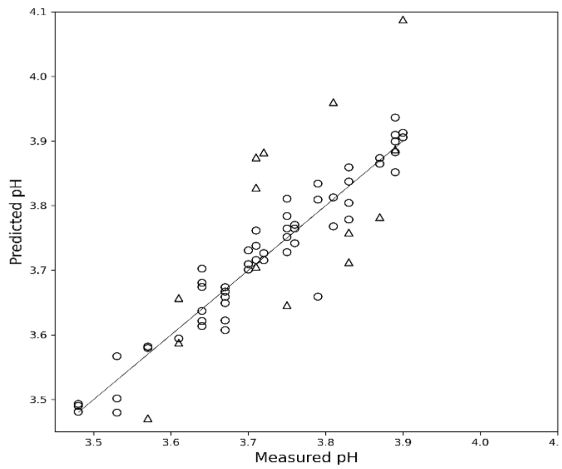

(a)

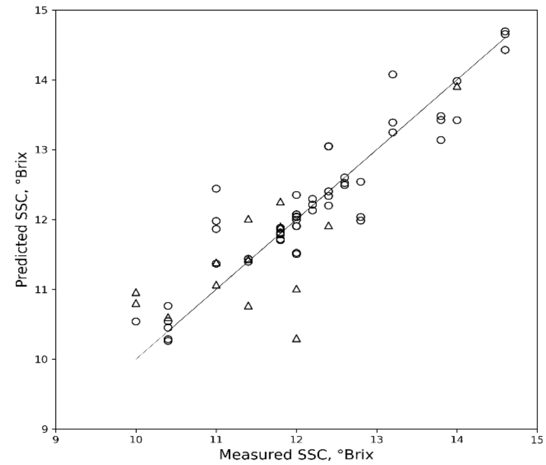

(b)

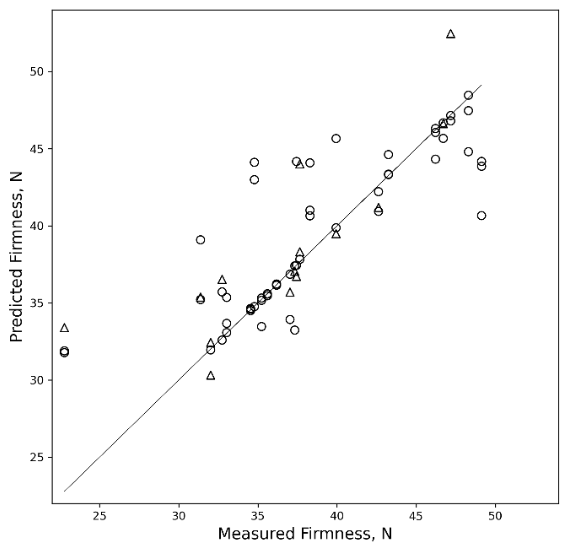

(c)

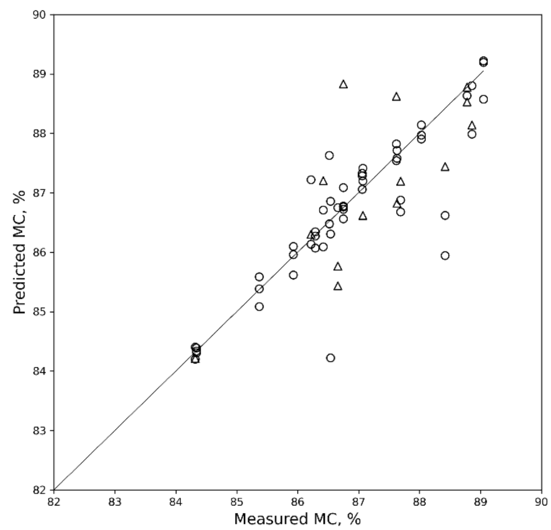

(d)

Figure 7.5 The measured vs. predicted values for pH (a), SSC (b), Firmness (c) and moisture content (d) for apples at 0 °C for calibration and prediction sets (Circles and triangles for training and predicting data points, respectively)

As shown in Table 7.5, for example, the PLSR prediction model for firmness uses seven wavelengths (957, 1164, 1184, 1248, 1321, 1324, and 1477 nm), which only account for 0.02% of the full spectrum, achieving a relatively optimal prediction effect with R_P of

0.95. When less variables are used, the model is more efficient. Therefore, it is concluded that PLSR is the best model for firmness prediction in this context.

Table 7.5 Prediction performance of regression models for apples stored 0 °C

Quality parameter	Selected wavelengths (nm)	Regression model	R_C	RMSEC	R_P	RMSEP
pH	950, 1161, 1221, 1224, 1271, 1274, 1334, 1378, 1381, 1471, 1474, 1477, 1481, 1584	PLSR	0.90	0.20	0.92	0.26
		SVR	0.98	0.12	0.92	0.29
SSC	1081, 1117, 1157, 1161, 1164, 1167, 1238, 1241, 1244, 1248, 1251, 1254, 1258, 1301, 1354, 1358, 1368, 1477, 1481	PLSR	0.97	0.48	0.91	0.84
		SVR	0.94	0.57	0.92	0.85
Firmness	957, 1164, 1184, 1248, 1321, 1324, 1477	PLSR	0.80	1.77	0.95	1.66
		SVR	0.87	1.68	0.94	1.84
MC	953, 957, 1020, 1054, 1071, 1074, 1184, 1188, 1241, 1291, 1344, 1348	PLSR	0.83	0.83	0.89	0.80
		SVR	0.83	0.84	0.90	0.85

Test split and with selected wavelength, SSC: soluble solids content, MC: moisture content, Rc: correlation coefficient of calibration, Rp: correlation coefficient of prediction, RMSEC: root mean square error of calibration, RMSEP: root mean square error of prediction

7.4 Conclusion

Using FANOVA to analyze the effect of biological variability on the measured spectra, it was found that the storage time and CM infestation effects significantly affect the spectra, creating a lot of variability in the predictive models. However, by separating the data of the infested and control samples, the best results for the prediction of quality attributes of apples were achieved for the control samples stored at 0 °C with Rp of 0.92 for SSC, 0.95 for firmness, 0.97 for pH, and 0.91 for moisture content. Furthermore, the optimal wavelengths were selected using the CARS algorithm to develop multispectral models with satisfactory performance. Therefore, the SWNIR HSI method for apple quality prediction demonstrated high accuracy for post-harvest apple quality prediction with potential in inline/online apple sorting applications.

CONNECTING STATEMENT

In Chapter 6, the HSI method was applied to detect and classify the CM-infested apples for freshly harvested samples. As discussed in chapter 7, the long-term storage of apples will change the quality characteristics of the fruit. Also, for the stored apples CM infestation damage is expected to develop to different degrees depending on the storage condition. In Chapter 8 the effect of storage time and condition on the detectability of CM infestation is investigated. The findings of this section will help determine the effectiveness of nondestructive methods for detection and classification of infested apples under different storage conditions.

CHAPTER 8. OBJECTIVE SIX

IMPACT OF STORAGE TIME AND CONDITION ON NONDESTRUCTIVE DETECTABILITY OF CM-INFESTED APPLES USING HYPERSPECTRAL IMAGING

Abstract

Different conditions during cold storage of CM-infested apples leads to different infestation levels, which affect the overall product quality. In this study the effect of postharvest storage duration (up to 20 weeks) and temperature (0 °C, 4 °C, and 10 °C) on the detectability of CM-infested apples using the near-infrared (NIR) hyperspectral imaging (HSI) method (900–1700 nm) was investigated. Fresh organic Gala apples were obtained directly from a commercial market and stored in the controlled environmental chamber at three temperatures for 20 weeks in two groups of control and CM-infested samples. Every four weeks, the NIR hyperspectral images in the reflectance mode were acquired directly for each set of samples. Machine learning models for classification of CM-infested apples were then developed based on the hyperspectral image data. Results revealed that storage duration and temperature had a significant effect on the performance of classification of the CM-infested and control apples. Overall, the best classification rates were obtained for apples stored for 16 weeks with accuracies of 97%, 94%, and 100% for storage temperatures of 0 °C, 4 °C, and 10 °C, respectively.

8.1 Introduction

Apples are among the top three most consumed fruits in the world with a high year-round demand. Cold storage is usually applied to extend their shelf life to be available after season. It has been reported that different cultivars of mature apples can be stored at 0 °C to 4 °C for 6 months to maintain their quality attributes. This can be extended to 12 months with close monitoring (University of Meryland Extension, 2021).

Cold storage has also been used as part of the system approach (SA) against insect pest infestation of apples such as the apple maggot (*Rhagoletis pomonella* (Diptera: Tephritidae)) (Hallman, 2004) and the oriental fruit moth (*Grapholita molesta* (Lepidoptera: Tortricidae)) (Hansen, 2002). However, the full control of CM activities using cold storage approach is rarely possible, and it depends on the storage condition and duration as well as physiological state of the insect at time of storage. For instance, Toba and Moffitt (1991) reported that, out of total of 142,000 CM larvae, no live larva survived after 13 weeks of storage at 0 °C, with 1.5% to 2.0% oxygen (O_2) and less than 1% carbon dioxide (CO_2). However, they were only concerned about the emergence of adult CM regardless of the larval damage. In addition, the effect of cold storage on the mortality of CM depends on the physiological state of the insect, with the diapause stage allowing them to survive really cold weather (Hansen et al. 2008). Therefore, the cold storage treatment will not fully eliminate the CM larvae and `there could exist some already infested apples in the batch. So, there is a need for nondestructive monitoring of the stored apples against the CM infestation in an effective and accurate way.

While long-term storage usually affects the quality of the fruit, the quality decline will be more significant in CM-infested apples since the pest can continue to develop and damage the fruit during storage. There has been a plethora of research on apple quality changes during cold storage (Zhang et al., 2021). However, there in a lack of study on the effect of storage on CM infestation detection in apples. Therefore, it is necessary to study the detectability of CM infestation in apples at different storage time and condition. This is of great significance in determining the best manageable approach to apple storage to reduce the impact of CM infestation in stored apples, especially from the standpoint of the efficacy of nondestructive HSI detection capability for apples under different storage conditions. Therefore, the objective of this chapter is to investigate the impact of storage condition and duration on the detection and classification accuracy of CM infestation in apples using the HSI method.

8.2 Material and Methods

A total of 180 organic Gala apple samples were purchased from a local market in Lexington, KY, USA in February 2021. The samples were artificially infested with one first instar larva each and held one day to allow the larva to chew into the fruit before putting it into storage system. Each sample was placed in an isolating plastic container with removable lid for respiration. Samples were divided randomly into three groups of 60 apples (20 control and 40 infested) and placed into three different storage conditions at 0 °C, 4 °C and 10 °C and a relative humidity of ≈ 90%. Hyperspectral images of the samples were acquired on the first day and after being refrigerated for 4, 8, 12, 16 and 20 weeks. On each sampling time a total of 36 apples (4 control and 8 infested for each treatment) were used. After hyperspectral image acquisition of each sample, they were cut open to confirm CM infestation and to search for live larva.

The shortwave near-infrared (SWNIR) HSI system used in this study consisted of a NIR spectrograph with a wavelength range from 900 to 1700 nm and a spectral resolution of 3 nm (N17E, Specim, Oulu, Finland), a moving stage driven by a stepping motor (MRC-999-031, Middleton Spectral Vision, Middleton, WI, USA), a 150 W halogen lamp (A20800, Schott, Southbridge, MA, USA), an InGaAs camera (Goldeye infrared camera: G-032, Allied Vision, Stradtroda, Germany) mounted perpendicular to the sample stage and a computer with data acquisition and analysis software (FastFrame™ Acquisition Software, Middleton Spectral Vision com, Middleton, WI, USA) (Figure 8.1). The parameters of the sample stage speed, the exposure time of the camera, the halogen lamp angle, and the vertical distance between the lens and the sample were adjusted to 10 mm/s, 40 ms, 45°, and 25 cm, respectively, in order to acquire clear images. The size of each acquired hyperspectral image was 266×320×256 (X, Y, λ) which was saved as "*.raw" file along with a header file as "*.hdr".

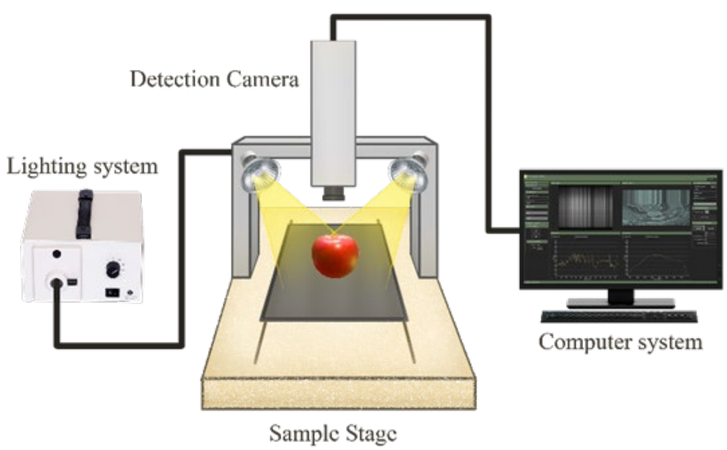

Figure 8.1 Schematic diagram of the hyperspectral imaging system

After the images acquisition, it was necessary to calibrate the raw hyperspectral images with white and dark reference images to compensate for the effect of illumination as well as the dark current of the detector. A white board with reflectance of 99% from a polytetrafluoroethylene (PTFE) Teflon plate was used to acquire the white reference image. Then lights were turned off and the camera lens was covered completely with a cap to acquire the dark reference image. The hyperspectral images were corrected with the white and dark reference according to the following equation (Tian et al., 2019):

$$R = \frac{R_0 - R_d}{R_w - R_d}$$

where R is the corrected image, R_o is the raw hyperspectral image, R_d is the dark image, and R_w is the white reflectance image.

After the acquisition and correction of the hyperspectral images, to acquire spectral data, the ROI was segmented using thresholding for each apple in the images. Then the average spectral information of all the pixels within the ROI was extracted and represented as the spectral data of the sample in the form of reflectance intensity versus wavelength.

The spectrum for each apple was labeled as either infested or healthy. Then these spectra were pre-processed by wavelength trimming, maximum normalization, a Savitzky-Golay smoothing filter, and mean centering to remove the noisy wavelengths at the edges of each spectrum, to get all data to the same scale, to account for particle size scattering and path length difference effects, and to keep only significant features, respectively. The maximum normalization was carried out by dividing each spectrum by the maximum value. The Savitzky-Golay method involves the application of the second-order polynomial and the filter window of length 31.

Having the spectral data for healthy and infested image pixels from all the samples, the labeled dataset was built by organizing pixels (observations) as rows, and the features (spectral data) as columns. After building the dataset, dimensionality reduction was carried out using PCA to obtain ten extracted features to be applied for building the machine learning models. Different machine learning classification algorithms including linear discriminant analysis (LDA), k-Nearest Neighbors (kNN), PLS-DA, and two ensemble methods, namely Random Forest (RF) and AdaBoost were applied and compared based on their classification rates. In order to analyze the effect of temperature and time on the classification performance of the models, two-way ANOVA was performed.

All the algorithms used in this study for pre-processing, image data analysis and post-processing were performed on the Python 3.7 (Python Software Foundation, https://www.python.org/ (accessed on 15/10/2021)) platform and in Jupyter Editor Notebook. The open-source libraries of spectral, Numpy, Scikit-learning, and Matplotlib were used in this work. The ANOVA was performed in MATLAB (R2020b, The MathWorks, Inc., Natick, Massachusetts, United States).

8.3 Results and Discussion:

The results showed that there were live larvae in apples until the 4th, 8th, and 17th week for samples stored at 0 °C, 4 °C, and 10 °C, respectively. While no live larvae were observed after these storage times, there were still previously infested apples without live larvae inside them among the samples of all three storage groups. Thus, it was desired to find out which condition was best for detecting and classifying CM-infested apples.

The results of ANOVA showed that the effect of storage temperature and duration on the accuracy, recall, and precision in classification of CM-infested and control apples were significant ($P < 0.05$). Tables 8.1 to 8.5 provide the mean values of classification rates for the models for apples stored at three different storage temperatures and for different periods. Statistically the fourth four-week (16 weeks of storage) gave higher classification rates than other storage periods that were not significantly different from each other. At the beginning of storage when CM larva is still at the early stage of development and infestation probably had just occurred, their damage may be less detectable by the HSI method. This might explain why the classification rate for the first few weeks are lower than the fourth four-week. The best classification rates were achieved for apples stored for 16 weeks following a decline in the classification results towards the end of the 20-week storage. Generally, PLS-DA models gave the highest classification rates for all the datasets.

Table 8.1 Classification performance (Average values) for apples stored for four weeks

Sample	Classifier [1]	Training Set (%)			Validation Set (%)		
		Precision	Recall	Accuracy	Precision	Recall	Accuracy
0 °C	LDA	83	83	83	86	80	80
	kNN	88	88	88	81	70	70
	RF	100	100	100	86	80	80
	AdaBoost	100	100	100	80	80	80
	PLS-DA	**98**	**97**	**97**	**98**	**97**	**97**
4 °C	LDA	100	100	100	69	67	70
	kNN	73	75	74	70	71	70
	RF	100	100	100	88	75	80
	AdaBoost	100	100	100	88	75	80
	PLS-DA	**92**	**92**	**92**	**92**	**88**	**91**
10 °C	LDA	92	92	92	88	80	82
	kNN	79	75	76	73	73	73
	RF	100	100	100	73	72	73
	AdaBoost	92	92	92	63	63	64
	PLS-DA	**83**	**83**	**83**	**84**	**83**	**83**

RF: Random Forest, kNN: k-Nearest Neighbors, LDA: Linear Discriminant Analysis, PLSDA: Partial Least Square Discriminant Analysis

Table 8.2 Classification performance (Average values) for apples stored for eight weeks

Sample	Classifier [1]	Training Set (%)			Validation Set (%)		
		Precision	Recall	Accuracy	Precision	Recall	Accuracy
0 °C	LDA	93	97	96	100	100	100

	kNN	80	72	84	36	50	73
	RF	100	100	100	90	67	82
	AdaBoost	100	100	100	90	67	82
	PLS-DA	**100**	**100**	**100**	**100**	**100**	**100**
4 °C	LDA	96	96	96	94	88	91
	kNN	53	53	52	65	66	64
	RF	100	100	100	89	75	82
	AdaBoost	100	100	100	94	88	91
	PLS-DA	**88**	**89**	**89**	**89**	**89**	**89**
10 °C	LDA	100	100	100	71	70	70
	kNN	88	88	88	25	50	50
	RF	100	100	100	71	70	70
	AdaBoost	100	100	100	86	80	80
	PLS-DA	**100**	**100**	**100**	**88**	**89**	**88**

RF: Random Forest, kNN: k-Nearest Neighbors, LDA: Linear Discriminant Analysis, PLSDA: Partial Least Square Discriminant Analysis

Table 8.3 Classification performance (Average values) for apples stored for twelve weeks

Sample	**Classifier [1]**	**Training Set (%)**			**Validation Set (%)**		
		Precision	**Recall**	**Accuracy**	**Precision**	**Recall**	**Accuracy**
0 °C	LDA	97	94	96	71	68	73
	kNN	33	50	67	32	50	63
	RF	100	100	100	89	75	82
	AdaBoost	100	100	100	94	88	91
	PLS-DA	**86**	**86**	**88**	**88**	**88**	**88**
4 °C	LDA	98	90	96	45	45	82
	kNN	95	80	92	45	50	91
	RF	100	100	100	45	50	91
	AdaBoost	100	100	100	45	50	91
	PLS-DA	**93**	**98**	**97**	**92**	**98**	**97**
10 °C	LDA	90	88	88	86	83	82
	kNN	45	47	48	75	58	55
	RF	100	100	100	86	83	82
	AdaBoost	100	100	100	86	83	82
	PLS-DA	**92**	**92**	**92**	**89**	**89**	**89**

RF: Random Forest, kNN: k-Nearest Neighbors, LDA: Linear Discriminant Analysis, PLSDA: Partial Least Square Discriminant Analysis

Table 8.4 Classification performance (Average values) for apples stored for 16 weeks

Sample	**Classifier [1]**	**Training Set (%)**			**Validation Set (%)**		
		Precision	**Recall**	**Accuracy**	**Precision**	**Recall**	**Accuracy**
0 °C	LDA	97	93	96	93	90	91
	kNN	75	73	80	66	65	64
	RF	100	100	100	88	80	82
	AdaBoost	100	100	100	83	70	73
	PLS-DA	**98**	**96**	**98**	**98**	**95**	**97**

4 °C	LDA	92	83	88	81	75	73
	kNN	91	94	92	86	83	82
	RF	100	100	100	92	92	91
	AdaBoost	100	100	100	92	92	91
	PLS-DA	**96**	**93**	**94**	**96**	**93**	**94**
10 °C	LDA	100	100	100	100	100	100
	kNN	100	100	100	100	100	100
	RF	100	100	100	100	100	100
	AdaBoost	100	100	100	100	100	100
	PLS-DA	100	100	100	100	100	100

RF: Random Forest, kNN: k-Nearest Neighbors, LDA: Linear Discriminant Analysis, PLSDA: Partial Least Square Discriminant Analysis

Table 8.5 Classification performance (Average values) for apples stored for 20 weeks

Sample	Classifier [1]	Training Set (%)			Validation Set (%)		
		Precision	Recall	Accuracy	Precision	Recall	Accuracy
0 °C	LDA	100	100	100	54	53	55
	kNN	92	85	88	83	70	73
	RF	100	100	100	65	62	64
	AdaBoost	100	100	100	65	62	64
	PLS-DA	**86**	**86**	**86**	**86**	**84**	**86**
4 °C	LDA	100	100	100	72	58	50
	kNN	43	50	87	20	50	40
	RF	100	100	100	72	58	50
	AdaBoost	100	100	100	20	50	40
	PLS-DA	**93**	**78**	**87**	**93**	**82**	**88**
10 °C	LDA	100	100	100	90	90	89
	kNN	89	85	86	79	70	67
	RF	100	100	100	83	80	78
	AdaBoost	100	100	100	90	90	89
	PLS-DA	**97**	**93**	**94**	**95**	**93**	**93**

RF: Random Forest, kNN: k-Nearest Neighbors, LDA: Linear Discriminant Analysis, PLSDA: Partial Least Square Discriminant Analysis

Based on the comparison of means, it was found that the mean classification rates were significantly higher in the fourth four-week period (week 13 to 16) than the other four-week periods in the whole 20 weeks of storage. This could be as a result of infestation development until week 16 while the majority of control samples were still in good shape. However, in the period between the 16th and 20th week of storage, the control samples were degraded as shown in Figure 8.2. This change again will be a source of variability added to the classification models, which probably interfered with the discriminative power of classifiers.

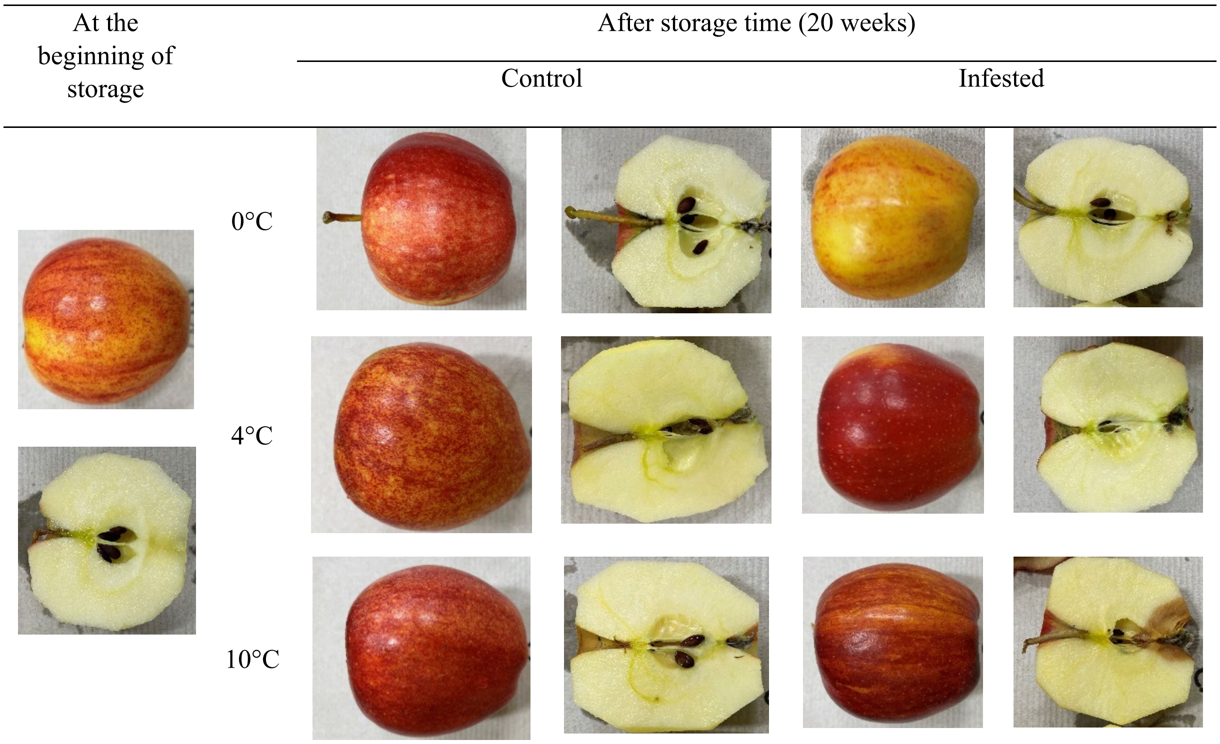

Figure 8.2 Typical CM-infested and healthy apple samples at different storage conditions

Table 8.6 illustrates the classification performance of the different models for all the apple samples stored at three temperatures and different storage times. From the table, it was observed that the classification rates for the combined samples were remarkably lower than when the samples were studied separately (see Tables 8.1 to 8.5). This is probably because of increased variability from the individual data set from each cultivar that reflects in the combined classification model, which resulted in a decrease in the discrimination power of the classification models.

Table 8.6 Classification results for the Gala apples from all the storage temperatures and times combined.

Sample	Classifier [1]	Training Set (%)			Validation Set (%)		
		Precision	Recall	Accuracy	Precision	Recall	Accuracy
	LDA	71	70	73	70	70	70
	kNN	75	74	76	66	66	65
All	RF	**100**	**100**	**100**	67	66	66
	AdaBoost	76	78	75	71	71	70
	PLS-DA	**73**	**73**	**75**	**73**	**73**	**74**

RF: Random Forest, kNN: k-Nearest Neighbors, LDA: Linear Discriminant Analysis, PLSDA: Partial Least Square Discriminant Analysis

Table 8.7 shows that the classification rates for Gala apples at 0 °C are higher than the samples at 4 °C and 10 °C. Higher classification rates at 0 °C is probably due to better preservative effect of low temperature on apple quality and yet allowing the detectability of infested samples. But at high temperatures like 10 °C, the rate of senescence or deterioration of both the control and infested samples were much higher. The obvious changes in the physicochemical properties of apples at higher temperatures were similar to the changes in the CM-infested apples resulting in the poor performance rate in the classification of the two classes. This source of variability between the two classes at high temperature might have caused similar changes making it harder for the models to classify the two.

Table 8.7 Classification results for the entire storage duration at each temperature for Gala apples

Sample	Classifier [1]	Training Set (%)			Validation Set (%)		
		Precision	Recall	Accuracy	Precision	Recall	Accuracy
0°C	LDA	83	81	85	78	77	75

	kNN	74	72	77	75	72	70
	RF	**100**	**100**	**100**	79	79	79
	AdaBoost	87	87	89	81	74	72
	PLS-DA	**85**	**87**	**86**	**84**	**87**	**86**
4°C	LDA	79	77	81	69	65	69
	kNN	74	70	76	61	61	62
	RF	100	100	100	70	61	67
	AdaBoost	91	86	90	84	67	73
	PLS-DA	**81**	**77**	**82**	**82**	**82**	**82**
10°C	LDA	71	71	71	72	71	75
	kNN	76	76	77	71	72	73
	RF	**100**	**100**	**100**	**79**	**80**	**80**
	AdaBoost	85	86	85	70	67	73
	PLS-DA	**81**	**80**	**80**	**80**	**80**	**80**

RF: Random Forest, kNN: k-Nearest Neighbors, LDA: Linear Discriminant Analysis, PLSDA: Partial Least Square Discriminant Analysis

8.4 Conclusion

In this chapter, the detectability and classification rate of CM-infested apples were investigated over a 20-week storage period. The results concluded that storage temperature and duration had significant effect on the classification performance of CM-infested and control Gala apples. No live CM larva were found in the samples stored at 0 °C, 4 °C, and 10 °C after 4, 8, and 17 weeks, respectively. While the classification rates for all the treatments using PLS-DA gave good results, the apples at the lowest cold storage condition (0 °C) for a period of 16 weeks showed the highest detectability and classification rate. The combined samples from all the different storage conditions and times gave relatively poor results, therefore, the suggestion is that classification models be developed and applied for different apple conditions separately. This study shows that nondestructive HSI approach is a practical and effective method for detecting and classifying CM infestation in stored apples along the supply chain.

CONNECTING STATEMENT

In the previous chapters, the acoustic and HSI methods were examined for the detecting and classifying CM-infested apples. While both methods gave promising results, they have their own advantages and limitations. If data from both are fused, we hypothesized that it might be possible to harness the merits of both to increase CM-detection rate in apples. In chapter 9, sensor data fusion method for the raw data (low-level) and the selected features (mid-level) will be implemented to investigate its effect on improving nondestructive CM infestation detection and classification performance in apples.

CHAPTER 9. OBJECTIVE SEVEN

CLASSIFICATION OF CM-INFESTED APPLES USING SENSOR DATA FUSION OF ACOUSTIC AND HYPERSPECTRAL IMAGING FEATURES COUPLED WITH MACHINE LEARNING

Abstract

Our previous studies demonstrated the potential of hyperspectral imaging (HSI) and acoustic methods as suitable techniques for the nondestructive codling moth (CM) infestation detection and classification in apples. However, both have limitations that can be addressed by the strength of the other. For example, acoustic methods are incapable of detecting CM external symptoms such as eggs but could determine internal morphological damages, whereas HSI can detect CM eggs but only capable of surface detection of changes in apples. This study investigated the possibility of sensor data fusion from HSI and acoustic signals on improved detection of CM-infestation in apples. The time and frequency domain acoustic features were combined with the spectral features obtained from HSI and various classification models were applied. The results showed that the sensor data fusion using the selected features (mid-level) gave high result in term of classification performance and reduced model complexity with a classification accuracy of up to 97% using only six acoustic and six hyperspectral image features. Therefore, this result suggests that sensor fusion technique can improve CM- infestation detection in pome fruits like apples.

9.1 Introduction

Apples are one of the most valuable fruits in the U.S. with a domestic consumption and total exports of around 4.1 and 0.87 million metric tons, respectively (USDA, 2020). Codling moth pest causes significant damages in apples. The presence of CM can cause a reject of a fruit shipment from most U.S. export destinations (Suffert et al., 2018). To improve the detection approach, there is a need to develop rapid, effective, and accurate nondestructive detection methods for CM infested apples.

In general, fruits have complex and dynamic textures with different characteristics. As a result, only limited information of fruit samples can be obtained using an individual sensing technique (Zhou et al., 2020). Thus, merging the data from different sensors can give a comprehensive information about the characteristics of fruits and improve the prediction and classification rates through better understanding of internal and external states of the produce.

Information fusion strategy has been defined as a way of fusing data from different sensors or knowledge from different models, while the relationship between the fused information and the target parameter is represented as mathematical models (Zhou et al., 2019). Based on the type of information to be fused, three level of fusion strategies have been defined: (1) measurement or low-level fusion, (2) feature or mid-level fusion, and (3) decision or high-level fusion (Khaleghi et al., 2013). In the first level of fusion, raw data from sensors are simply integrated as a new dataset for further processing. This strategy suffers from high amounts of redundant and noisy data. For the second level of fusion, the extracted features from each sensing techniques are fused as input to the final model. This method can address the redundancy and noise issues for achieving improved results. In the third level of fusion, the output of multiple models is combined for full evaluation of the final decision. As an example, the majority voting method takes into account the results of many classifiers to provide an overall decision. While the decision fusion strategy potentially reduces the interference by the limitations of different models, it has the risk of losing important information in the raw data (Khaleghi et al., 2013).

Recently, the fusion strategies have been used in some studies on defect detection and quality assessment of fruits. Liu et al. (2019) applied a mid-level/feature fusion method based on HSI and E-nose data for fungal contamination detection in strawberries. They concluded that while the raw data fusion of HSI and E-nose resulted in low prediction rate and high processing time, the feature fusion method improved the detection accuracy compared to each of those individual sensing methods. In another study, the application of the fusion of acoustic measurements and convolutional neural networks method for mealiness determination in Red Delicious apples was investigated. From the results presented, the accuracy of the fused model for classifying mealy and normal apples was 91.11% and 86.94%, respectively.

CM attack leads to changes in both external and internal physicochemical characteristics of apples. While fusion of different sensing methods can provide comprehensive and combined information related to the infestation, individual sensing techniques will only capture one (or a few) of the many aspects of infestation damage. For example, HSI provides physical and chemical information from the top layers of fruit tissue and flesh (Liu et al., 2019); it is not able to capture data from the core of apples. On the other hand, vibrational/acoustic methods can be used to monitor and detect the infested apples through sensing either the activities of the insects that bored deep into the fruit or the internal textural changes related to the infestation. The output of the two sensing systems can be analyzed using multivariate data analysis methods to detect specific patterns in the data. Thus, the goal of this study was to investigate the application of the sensor fusion approach (HSI and acoustic) for improving classification accuracy for the detection of CM infestation in apples. Since the capability of rapid detection by HSI and acoustic can be negatively affected by large data dimensionality, the specific objective was to perform the mid-level fusion with feature extraction and feature selection from the raw HSI and acoustic data and then develop the fusion models based on multiple optimum features.

9.2 Material and Methods

9.2.1 Sample Preparation

The apple samples used in the experiments were organic Gala, Fuji, and Granny Smith cultivars purchased from a commercial market in Princeton, KY, USA in October 2020. After careful inspection, 60 apple samples without any form of mechanical damage which were similar in size, diameter and shape were chosen from each cultivar (180 samples in total). The apples were then disinfected against fungal and bacterial decay in a 0.5% (v/v) sodium hypochlorite solution. The samples were washed with distilled water and dried in open air at ambient conditions at 25±2 °C in the lab (Department of Entomology, University of Kentucky, USA). To artificially infest the apples, a first instar CM larva was placed near the calyx end of each apple in an isolated cup (8 cm bottom diameter, 10 cm top diameter, 10 cm high) with a plastic lid for respiration purpose. Apples of each cultivar were divided into 20 control and 40 infested groups and stored in an environmental control chamber at 27 °C and 85% relative humidity for three weeks to cause infestation to occur. The hyperspectral data acquisition was carried out in the Food Engineering lab at Biosystems and Agricultural Engineering Department, University of Kentucky, Lexington, KY, USA.

9.2.2 Hyperspectral Image Acquisition and Spectra Extraction

The short wave near-infrared (SWNIR) HSI system in the spectral range of 900–1,700 nm was used to acquire hyperspectral images of healthy and infected apples for each cultivar. This system was composed of an imaging spectrograph (N17E, Specim, Oulu, Finland), a InGaAs camera (Goldeye infrared camera: G-032, Allied Vision, Stradtroda, Germany), a stepping-motor-driven moving stage (MRC-999-031, Middleton Spectral Vision, Middleton, WI), and a 150 W halogen lamp (A20800, Schott, Southbridge, MA, USA). The hyperspectral imaging system was a push broom (line scanning) type. To acquire clear images, the parameters of the sample stage speed, the exposure time of the camera, the halogen lamp angle, and the vertical distance between the lens and the sample, were set to 10 mm/s, 40 ms. 45° and 25 cm, respectively. Samples were placed on the sample stage and captured in a line scanning or pushbroom mode. The acquired hyperspectral images contained wavelength bands stored in "*.raw" format along with a header file in "*.hdr" format.

9.2.3. Acoustic Impulse Response Test and Signal Recording

After the hyperspectral image acquisition, each sample was used for the acoustic test. A schematic of the acoustic impulse response test is shown in Figure 9.1. It consisted of two main parts: the acoustic recording unit and the impulse or knocking unit. The impulse or knocking test unit consisted of two major components: an impulse generator, and a mechanical support structure (retort stand) to securely hold the apple, impulse generator, and a sensor in repeatable relative positions (Figure 9.1). The support structure was constructed from standard lab metalware. The structure was supported on a single ring-stand with a cast-iron base to minimize resonance (American Educational 7-G15-A). A three-prong gripper was hung from the stand using a 90° bosshead. The outer two grippers are 0-30 mm rubber coated Zinc alloy flask clamps (from Dtacke), which hold the solenoid used to generate the impulse in the bottom gripper and the sensor pickup in the top gripper. The apple is held between them with 10-90 mm rubber-coated three-prong grips as shown in Figure 9.1.

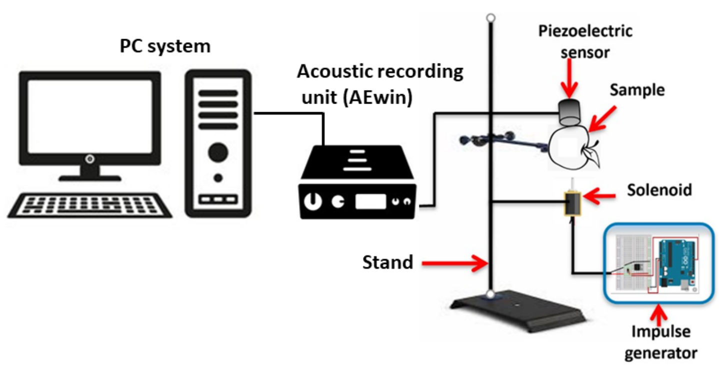

Figure 9.1 A schematic diagram of the acoustic impulse response system for data acquisition from apple

To collect data, the apple to be tested was placed between the large central three-prong gripper and secured with its actuating screw. The other two grippers were then adjusted vertically on the rod and laterally in their bosses such that they made firm contact with the top and bottom of the apple. A spacer attached to the end of the solenoid was used so its head could be placed at a consistent distance from the surface of the apple such that the same portion of the stroke was in contact with the apple for each test. This configuration gave the necessary degrees of freedom to consistently accommodate apples with a variety of sizes and shapes, while still firmly and repeatably securing them during the test.

The impulse generator was a solenoid precisely driven by a microcontroller (Apex AGM32F103CB, RobotDyn, Arduino, Ivrea, Italy) through an amplifying transistor. The solenoid used was a Guardian Electric model A420-067074-01 (Guardian Electric Manufacturing, Woodstock, Illinois, USA). The solenoid delivered impact through a 6.35 mm radiused nose on the armature. The impulse was triggered by a simple push-button pressed by the experimenter after data capture had been initiated. The input button was connected to the microcontroller and pulled up through the internal resistor. The microcontroller tying the system together was an Apex AGM32F103CB in a “Black Pill” breakout board from RobotDyn, running the Arduino bootloader. It was configured with a simple circuit to make it act as a one-shot pulse generator, producing a single 50 μs output pulse on each button press, with hold-off to filter any potential switch bounce. The 50 μs charge was chosen as it is adequate to reliably “bottom out” the solenoid's pin to maximum extension against gravity at 9 V. The output pulse from the microcontroller was then driven into the base of a TIP-31c NPN transistor through a 130 Ω resistor, to handle the large current requirement and EMF kick of the solenoid. The solenoid was lower side switched by the transistor. Power for the system was supplied by a commodity 9 V DC “wall wart” power adapter.

The acoustic recording unit was a custom-designed system to record the high-frequency acoustic response signals from apples generated by the impulse/knocking test. This system consisted of a contact piezoelectric sensor (R6α-SNAD 52, Physical Acoustics Corporation, New Jersey, USA) with a frequency range of 35 to 100 kHz, a preamplifier (model1220A, Physical Acoustics Corp., Princeton Junction, N.J.), an I/O board (PCI-2, Physical Acoustics Corp.), and signal processing software (AEwin by MISTRAS).

To reduce the ambient noise, the acoustic impulse response experimental unit was set above an isolated table that had a 15 cm layer of sand, topped with a 5 cm slab of granite with acoustic padding. This unit was in a room with a concrete padded floor built on 20 cm of gravel above the loam soil bed in an isolated room in Food Engineering lab at the Biosystems and Agricultural Engineering Department, University of Kentucky, Lexington, KY, USA. To carry out each test, an apple was placed between the sensor and the impulse generator (solenoid). Signal recording for each test was performed for 10 seconds with two impulses for each apple where the first impulse was generated in the 5th second and the second impulse in the 10th second. The acoustic signals derived from the knocking impulse on apples were collected and processed by different signal processing methods and then the time-domain and frequency-domain features of vibration acoustic signals were extracted to be used in machine learning classification models.

After manually segmenting the actual impulse moment from the entire signal, 21 important time and frequency domain features were extracted (Table 3.1) using a code (Appendix A) created in MATLAB. Having these features as the variables (columns) for all the sample (as rows), the dataset was built to be used for the machine learning classification. Also, these features were concatenated with the HSI features to build the data fusion models.

9.2.4 Data Fusion Strategies

Data fusion has been defined as the fusion of the data acquired using different sensors (Doeswijk et al., 2011). In this study low-level and mid-level data fusion strategies were implemented to combine information from the hyperspectral and acoustic datasets for CM infestation detection in apples. In low-level fusion, the raw hyperspectral, and acoustic datasets were concatenated into a single matrix by merging them along the rows. This resulted a combined data matrix with the same number of rows as the number of samples. The columns were the combined variables from each dataset (241 spectral plus 21 acoustic). However, since the features from different sensors had different scales, a z-score normalization was used for rescaling purpose before building the model. In mid-level fusion, the extracted features from the hyperspectral dataset using the PCA method were fused with the optimum acoustic features selected by the Pearson correlation method (six HSI and six acoustic features). Then these merged data matrices from the low-level and mid-level methods were used to build multivariate calibration models.

9.2.5 Classification Models

After creating the datasets, to build and compare different classifiers, PyCaret (version 2.3.10) machine learning library in Python was used. The result of 15 different classifiers were analyzed and compared and the best model obtained was the ensemble AdaBoost method based on the total accuracy, recall, and precision. Then the average values for the accuracy, recall, precision, and F1-score were calculated in a five-fold cross validation process.

9.3 Results and Discussion

9.3.1 Classification Models Using Single Acoustic and HSI Datasets

The results of the classification models using each of the acoustic and hyperspectral datasets are shown in Table 9.1. Between the two datasets, the acoustic data gave higher classification rates than the mean spectra hyperspectral data. AdaBoost model with acoustic data from Gala apples achieved an accuracy of 97% for the test set. The best classification accuracy for the HSI method was obtained for Fuji apples as 88%.

For the combination of all three cultivars, while the acoustic method achieved an acceptable classification rate in lower ninety percent range, the HSI gave a poor classification accuracy. The lower classification results for the combined samples could be related to the different textural and surface color characteristics of the three cultivars, causing extra biological variability into the model.

Table 9.1 The test-set classification results based on different sources of data from each individual sensor using ensemble AdaBoost classifier.

Cultivar	Features	Variables	Accuracy	Recall	Precision	F1 score
Fuji	Full-HSI	241	88	88	91	88
	Acoustic	21	90	87	89	88
Gala	Full-HSI	241	79	62	67	79
	Acoustic	21	97	97	96	97
GS	Full-HSI	241	71	71	71	71
	Acoustic	21	95	92	91	91

Combined	Full-HSI	241	64	65	68	64
	Acoustic	21	94	93	93	93

HSI: Hyperspectral Imaging

9.3.2 Classification Models Based on Selected Feature

The results of machine learning classification based on the HSI features extracted by PCA and the acoustic features selected by Pearson correlation method are presented in Table 9.2. Overall, PCA-based HSI models showed better performance than models based on full HSI spectra while the dimensionality of the data decreased significantly from 241 to 5, 10, or 15 features. This improved classification performance was due to reducing both the dimension of data and the redundancy of variables. However, for the acoustic models with the selected features a slight decrease in the classification performance was observed because the dimension of the acoustic data was low and in the feature selection process some of the information (less significant features) were probably removed from the dataset. Although, this slight decrease in the classification rate will be compensated by having a model with only six features in comparison to 21 features.

Table 9.2 The classification results based on selected features from individual HSI and acoustic sensors using AdaBoost classifier.

Cultivar	Features	Variables	Accuracy	Recall	Precision	F1 score
Fuji	PCA-HSI	10	88	91	88	90
	Acoustic	6	84	92	90	91
Gala	PCA-HSI	5	86	50	43	86
	Acoustic	6	95	97	96	97
GS	PCA-HSI	10	71	71	71	71
	Acoustic	6	93	91	89	90

Combined	PCA -HSI	15	69	70	70	69
	Acoustic	6	92	91	92	91

HSI: Hyperspectral Imaging

9.3.3 Classification Models Based on Data Fusion

In the low-level data fusion, the acoustic dataset was directly concatenated with the HSI dataset. The results of classification of CM-infested apples for the three cultivars are presented in Table 9.3. In terms of the Gala cultivar, the classification performance of the low-level data fusion model was superior to each of the individual acoustic and HSI models, with all the performance metrics surpassing 98% for the test set. The combination of acoustic and HSI improved the classification accuracy for Gala apples by 24% compared with Full-HSI spectra and by around 2% compared to full acoustic dataset. Particularly important is the perfect recall result for Fuji and Gala apple cultivars. The implication of 100% result is that all the infested apples were 100% classified correctly with zero false negative. The high misclassification of infested apples in the GS apples, which have clearly different color and surface reflectance, may be attributed to the skin pigmentation and reflection during HSI scanning. This pigmentation effect can also be reflected in the combined data from all the three cultivars.

Table 9.3 The performance of classification models based on complete data fusion.

Cultivar	Features	Variables	Accuracy	Recall	Precision	F1 score
Fuji	Acoustic -HSI	21+241	98	100	97	98
Gala	Acoustic - HSI	21+241	98	100	98	99
GS	Acoustic -HSI	21+241	92	91	97	94

Combined	Acoustic -HSI	21+241	90	93	92	93

HSI: Hyperspectral Imaging

In the mid-level fusion, the optimum features separately extracted by Pearson correlation and PCA for the acoustic and HSI datasets, respectively, were merged as a single matrix to be used for classification analysis (Table 9.4). The mid-level data fusion gave highly satisfactory results for all the three apple cultivars. For example, for Gala apples, the accuracy, recall, precision, and F1-score were 98%, 98%, 100%, and 99%, respectively. This high classification rates using the mid-level data fusion is specifically noticeable in combined samples from all the cultivars compared to the low-level fusion. Using the mid-level fusion approach, it is possible to classify CM-infested apples in a sample of the three different cultivars with an accuracy, recall, precision, and F1 score of 94%, 97%, 95%, and 96%, respectively.

Table 9.4 The classification performance based on fusion of selected acoustic and HSI features.

Cultivar	Features	Variables	Accuracy	Recall	Precision	F1 score
Fuji	Acoustic -PCA-HSI	6+6	94	97	94	96
Gala	Acoustic - PCA-HSI	6+6	97	97	100	98
GS	Acoustic -PCA-HSI	6+6	88	91	92	91
Combined	Acoustic -PCA-HSI	6+6	94	97	95	96

9.4 Conclusion

In this chapter, the fusion of acoustic and hyperspectral images of apples were studied at two levels for classifying CM-infested apples. Features were fused using the low- and mid-level approach and with the application of AdaBoost, a pre-determined best classifier. The performance of the classifications based on individual raw data was improved by the fusion methods leading to more reliable results. Results showed that the combined selected features (mid-level fusion) were better than using all the combined features (low-level fusion) in the classification of CM-infested apples. This improvement is particularly important in the case of the combined apples where the data fusion gave the accuracy, recall, precision, and F1-score of 96%, to 94%, 97%, 95%, and 96% in the classification of CM-infested apples regardless of the cultivar, respectively. These results proved that sensor/data fusion approach can improve classification accuracy for any CM-infested apples and consequently help improve the sorting process for CM-damaged apples from three different cultivars.

CHAPTER 10. CONCLUSION AND FUTURE WORK

The demand for apples, as one of the most popular and valuable fruits in the world, is seeing a considerable growth in the global market. This increased demand is even more noticeable for organic apples due to the consumers' growing concern for health and wellness. Moreover, after the COVID-19 pandemic, the production of fresh apples is projected to witness a compound annual growth rate (CAGR) of 4.0% during 2022-2027 to meet the global market needs. On the other hand, the problem of insect pests and invasive species continues to impose a threat to the apple industry due to the considerable growth in global supply chain of apples, especially for more susceptible organic produce. Among the worst invasive alien insect pests in the world is the codling moth, which is considered as the most devastating pest of apples. Notwithstanding, the current method of sorting apples against this pest is mostly manual and random that is inefficient, laborious, and often unreliable. While there have been some nondestructive technologies introduced to the modern apple processing, a lot of research is needed to overcome the limitations of the current methods. For instance, machine vision is not capable of detecting CM infested apples where the damage is mostly internal. Thus, in this research, two effective nondestructive quality evaluation methods were developed to detect and classify CM infestation in apples.

The first approach was based on the acoustic methods. The initial results showed a difference in the acoustic signals coming from CM-infested and control apples. But we faced the question of "what is the source of these acoustic events?" as a first consideration. Two acoustic techniques were used to answer this question: low frequency vibro-acoustic and high-frequency impulse response tests. In a study which may be first of its kind, it was shown that the different activities of the CM larva have different repeatable patterns in the low-frequency range. For example, the larva chewing signals showed a chewing rate of 1 to 2.3 times a second and the internal movement of larva showed large transient spikes at irregular intervals. Additionally, our findings showed that it is possible to accurately detect these signal patterns using a newly designed matched filter coupled with machine learning models with a classification rate of 100% for test data set with a signal recording of 5 s. Also, as the second acoustic technique, we applied a novel knocking test to correlate the acoustic impulse response from CM-infested apples to the mechanical and textural changes in the infested samples. Results showed that there is a difference in the spectral properties of the signals for infested versus control apples. These differences in the signals led to a fast impulse signal length of 60 - 80 ms and accuracy up to 99% for the classification of infested samples using the optimally selected features and machine learning classifies.

The second approach used in this dissertation for nondestructive detection of CM-infested apples was the HSI method. Some main questions regarding the application of this method were: can we determine and predict the important quality characteristics of CM-infested apples in comparison to control ones using HSI? Is there any difference between the spectral information of the CM-infested apples and healthy ones? Is the HSI method capable of detecting and classifying CM infestation in apples with high performance? How do storage conditions and external stimulation impact classification accuracy? The results in this dissertation showed that CM infested apples can be classified using NIR HSI method with high accuracy up to 97% for test dataset.

In the last objective, consideration was given to sensor data fusion from the acoustic and HSI methods to achieve better classification performance. Since the high-frequency acoustic impulse method gave higher accuracies in shorter time, it was used for the acoustic method in the fusion approach with the HSI. Our findings revealed that fusion of selected features (mid-level fusion) was superior to models from using all the combined features (low-level fusion) with an accuracy of 97% with only 6 acoustic and 6 hyperspectral features.

Future Work

This dissertation showed the high potential of the novel approaches developed for the nondestructive detection of CM-infested apples. However, there are some opportunities for future research that could potentially improve the outcomes presented in this body of work.

The application of acoustic methods as a nondestructive approach in the apple industry is a novel approach we have proposed. However, there are some challenges in the implementation of this method such as cost, noise-tolerance, and the target signal activity issues that we tried to address in this dissertation. The cost of acoustic system depends on some factors like the frequency range, the sensor technology, and the signal recording technology. Usually the higher-frequency systems are more expensive because of the need for higher sampling rate than lower-frequency ones. In my dissertation, we obtained high classification rates using the cheap low-frequency sensors, which can be designed for simultaneous multiple sensor scanning. Another main issue to consider in acoustic methods is the noise-tolerance which means isolating the subject from the background noise. This issue is more challenging in the passive and lower frequency methods. In this regard, the high-frequency active impulse test used in the current dissertation is superior for the applications in noisy industrial environments. The concept of activity of the target signal is an issue where the larval activity of the insect is desired. For example, the low-frequency vibro-acoustic method developed in this dissertation detects the known signal patterns generated by the CM larva. Since there are some moments when the larva is inactive, there may be no detection for a truly infested sample (false negative). Two approaches studied in this dissertation to tackle this problem were to artificially stimulate the insect with example heat, and to develop an active impulse test, which does not depend on the larval activity. Thus, for future work I suggest studying other insect stimulation methods as well as developing hardware (sensors and signal recording equipment) and software (algorithms) to detect the underlying patterns in more noisy data collection environments.

For the HSI method, one major area to work on in the future for the apple quality evaluation is assessing the robustness of the models for non-controlled (out-door or industrial) conditions. This can open new doors for the application of the HSI method used in this dissertation in orchards for drone based or robotic driven apple quality assessment. One other area to consider as future work is the application of deep learning and convolutional neural networks (CNN) for the classification of the hyperspectral images regarding CM infestation.

APPENDIX

MATLAB Codes used for defining and extracting the acoustic features.

1) The function to define acoustic features

```
function fm = ACM_tdfe(sig,fs)
Amplitude = (max(sig)/10);
Duration = (length(sig)/1000000);
fftsig = fft(sig,2^nextpow2(length(sig)));
Length_Signal = length(sig);
fs=1e6
faxfft = [0:length(fftsig)-1]/length(fftsig)*fs;
fftsigOSS = fftsig(1:ceil(length(fftsig)/2));
Average_signal_level = mean(sig);
Variance = var(sig);
Kurtosis = kurtosis (sig);
Skewness = skewness (sig);
Mean_absolute_deviation = mad (sig);
Crest_factor = peak2rms(sig);
Root_mean_square = rms(sig);
Entropy = entropy(sig);
Rise_time = risetime (sig);
Mean_rise_time = mean(Rise_time);
Square = (sig).^2;
Absolute_Energy = sum(Square);
Area_under_curve = sum(sig);
Signal_Strength = Absolute_Energy/Length_Signal;
pks = findpeaks(sig);
Average_number_of_peaks = length (pks)/Length_Signal;
t = [0:1/fs:length(sig)/fs-(1/fs)];
```

```
zci = @(v) find(v(:).*circshift(v(:), [-1 0]) <= 0);

zx = zci(sig);

Number_zero_crossing = length (zx);

Energy_spectral_density = abs(sum(fftsigOSS.^2));

[p,fax] = pwelch(sig,hamming(256),128,512,1e3);

[~,i] = max(p);

Maximum_PSD = fax(i);

[freq_response,freq_index] = freqz(fftsig,1,length(sig),fs);

pM = max(abs(freq_response));

pF = freq_index(abs(freq_response)==pM);

power_BW = powerbw(p,fax);

[S,F,T,P] = spectrogram(sig);

Spectral_Entropy = pentropy(P,F,T)';

Max_Spectral_Entropy = max(Spectral_Entropy);

pks = findpeaks(abs(fftsig));

numpks = length(pks);

FFT_Mean_Coe = mean(abs(fftsigOSS));


fm =
[Amplitude,Duration,Average_signal_level,Variance,Kurtosis,Skewness,Mean_absolute_
deviation,...

    Root_mean_square,Entropy,Mean_rise_time,Absolute_Energy,Area_under_curve,...

    Signal_Strength,Average_number_of_peaks,
Number_zero_crossing,Energy_spectral_density,...

    Maximum_PSD,pF,power_BW,Max_Spectral_Entropy,numpks,FFT_Mean_Coe];


End
```

---

2) The function to read the signals from the recording system to MATLAB

```
function [sigout1, sigout2, eof] = cmwfread2att2(f,p,startsamp,numsamp)

%  Function will read waveform files from the PCI-2 system from mistras into a vector.
```

```
%  sigout = cmwfread(f,p,startsamp,endsamp)
%  f => String indicating file name
%  p => String indicating path name
%  startsamp => Integer indicating the starting sample from the beginning
%  endsamp => Integer indicating how many samples to read
%  sigout => output vector
%
%  written by Kevin D. Donohue kevin.donohue1@uky.edu, 7/20/2019
%
%  fuction will read in a few samples before and after the requested number
%  if the starting and ending samples do not correspond to the begining and
%  ending of a block

headerbytes = 310; %310; %236; %304; %  Bytes in header
blksize = 1039;  % data plus tralier record
recsize = 15;  % 16 bit samples in record header
datasize = 1024;  % 16 bit signed number is record
fid = fopen([p,f],'r'); %open file
fseek(fid,headerbytes,-1); % skip header bytes

eof = 0;  % Set end of file flag
% figure out which block the starting sample occurs in
numblocks = floor(startsamp/datasize);
%  Just read the whole block in with the starting sample.
fseek(fid,2*numblocks*blksize,0);

sigout1 = []; % initialize output vector
sigout2 = []; % initialize output vector
```

```
sampcnt = 0;  % initialize  sample counter to test for end of segment
%  Loop to read in each block until number of samples reached or end of
%  file
channel = 1;
while eof == 0 && sampcnt <= numsamp
[da, cnt] = fread(fid,blksize,'int16','b');  % read in block
sampcnt = sampcnt+datasize;
if feof(fid)
   eof = 1;
end
% sigout1 = [sigout1; da(1:2:datasize)];
% sigout2 = [sigout2; da(2:2:datasize)];

   if channel == 1
      sigout1 = [sigout1; da(1:datasize)];
      channel = 2;
   else
      sigout2 = [sigout2; da(1:datasize)];
      channel = 1;
   end


end


if length(sigout1) > length(sigout2)
   sigout1 = sigout1(1:length(sigout2));
else
   sigout2 = sigout2(1:length(sigout1));
end
```

```
fclose(fid)
```

---

3)

```
% This script prompts to open a single file and then slides an analysis
% window over the signal extract features from every window with 50%
% overlap. The array of feature vectors are stored row-wise and saved to
% a csv file and a mat file.
clear

fc = [300 16e3]; % low-pass cutoff (You may want to raise this, transducer was at
60kHz)
window = 4096;
noverlap = window/2;
nfft = window*2;
fs = 1e6;

cd 'Data\';
kk = dir;
cd ..

numfiles = length(kk);
files = kk(3:end);

for k =1:length(files)
   fname = files(k).name;
   pname = 'Data\';
   %fprintf("File name  %7s\n", fname);
   %cc = input('What is the name of this apple?: ', 's');
   % read in segment by segment
```

```
    %eof = 0; % end of file flag, eof = 1 means end of file reached
    startsec = 0;  % start in second
    endsec = 10;  % end in seconds, 0.25 seconds longer than wanted. Excess will be
removed.
%
    [sig,sigout2,eof] = cmwfread2att2(fname,pname,2*startsec * fs, 2*(endsec-
startsec)*fs); %Multiply duration *2 since there are 2 signals
% %     if eof ~= 1
% %         sig1cut = sig(1:(endsec-0.25)*fs);
% %         sig2cut = sigout2(1:(endsec-0.25)*fs);
% %     else
% %         error('not enough signal');
% %     end
%
    [s1,f1,t1] = spectrogram(sig,hamming(window),noverlap,nfft,fs);
%     %[s2,f2,t2] = spectrogram(sig2cut,hamming(window),noverlap,nfft,fs);
%
    figure,imagesc(t1,f1,abs(s1))
    temp = strcat(fname, '-Pulse');
    title(temp)
    axis('xy')
    colorbar
    set(gca, 'ColorScale', 'log')
    caxis([1e3 1e6]);
    xlabel('Time (s)')
    ylabel('Frequency (Hz)')
%     saveas(gcf,sprintf('Fig_Infested%d.png',k));
%     clf


% save(
```

```
%    figure,imagesc(t2,f2,abs(s2))
%    temp = strcat(cc, 'Channel 2');
%    title(temp)
%    axis('xy')
%    colorbar
%    set(gca, 'ColorScale', 'log')
%    xlabel('Time (s)')
%    ylabel('Frequency (Hz)')

end
```

REFERENCES:

Abdi, H., & Williams, L. J. (2010). Principal component analysis. *Wiley interdisciplinary reviews: computational statistics, 2*(4), 433-459.

Adedeji, A. (2011). Microstructural characterization of deep-fat fried breaded chicken nuggets using X-ray micro-computed tomography. *Food Process Engineering, 34*. doi:10.1111/j.1745-4530.2009.00565.x

Adedeji, A. A., & Ngadi, M. O. (2009). 3-D Imaging of Deep-Fat Fried Chicken Nuggets Breading Coating Using X-Ray Micro-CT. *Food Process Engineering, 5*(4). doi:https://doi.org/10.2202/1556-3758.1452

Al-Mezeini, N., Manickavasagan, A., Al-Yahyai, R., Al-Wahaibi, A., Al-Raeesi, A., & Khriji, L. (2015). X-ray Imaging of Stored Dates to Detect Infestation by Saw-Toothed Beetles. *International Journal of Fruit Science, 16*. doi:10.1080/15538362.2015.1044692

Alagna, F., Kallenbach, M., Pompa, A., De Marchis, F., Rao, R., Baldwin, I. T., . . . Baldoni, L. (2016). Olive fruits infested with olive fly larvae respond with an ethylene burst and the emission of specific volatiles. *Journal of integrative plant biology, 58*(4), 413-425. doi:10.1111/jipb.12343

Ammari, H. (2008). *An introduction to mathematics of emerging biomedical imaging* (Vol. 62): Springer.

Appel, H. M., & Cocroft, R. (2014). Plants respond to leaf vibrations caused by insect herbivore chewing. *Oecologia, 175*(4), 1257-1266.

Armstrong, P., Stone, M., & Brusewitz, G. (1997). Nondestructive acoustic and compression measurements of watermelon for internal damage detection. *Applied Engineering in Agriculture, 13*(5), 641-645.

Arthur, F., Johnson, J., Neven, L., Hallman, G., & Follett, P. (2010). Insect Pest Management in Postharvest Ecosystems in the United States of America. *Outlooks on Pest Management, 20*. doi:10.1564/20dec10

Association, U. S. A. (2018). Retrieved from https://usapple.org/

Badii, K., Billah, M., Afreh-Nuamah, K., Obeng-Ofori, D., & Nyarko, G. (2015). Review of the pest status, economic impact and management of fruit-infesting flies (Diptera: Tephritidae) in Africa.

Baldwin, E. A., Bai, J., Plotto, A., & Dea, S. (2011). Electronic noses and tongues: Applications for the food and pharmaceutical industries. *Sensors, 11*(5), 4744-4766.

Banga, K. S., Kotwaliwale, N., Mohapatra, D., Giri, S. K., & Babu, V. B. (2019). Bioacoustic detection of Callosobruchus chinensis and Callosobruchus maculatus in bulk stored chickpea (Cicer arietinum) and green gram (Vigna radiata). *Food Control, 104*, 278-287. doi:https://doi.org/10.1016/j.foodcont.2019.02.026

Blasco, J., Aleixos, N., Gómez-Sanchis, J., & Moltó, E. (2009). Recognition and classification of external skin damage in citrus fruits using multispectral data and morphological features. *Biosystems engineering, 103*(2), 137-145.

Blasco, J., Aleixos, N., Gómez, J., & Moltó, E. (2007). Citrus sorting by identification of the most common defects using multispectral computer vision. *Journal of Food Engineering, 83*(3), 384-393.

Blasco, J., Aleixos, N., & Moltó, E. (2007). Computer vision detection of peel defects in citrus by means of a region oriented segmentation algorithm. *Journal of Food Engineering, 81*(3), 535-543.

Blasco, J., Cubero, S., & Moltó, E. (2016). Quality evaluation of citrus fruits. In *Computer vision technology for food quality evaluation* (pp. 305-325): Elsevier.

Blasco, J., Munera, S., Aleixos, N., Cubero, S., & Molto, E. (2017). Machine vision-based measurement systems for fruit and vegetable quality control in postharvest. In *Measurement, Modeling and Automation in Advanced Food Processing* (pp. 71-91): Springer.

Blažek, J., Hlušičková, I., & Varga, A. (2003). Changes in quality characteristics of Golden Delicious apples under different storage conditions and correlations between them. *Horticultural Science (Prague), 30*(3), 81-89.

Bobelyn, E., Serban, A.-S., Nicu, M., Lammertyn, J., Nicolai, B. M., & Saeys, W. (2010). Postharvest quality of apple predicted by NIR-spectroscopy: Study of the effect of biological variability on spectra and model performance. *Postharvest Biology and Technology, 55*(3), 133-143.

Breth, D. I. (2002). Controlling Oriental Fruit Moth in Peaches Using Mating Disruption and Assessing the Problem in Apples.

Burks, C., Dowell, F., & Xie, F. (2000). Measuring fig quality using near-infrared spectroscopy. *Journal of stored products Research, 36*(3), 289-296.

Burns, D. A., & Ciurczak, E. W. (2007). *Handbook of near-infrared analysis*: CRC press.

Cárdenas-Pérez, S., Chanona-Pérez, J., Méndez-Méndez, J. V., Calderón-Domínguez, G., López-Santiago, R., Perea-Flores, M. J., & Arzate-Vázquez, I. (2017). Evaluation of the ripening stages of apple (Golden Delicious) by means of computer vision system. *Biosystems engineering, 159*, 46-58.

Cen, H., Lu, R., Ariana, D., & Mendoza, F. (2013). *Hyperspectral imaging-based classification and wavebands selection for internal defect detection of pickling cucumbers.* Paper presented at the 2013 Kansas City, Missouri, July 21-July 24, 2013.

Center, A. M. R. (2021). Retrieved from https://www.agmrc.org/commodities-products/fruits/apples

Chapman, G. W., Horvat, R. J., & Forbus, W. R. (1991). Physical and chemical changes during the maturation of peaches (cv. Majestic). *Journal of Agricultural and Food Chemistry, 39*(5), 867-870. doi:10.1021/jf00005a010

Che, W., Sun, L., Zhang, Q., Tan, W., Ye, D., Zhang, D., & Liu, Y. (2018). Pixel based bruise region extraction of apple using Vis-NIR hyperspectral imaging. *Computers and Electronics in Agriculture, 146*, 12-21.

Chen, P., & Sun, Z. (1991). A review of non-destructive methods for quality evaluation and sorting of agricultural products. *Journal of Agricultural Engineering Research, 49*, 85-98.

Chen, Y., Yang, W., Li, M., Hao, Z., Zhou, P., & Sun, H. (2018). Research on pest image processing method based on Android thermal infrared lens. *IFAC-PapersOnLine, 51*(17), 173-178.

Chuang, C.-L., Ouyang, C.-S., Lin, T.-T., Yang, M.-M., Yang, E.-C., Huang, T.-W., . . . agriculture, e. i. (2011). Automatic X-ray quarantine scanner and pest infestation detector for agricultural products. *Computers, 77*(1), 41-59.

Cocetta, G., Beghi, R., Mignani, I., & Spinardi, A. (2017). Nondestructive apple ripening stage determination using the delta absorbance meter at harvest and after storage. *HortTechnology, 27*(1), 54-64.

Cortés, V., Blasco, J., Aleixos, N., Cubero, S., & Talens, P. (2019). Monitoring strategies for quality control of agricultural products using visible and near-infrared spectroscopy: A review. *Trends in Food Science & Technology, 85*, 138-148.

Costa, F., Cappellin, L., Longhi, S., Guerra, W., Magnago, P., Porro, D., . . . Biasioli, F. (2011). Assessment of apple (Malus× domestica Borkh.) fruit texture by a combined acoustic-mechanical profiling strategy. *Postharvest Biology and Technology, 61*(1), 21-28.

Cox, T. J. (2014). *The Acoustic Emissions Produced by Escherichia Coli During the Growth Cycle.*

Craig, A. P., Franca, A. S., & Irudayaraj, J. (2013). Surface-enhanced Raman spectroscopy applied to food safety. *Annual review of food science and technology, 4*, 369-380.

Cubero, S., Aleixos, N., Moltó, E., Gómez-Sanchis, J., Blasco, J., & technology, b. (2011). Advances in machine vision applications for automatic inspection and quality evaluation of fruits and vegetables. *Food, 4*(4), 487-504.
Cui, S., Ling, P., Zhu, H., & Keener, H. M. (2018). Plant pest detection using an artificial nose system: a review. *Sensors, 18*(2), 378.
Del Fiore, A., Reverberi, M., Ricelli, A., Pinzari, F., Serranti, S., Fabbri, A., . . . Fanelli, C. (2010). Early detection of toxigenic fungi on maize by hyperspectral imaging analysis. *International journal of food microbiology, 144*(1), 64-71.
Diezma-Iglesias, B., Ruiz-Altisent, M., & Barreiro, P. (2004). Detection of internal quality in seedless watermelon by acoustic impulse response. *Biosystems engineering, 88*(2), 221-230.
Doeswijk, T., Smilde, A., Hageman, J., Westerhuis, J., & Van Eeuwijk, F. (2011). On the increase of predictive performance with high-level data fusion. *Analytica chimica acta, 705*(1-2), 41-47.
Dong, J., & Guo, W. (2015). Nondestructive determination of apple internal qualities using near-infrared hyperspectral reflectance imaging. *Food Analytical Methods, 8*(10), 2635-2646.
Dosunmu, O. G., Herrick, N. J., Haseeb, M., Hix, R. L., & Mankin, R. W. (2014). Acoustic detectability of Rhynchophorus cruentatus (Coleoptera: Dryophthoridae). *Florida Entomologist, 97*(2), 431-438.
Dosunmu, O. G., Herrick, N. J., Haseeb, M., Hix, R. L., & Mankin, R. W. (2014). Acoustic Detectability of Rhynchophorus cruentatus (Coleoptera: Dryophthoridae). *The Florida entomologist, 97*(2), 431-438. doi:10.1653/024.097.0213
Du Plessis, A., Broeckhoven, C., Guelpa, A., & Le Roux, S. G. (2017). Laboratory x-ray micro-computed tomography: a user guideline for biological samples. *Gigascience, 6*(6), gix027.
Ekramirad, N., Adedeji, A. A., & Alimardani, R. (2016). A review of non-destructive methods for detection of insect infestation in fruits and vegetables. *Innovations in Food Research, 2*, 6-12.
Ekramirad, N., Khaled, A. Y., Doyle, L. E., Loeb, J. R., Donohue, K. D., Villanueva, R. T., & Adedeji, A. A. (2022). Nondestructive Detection of Codling Moth Infestation in Apples Using Pixel-Based NIR Hyperspectral Imaging with Machine Learning and Feature Selection. *Foods, 11*(1), 8. Retrieved from https://www.mdpi.com/2304-8158/11/1/8
Ekramirad, N., Parrish, C. A., Villanueva, R. T., Donohue, K. D., & Adedeji, A. A. (2020). *Low frequency signal patterns for codling moth larvae activity in apples.* Paper presented at the 2020 ASABE Annual International Virtual Meeting.
El-Mesery, H. S., Mao, H., & Abomohra, A. E.-F. (2019). Applications of non-destructive technologies for agricultural and food products quality inspection. *Sensors, 19*(4), 846.
Elbashir, H., & Abu-Goukh, P. A.-B. (2003). Compositional changes during guava fruit ripening. *Food Chemistry, 80*, 557-563. doi:10.1016/S0308-8146(02)00345-X
Elbatawi, I. (2008). An acoustic impact method to detect hollow heart of potato tubers. *Biosystems engineering, 100*(2), 206-213.
Extension, U. o. M. (2021). Retrieved from https://extension.umd.edu/resource/keeping-it-cool-cold-storage-recommendations-apples-and-peaches#:~:text=Mature%20apples%20can%20typically%20be,a%20month%20in%20cold%20storage.
Fan, S., Li, J., Zhang, Y., Tian, X., Wang, Q., He, X., . . . Huang, W. (2020). On line detection of defective apples using computer vision system combined with deep learning methods. *Journal of Food Engineering, 286*, 110102.
Fathizadeh, Z., Aboonajmi, M., & Beygi, S. R. H. (2020). Nondestructive firmness prediction of apple fruit using acoustic vibration response. *Scientia Horticulturae, 262*, 109073.
Fathizadeh, Z., Aboonajmi, M., & Hassan-Beygi, S. R. (2021). Nondestructive methods for determining the firmness of apple fruit flesh. *Information Processing in Agriculture*.

Feldman, M. (2011). *Hilbert transform applications in mechanical vibration*. Hoboken, N.J.: Wiley.

Feng, Y.-Z., & Sun, D.-W. (2012). Application of hyperspectral imaging in food safety inspection and control: a review. *Critical Reviews in Food Science and Nutrition, 52*(11), 1039-1058.

Firtha, F. (2007). Development of data reduction function for hyperspectral imaging. *Progress in Agricultural Engineering Sciences, 3*(1), 67-88.

Firtha, F., Fekete, A., Kaszab, T., Gillay, B., Nogula-Nagy, M., Kovács, Z., & Kantor, D. B. (2008). Methods for improving image quality and reducing data load of NIR hyperspectral images. *Sensors, 8*(5), 3287-3298.

Follett, P. A., & Armstrong, J. W. (2004). Revised irradiation doses to control melon fly, Mediterranean fruit fly, and oriental fruit fly (Diptera: Tephritidae) and a generic dose for tephritid fruit flies. *Journal of economic entomology, 97*(4), 1254-1262.

Garillos-Manliguez, C. A., & Chiang, J. Y. (2021). Multimodal Deep Learning and Visible-Light and Hyperspectral Imaging for Fruit Maturity Estimation. *Sensors, 21*(4), 1288.

Ghaffari, R., Zhang, F., Iliescu, D., Hines, E. L., Leeson, M. S., & Napier, R. (2011). Detection of Diseases and Volatile Discrimination of Plants: An Electronic Nose and Self-Organizing Maps Approach. In *Intelligent Systems for Machine Olfaction: Tools and Methodologies* (pp. 214-230). Hershey, Pennsylvania, USA,: IGI Global.

Ghafir, S. A., Gadalla, S. O., Murajei, B. N., & El-Nady, M. F. (2009). Physiological and anatomical comparison between four different apple cultivars under cold-storage conditions. *African Journal of Plant Science, 3*(6), 133-138.

Ghosh, D., Stencel, J. M., Hicks, C. D., Payne, F., & Ozevin, D. J. I. m. (2013). Acoustic Emission Signal of Lactococcus lactis before and after Inhibition with NaN 3 and Infection with Bacteriophage c2. *ISRN microbiology, 2013*.

Ghosh, P. K., & Jayas, D. S. (2009). Use of spectroscopic data for automation in food processing industry. *Sensing and Instrumentation for Food Quality and Safety, 3*(1), 3-11.

Gomes, J. F. S., Leta, F. R., & Technology. (2012). Applications of computer vision techniques in the agriculture and food industry: a review. *European Food Research, 235*(6), 989-1000.

Gongal, A., Silwal, A., Amatya, S., Karkee, M., Zhang, Q., & Lewis, K. (2016). Apple crop-load estimation with over-the-row machine vision system. *Computers and Electronics in Agriculture, 120*, 26-35.

Greenwood, P. (2000). *American Horticultural Society Pests & Diseases: Pests and Diseases*: Dorling Kindersley.

Gulati, P., Weier, S. A., Santra, D., Subbiah, J., Rose, D. J., & Technology. (2016). Effects of feed moisture and extruder screw speed and temperature on physical characteristics and antioxidant activity of extruded proso millet (P Anicum Miliaceum) flour. *International Journal of Food Science, 51*(1), 114-122.

Guo, Z.-m., Huang, W.-q., Peng, Y.-k., Wang, X., & Li, J. (2014). Impact of region of interest selection for hyperspectral imaging and modeling of sugar content in apple. *Mod. Food Sci. Technol, 30*, 59-63.

Haff, R., & Pearson, T. (2007). An automatic algorithm for detection of infestations in X-ray images of agricultural products. *Sensing Instrumentation for Food Quality Safety, 1*(3), 143-150.

Haff, R. P., Jackson, E. S., Moscetti, R., & Massantini, R. (2015). Detection of fruit-fly infestation in olives using x-ray imaging: Algorithm development and prospects. *American Journal of Agricultural Science and Technology, 4*(1), 1-8.

Haff, R. P., Saranwong, S., Thanapase, W., Janhiran, A., Kasemsumran, S., & Kawano, S. (2013). Automatic image analysis and spot classification for detection of fruit fly infestation in hyperspectral images of mangoes. *Journal of near infrared spectroscopy, 86*, 23-28.

Haff, R. P., & Toyofuku, N. (2008). X-ray detection of defects and contaminants in the food industry. *Sensing and Instrumentation for Food Quality and Safety, 2*(4), 262-273.

Hagstrum, D. W., Flinn, P. W., & Gaffney, J. J. (1998). Temperature gradient on Tribolium castaneum (Coleoptera: Tenebrionidae) adult dispersal in stored wheat. *Environmental entomology, 27*(1), 123-129.

Hagstrum, D. W., Flinn, P. W., & Shuman, D. (1996). Automated monitoring using acoustical sensors for insects in farm-stored wheat. *Journal of economic entomology, 89*(1), 211-217.

Haishi, T., Koizumi, H., Arai, T., Koizumi, M., & Kano, H. (2011). Rapid detection of infestation of apple fruits by the peach fruit moth, Carposina sasakii Matsumura, larvae using a 0.2-T dedicated magnetic resonance imaging apparatus. *Applied magnetic resonance, 41*(1), 1.

Hallman, G. J. (2004). Irradiation disinfestation of apple maggot (Diptera: Tephritidae) in hypoxic and low-temperature storage. *Journal of economic entomology, 97*(4), 1245-1248.

Hallman, G. J., & Hellmich, R. L. (2009). Ionizing radiation as a phytosanitary treatment against European corn borer (Lepidoptera: Crambidae) in ambient, low oxygen, and cold conditions. *J Econ Entomol, 102*(1), 64-68. doi:10.1603/029.102.0110

Hamidisepehr, A., Sama, M. P., Turner, A. P., & Wendroth, O. O. (2017). A method for reflectance index wavelength selection from moisture-controlled soil and crop residue samples. *Transactions of the ASABE, 60*(5), 1479-1487.

Hansen, J. D. (2002). Effect of cold temperature treatments on the mortality of eggs and feeding larvae of the oriental fruit moth. *HortTechnology, 12*(2), 203-205.

Hansen, J. D., Carlton, R., Adams, S., & Lacey, L. A. (2008). Infrared detection of internal feeders of deciduous tree fruits. *Journal of Entomological Science, 43*(1), 52-56.

Harold Toba, H., & Moffitt, H. R. (1991). Controlled-atmosphere cold storage as a quarantine treatment for nondiapausing codling moth (Lepidoptera: Tortricidae) larvae in apples. *Journal of economic entomology, 84*(4), 1316-1319.

Hong, Y. A., Gallardo, R. K., Fan, X., Atallah, S., & Gómez, M. I. (2019). Phytosanitary Regulation of Washington Apple Producers under an Apple Maggot Quarantine Program. *Journal of Agricultural and Resource Economics, 44*(3), 646-663.

Huang, M., Wan, X., Zhang, M., & Zhu, Q. (2013). Detection of insect-damaged vegetable soybeans using hyperspectral transmittance image. *Journal of Food Engineering, 116*(1), 45-49.

Hussain, A., Pu, H., Sun, D.-W., & technology. (2018). Innovative nondestructive imaging techniques for ripening and maturity of fruits–a review of recent applications. *Trends in food science, 72*, 144-152.

Ishimwe, R., Abutaleb, K., & Ahmed, F. (2014). Applications of thermal imaging in agriculture—a review. *Advances in remote Sensing, 3*(03), 128.

Jackman, R., Marangoni, A., & Stanley, D. (2007). The effects of turgor pressure on puncture and viscoelastic properties of tomato tissue. *Journal of texture studies, 23*, 491-505. doi:10.1111/j.1745-4603.1992.tb00036.x

Jaffe, B. D., Guédot, C., & Landolt, P. J. (2018). Mass-trapping codling moth, Cydia pomonella (Lepidopteran: Torticidae), using a kairomone lure reduces fruit damage in commercial apple orchards. *Journal of economic entomology, 111*(4), 1983-1986.

Jakhete, S., Allan, S., & Mankin, R. (2017). Wingbeat Frequency-Sweep and Visual Stimuli for Trapping Male Aedes aegypti (Diptera: Culicidae). *Journal of Medical Entomology, 54*. doi:10.1093/jme/tjx074

Jalinas, J., Gerri-Agull, B., Dosunmu, O., Haseeb, M., Lopez-Llorca, L., & Mankin, R. (2019). Acoustic Signal Applications in Detection and Management of Rhynchophorus spp. in Fruit-Crops and Ornamental Palms. *Florida Entomologist, 102*, 475-479. doi:10.1653/024.102.0303

Jalinas, J., Güerri-Agulló, B., Dosunmu, O. G., Lopez Llorca, L. V., & Mankin, R. W. (2017a). Acoustic Activity Cycles of Rhynchophorus ferrugineus (Coleoptera: Dryophthoridae)

Early Instars After Beauveria bassiana (Hypocreales: Clavicipitaceae) Treatments. *Annals of the Entomological Society of America, 110*(6), 551-557. doi:10.1093/aesa/sax061

Jalinas, J., Güerri-Agulló, B., Dosunmu, O. G., Lopez Llorca, L. V., & Mankin, R. W. (2017b). Acoustic activity cycles of Rhynchophorus ferrugineus (Coleoptera: Dryophthoridae) early instars after Beauveria bassiana (Hypocreales: Clavicipitaceae) treatments. *Annals of the Entomological Society of America, 110*(6), 551-557.

Jamieson, L., Wilkinson, R. T., Page-Weir, N. E. M., Hawthorne, A., Hartnett, D. E., Redpath, S., . . . Guo, L. F. (2018). Assessing the efficacy of controlled atmosphere temperature treatment system (CATTS) against codling moth inside harvested apples. *New Zealand Plant Protection, 71*, 306-313.

Jamshidi, B. (2020). Ability of near-infrared spectroscopy for non-destructive detection of internal insect infestation in fruits: Meta-analysis of spectral ranges and optical measurement modes. *Spectrochimica Acta Part A: Molecular and Biomolecular Spectroscopy, 225*, 117479. doi:https://doi.org/10.1016/j.saa.2019.117479

Jan, I., Rab, A., Sajid, M., Ali, A., & Shah, S. (2012). Response of apple cultivars to different storage durations. *Sarhad J. Agric, 28*(2), 219-225.

Jia, W., Liang, G., Jiang, Z., & Wang, J. (2019). Advances in electronic nose development for application to agricultural products. *Food Analytical Methods, 12*(10), 2226-2240.

Jiang, D., Chen, S., Hao, M., Fu, J., & Ding, F. (2018). Mapping the Potential Global Codling Moth (Cydia pomonella L.) Distribution Based on a Machine Learning Method. *Scientific Reports, 8*(1), 13093. doi:10.1038/s41598-018-31478-3

Jiang, J.-A., Chang, H.-Y., Wu, K.-H., Ouyang, C.-S., Yang, M.-M., Yang, E.-C., . . . agriculture, e. i. (2008). An adaptive image segmentation algorithm for X-ray quarantine inspection of selected fruits. *Computers, 60*(2), 190-200.

Johnston, J. W., Hewett, E. W., & Hertog, M. L. (2002). Postharvest softening of apple (Malus domestica) fruit: a review. *New Zealand Journal of Crop and Horticultural Science, 30*(3), 145-160.

Joshi, N. K., Hull, L. A., & Krawczyk, G. (2020). Insecticide Baseline Sensitivity in Codling Moth (Lepidoptera: Tortricidae) Populations From Orchards Under Different Management Practices. *Journal of Entomological Science, 55*(1), 105-116. doi:10.18474/0749-8004-55.1.105

Kadoić Balaško, M., Bažok, R., Mikac, K., Lemic, D., & Pajač Živković, I. (2020). Pest Management Challenges and Control Practices in Codling Moth: A Review. *Insects, 11*, 38. doi:10.3390/insects11010038

Kaliramesh, S., Chelladurai, V., Jayas, D., Alagusundaram, K., White, N., & Fields, P. (2013). Detection of infestation by Callosobruchus maculatus in mung bean using near-infrared hyperspectral imaging. *Journal of stored products Research, 52*, 107-111.

Keresztes, J. C., Goodarzi, M., & Saeys, W. (2016). Real-time pixel based early apple bruise detection using short wave infrared hyperspectral imaging in combination with calibration and glare correction techniques. *Food Control, 66*, 215-226.

Khaled, A. Y., Abd Aziz, S., Bejo, S. K., Nawi, N. M., Seman, I. A., & Izzuddin, M. A. (2018). Development of classification models for basal stem rot (BSR) disease in oil palm using dielectric spectroscopy. *Industrial Crops and Products, 124*, 99-107.

Khaleghi, B., Khamis, A., Karray, F. O., & Razavi, S. N. (2013). Multisensor data fusion: A review of the state-of-the-art. *Information fusion, 14*(1), 28-44.

Kotwaliwale, N., Singh, K., Kalne, A., Jha, S. N., Seth, N., & Kar, A. (2014). X-ray imaging methods for internal quality evaluation of agricultural produce. *Journal of food science technology, 51*(1), 1-15.

Kubat, M. (2015). *An Introduction to Machine Learning*: Springer Publishing Company, Incorporated.

Kuckenberg, J., Tartachnyk, I., & Noga, G. (2008). Evaluation of fluorescence and remission techniques for monitoring changes in peel chlorophyll and internal fruit characteristics in sunlit and shaded sides of apple fruit during shelf-life. *Postharvest Biology and Technology, 48*(2), 231-241.

Kumar, R., & Vishwakarma, R. (2018). Chapter 12 - Preharvest Approaches to Control Insect Infestation in Fruit. In M. W. Siddiqui (Ed.), *Preharvest Modulation of Postharvest Fruit and Vegetable Quality* (pp. 301-357): Academic Press.

Lammertyn, J., Dresselaers, T., Van Hecke, P., Jancsók, P., Wevers, M., & Nicolai, B. (2003). MRI and X-ray CT study of spatial distribution of core breakdown in 'Conference'pears. *Magnetic Resonance Imaging, 21*(7), 805-815.

Lan, Y.-b., Zheng, X.-z., Westbrook, J. K., Lopez, J., Lacey, R., & Hoffmann, W. C. (2008). Identification of Stink Bugs Using an Electronic Nose. *Journal of Bionic Engineering, 5*, 172-180. doi:https://doi.org/10.1016/S1672-6529(08)60090-6

Landolt, P., Brumley, J., Smithhisler, C., Biddick, L., & Hofstetter, R. (2000). Apple Fruit Infested with Codling Moth are More Attractive to Neonate Codling Moth Larvae and Possess Increased Amounts of (E,E)-α-Farnesene. *Journal of Chemical Ecology, 26*, 1685-1699. doi:10.1023/A:1005595014589

Li, H., Chen, Q., Zhao, J., & Wu, M. (2015). Nondestructive detection of total volatile basic nitrogen (TVB-N) content in pork meat by integrating hyperspectral imaging and colorimetric sensor combined with a nonlinear data fusion. *LWT - Food Science and Technology, 63*(1), 268-274. doi:https://doi.org/10.1016/j.lwt.2015.03.052

Li, H., Sun, X., Pan, W., Kutsanedzie, F., Zhao, J., & Chen, Q. (2016). Feasibility study on nondestructively sensing meat's freshness using light scattering imaging technique. *Meat science, 119*, 102-109. doi:https://doi.org/10.1016/j.meatsci.2016.04.031

Li, J., Rao, X., & Ying, Y. (2011). Detection of common defects on oranges using hyperspectral reflectance imaging. *Computers and Electronics in Agriculture, 78*(1), 38-48. doi:https://doi.org/10.1016/j.compag.2011.05.010

Li, M., Ekramirad, N., Rady, A. M., & Adedeji, A. (2018). Application of Acoustic Emission and Machine Learning to Detect Codling Moth Infested Apples. *Transactions of the ASABE (American Society of Agricultural and Biological Engineers), 61*. doi:10.13031/trans.12548

Li, Y.-S., & Church, J. S. (2014). Raman spectroscopy in the analysis of food and pharmaceutical nanomaterials. *Journal of food and drug analysis, 22*(1), 29-48.

Liljedahl, L., & Abbott, J. (1994). Changes in Sonic Resonance of Delicious and Golden Delicious Apples Undergoing Accelerated Ripening. *Transactions of the ASAE, 37*, 907-912. doi:10.13031/2013.28158

Liu, G., He, J., Wang, S., Luo, Y., Wang, W., Wu, L., . . . He, X. (2015). Application of Near-Infrared Hyperspectral Imaging for Detection of External Insect Infestations on Jujube Fruit. *International Journal of Food Properties, 19*, 41-52. doi:10.1080/10942912.2014.923439

Liu, G., Nie, R., Liu, Y., & Mehmood, A. (2022). Combined antimicrobial effect of bacteriocins with other hurdles of physicochemic and microbiome to prolong shelf life of food: A review. *Science of the Total Environment*, 154058.

Liu, H., Lee, S.-H., & Chahl, J. S. (2017). A review of recent sensing technologies to detect invertebrates on crops. *Precision Agriculture, 18*(4), 635-666. doi:10.1007/s11119-016-9473-6

Liu, Q., Sun, K., Zhao, N., Yang, J., Zhang, Y., Ma, C., . . . Tu, K. (2019). Information fusion of hyperspectral imaging and electronic nose for evaluation of fungal contamination in strawberries during decay. *Postharvest Biology and Technology, 153*, 152-160.

López-García, F., Andreu-García, G., Blasco, J., Aleixos, N., & Valiente, J.-M. (2010). Automatic detection of skin defects in citrus fruits using a multivariate image analysis approach.

Computers and Electronics in Agriculture, 71(2), 189-197. doi:https://doi.org/10.1016/j.compag.2010.02.001

Lorente, D., Aleixos, N., Gómez-Sanchís, J., Cubero, S., García-Navarrete, O., & Blasco, J. (2011). Recent Advances and Applications of Hyperspectral Imaging for Fruit and Vegetable Quality Assessment. *Food and Bioprocess Technology, 5*, 1121-1142. doi:10.1007/s11947-011-0725-1

Lorente, D., Aleixos, N., Gómez-Sanchis, J., Cubero, S., García-Navarrete, O. L., & Blasco, J. (2012). Recent advances and applications of hyperspectral imaging for fruit and vegetable quality assessment. *Food and Bioprocess Technology, 5*(4), 1121-1142.

Louzeiro, L. R., Souza-Filho, M., Raga, A., & Schmidt, F. (2020). Relationship between fruit fly (Diptera: Tephritidae) infestation and the physicochemical changes in fresh fruits. *African journal of agricultural research, 15*, 122-133. doi:10.5897/AJAR2019.14533

Lowe, A., Harrison, N., & French, A. P. (2017). Hyperspectral image analysis techniques for the detection and classification of the early onset of plant disease and stress. *Plant methods, 13*, 80-80. doi:10.1186/s13007-017-0233-z

Lu, R. (2007). Nondestructive measurement of firmness and soluble solids content for apple fruit using hyperspectral scattering images. *Sensing and Instrumentation for Food Quality and Safety, 1*(1), 19-27.

Lu, Y., Huang, Y., & Lu, R. (2017). Innovative Hyperspectral Imaging-Based Techniques for Quality Evaluation of Fruits and Vegetables: A Review. *Applied Sciences, 7*, 189. doi:10.3390/app7020189

Lu, Y., & Lu, R. (2017). Non-destructive defect detection of apples by spectroscopic and imaging technologies: a review. *Transactions of the ASABE, 60*(5), 1765-1790.

Ma, J., Sun, D.-W., Qu, J.-H., Liu, D., Pu, H., Gao, W.-H., & Zeng, X.-A. (2016). Applications of computer vision for assessing quality of agri-food products: a review of recent research advances. *Critical Reviews in Food Science and Nutrition, 56*(1), 113-127.

Ma, T., Li, X., Inagaki, T., Yang, H., & Tsuchikawa, S. (2018). Noncontact evaluation of soluble solids content in apples by near-infrared hyperspectral imaging. *Journal of Food Engineering, 224*, 53-61.

Ma, T., Xia, Y., Inagaki, T., & Tsuchikawa, S. (2021). Rapid and nondestructive evaluation of soluble solids content (SSC) and firmness in apple using Vis–NIR spatially resolved spectroscopy. *Postharvest Biology and Technology, 173*, 111417.

Ma, Y., Huang, M., Yang, B., & Zhu, Q. (2014). Automatic threshold method and optimal wavelength selection for insect-damaged vegetable soybean detection using hyperspectral images. *Computers and Electronics in Agriculture, 106*, 102-110. doi:https://doi.org/10.1016/j.compag.2014.05.014

Mankin, R. (2012). Recent Developments in the use of Acoustic Sensors and Signal Processing Tools to Target Early Infestations of Red Palm Weevil in Agricultural Environments1. *Florida Entomologist, 97*, 761-765. doi:10.1653/024.094.0405

Mankin, R., Al-Ayedh, H., Aldryhim, Y., & Rohde, B. (2016). Acoustic detection of Rhynchophorus ferrugineus (Coleoptera: Dryophthoridae) and Oryctes elegans (Coleoptera: Scarabaeidae) in Phoenix dactylifera (Arecales: Arecacae) trees and offshoots in Saudi Arabian orchards. *Journal of economic entomology, 109*(2), 622-628.

Mankin, R., Hodges, R., Nagle, J. H., Schal, C., Pereira, R., & Koehler, P. (2010). Acoustic Indicators for Targeted Detection of Stored Product and Urban Insect Pests by Inexpensive Infrared, Acoustic, and Vibrational Detection of Movement. *Journal of economic entomology, 103*, 1636-1646. doi:10.1603/EC10126

Mankin, R., Hubbard, J., & Flanders, K. (2007). Acoustic Indicators for Mapping Infestation Probabilities of Soil Invertebrates. *Journal of economic entomology, 100*, 790-800. doi:10.1603/0022-0493(2007)100[790:AIFMIP]2.0.CO;2

Mankin, R., Mizrach, A., Hetzroni, A., Levsky, S., Nakache, Y., & Soroker, V. (2009). Temporal and Spectral features of Sounds of wood-boring Beetle Larvae: Identifiable patterns of Activity enable improved discrimination from background noise. *Florida Entomologist, 91*, 241-248. doi:10.1653/0015-4040(2008)91[241:TASFOS]2.0.CO;2

Mankin, R., & Moore, A. (2010). Acoustic Detection of Oryctes rhinoceros (Coleoptera: Scarabaeidae: Dynastinae) and Nasutitermes luzonicus (Isoptera: Termitidae) in Palm Trees in Urban Guam. *Journal of economic entomology, 103*, 1135-1143. doi:10.1603/EC09214

Mankin, R. W., Hagstrum, D. W., Smith, M. T., Roda, A. L., & Kairo, M. T. K. (2011). Perspective and Promise: a Century of Insect Acoustic Detection and Monitoring. *American Entomologist, 57*(1), 30-44. doi:10.1093/ae/57.1.30

Mankin, R. W., Rohde, B., & McNeill, S. (2015, 2015/11/02). *Vibrational duetting mimics to trap and disrupt mating of the devastating Asian citrus psyllid insect pest.* Paper presented at the Proceedings of Meetings on Acoustics.

Mankin, R. W., Samson, P. R., & Chandler, K. J. (2009). Acoustic Detection of Melolonthine Larvae in Australian Sugarcane. *Journal of economic entomology, 102*(4), 1523-1535. doi:10.1603/029.102.0417

Mankin, R. W., Stanaland, D., Haseeb, M., Rohde, B., Menocal, O., & Carrillo, D. (2018). Assessment of plant structural characteristics, health, and ecology using bioacoustic tools. *Proceedings of Meetings on Acoustics, 33*(1), 010003. doi:10.1121/2.0000902

Mao, J., Yu, Y., Rao, X., & Wang, J. (2016). Firmness prediction and modeling by optimizing acoustic device for watermelons. *Journal of Food Engineering, 168*, 1-6. doi:https://doi.org/10.1016/j.jfoodeng.2015.07.009

Marzec, A., Lewicki, P. P., & Ranachowski, Z. (2007). Influence of water activity on acoustic emission of flat extruded bread. *Journal of Food Engineering, 79*(2), 410-422. doi:https://doi.org/10.1016/j.jfoodeng.2006.01.067

McNett, G., Miles, R., Homentcovschi, D., & Cocroft, R. (2007). A method for two-dimensional characterization of animal vibrational signals transmitted along plant stems. *Journal of comparative physiology. A, Neuroethology, sensory, neural, and behavioral physiology, 192*, 1245-1251. doi:10.1007/s00359-006-0153-2

Mditshwa, A., Fawole, O. A., & Opara, U. L. (2018). Recent developments on dynamic controlled atmosphere storage of apples—A review. *Food packaging and shelf life, 16*, 59-68.

Meng, L. (2016). *Acoustic Emission of Lactococcus lactis ssp. lactis C2 Infected with Three Bacteriophages c2, sk1 and ml3.*

Mireei, S. A., Amini-Pozveh, S., & Nazeri, M. (2017). Selecting optimal wavelengths for detection of insect infested tomatoes based on SIMCA-aided CFS algorithm. *Postharvest Biology and Technology, 123*, 22-32. doi:https://doi.org/10.1016/j.postharvbio.2016.08.009

Mitsuno, H., Sakurai, T., Namiki, S., Mitsuhashi, H., & Kanzaki, R. (2015). Novel cell-based odorant sensor elements based on insect odorant receptors. *Biosensors and Bioelectronics, 65*, 287-294. doi:https://doi.org/10.1016/j.bios.2014.10.026

Moscetti, R., Haff, R. P., Saranwong, S., Monarca, D., Cecchini, M., & Massantini, R. (2014). Nondestructive detection of insect infested chestnuts based on NIR spectroscopy. *Postharvest Biology and Technology, 87*, 88-94. doi:https://doi.org/10.1016/j.postharvbio.2013.08.010

Moscetti, R., Haff, R. P., Stella, E., Contini, M., Monarca, D., Cecchini, M., & Massantini, R. (2015). Feasibility of NIR spectroscopy to detect olive fruit infested by Bactrocera oleae. *Postharvest Biology and Technology, 99*, 58-62. doi:https://doi.org/10.1016/j.postharvbio.2014.07.015

Munera, S., Gómez-Sanchís, J., Aleixos, N., Vila-Francés, J., Colelli, G., Cubero, S., . . . Blasco, J. (2021). Discrimination of common defects in loquat fruit cv.'Algerie'using hyperspectral imaging and machine learning techniques. *Postharvest Biology and Technology, 171*, 111356.

Muravin, B. J. J. o. b., engineers, i. e. o. t. I. a. o., & architects. (2009). Acoustic emission science and technology. *1*, 4-5.

Nawar, S., & Mouazen, A. M. (2018). Optimal sample selection for measurement of soil organic carbon using on-line vis-NIR spectroscopy. *Computers and Electronics in Agriculture, 151*, 469-477.

Neven, L., Rehfield-Ray, L., & Obenland, D. (2006). Confirmation and Efficacy Tests Against Codling Moth and Oriental Fruit Moth in Peaches and Nectarines Using Combination Heat and Controlled Atmosphere Treatments. *Journal of economic entomology, 99*, 1610-1619. doi:10.1603/0022-0493-99.5.1610

Nicolaï, B. M., Defraeye, T., De Ketelaere, B., Herremans, E., Hertog, M. L., Saeys, W., . . . Verboven, P. (2014). Nondestructive measurement of fruit and vegetable quality. *Annual review of food science technology, 5*, 285-312.

Nicolai, B. M., Theron, K. I., & Lammertyn, J. (2007). Kernel PLS regression on wavelet transformed NIR spectra for prediction of sugar content of apple. *Chemometrics and intelligent laboratory systems, 85*(2), 243-252.

Nturambirwe, J. F. I., & Opara, U. L. (2020). Machine learning applications to non-destructive defect detection in horticultural products. *Biosystems engineering, 189*, 60-83.

Nylund, R., & Lutz, J. (1950). Separation of hollow heart potato tubers by means of size grading, specific gravity, and x-ray examination. *American Potato Journal, 27*(6), 214-222.

O'Donnell, C. P., Fagan, C., & Cullen, P. J. (2014). *Process analytical technology for the food industry*: Springer.

Omkar, S., & Karanth, R. (2008). Rule extraction for classification of acoustic emission signals using ant colony optimisation. *Engineering Applications of Artificial Intelligence, 21*(8), 1381-1388.

Onwude, D. I., Chen, G., Eke-Emezie, N., Kabutey, A., Khaled, A. Y., & Sturm, B. (2020). Recent advances in reducing food losses in the supply chain of fresh agricultural produce. *Processes, 8*(11), 1431.

Pajač, I., Pejić, I., & Barić, B. (2011). Codling moth, Cydia pomonella (Lepidoptera: Tortricidae)– major pest in apple production: an overview of its biology, resistance, genetic structure and control strategies. *Agriculturae Conspectus Scientificus, 76*(2), 87-92.

Pasquini, C. (2003). Near infrared spectroscopy: fundamentals, practical aspects and analytical applications. *Journal of the Brazilian chemical society, 14*(2), 198-219.

Patel, K. K., Kar, A., Jha, S., & Khan, M. (2012). Machine vision system: a tool for quality inspection of food and agricultural products. *Journal of food science technology, 49*(2), 123-141.

Pathmanaban, P., Gnanavel, B., & Anandan, S. S. (2019). Recent Application of imaging techniques for Fruit quality Assessment. *Trends in Food Science Technology*.

Pearson, T., Doster, M., & Michailides, T. (2001). Automated detection of pistachio defects by machine vision. *Applied Engineering in Agriculture, 17*(5), 729.

Peerbhay, K. Y., Mutanga, O., & Ismail, R. (2015). Random forests unsupervised classification: The detection and mapping of solanum mauritianum infestations in plantation forestry using hyperspectral data. *IEEE Journal of Selected Topics in Applied Earth Observations and Remote Sensing, 8*(6), 3107-3122.

Peirs, A., Schenk, A., & Nicolaï, B. M. (2005). Effect of natural variability among apples on the accuracy of VIS-NIR calibration models for optimal harvest date predictions. *Postharvest Biology and Technology, 35*(1), 1-13.

Peirs, A., Tirry, J., Verlinden, B., Darius, P., & Nicolaï, B. M. (2003). Effect of biological variability on the robustness of NIR models for soluble solids content of apples. *Postharvest Biology and Technology, 28*(2), 269-280.

Peshlov, B. N., Dowell, F. E., Drummond, F. A., & Donahue, D. W. (2009). Comparison of three near infrared spectrophotometers for infestation detection in wild blueberries using multivariate calibration models. *Journal of near infrared spectroscopy, 17*(4), 203-212.

Phung, Q. V., Ahmad, I., Habibi, D., & Hinckley, S. (2017). Automated Insect Detection Using Acoustic Features Based on Sound Generated from Insect Activities. *Acoustics Australia, 45*(2), 445-451. doi:10.1007/s40857-017-0095-6

Pimentel, D., Zuniga, R., & Morrison, D. (2005). Update on the environmental and economic costs associated with alien-invasive species in the United States. *Ecological economics, 52*(3), 273-288.

Pinhas, J., Soroker, V., Hetzroni, A., Mizrach, A., Teicher, M., & Goldberger, J. (2008). Automatic acoustic detection of the red palm weevil. *Computers electronics in agriculture, 63*(2), 131-139.

Pinhas, J., Soroker, V., Hetzroni, A., Mizrach, A., Teicher, M., & Goldberger, J. (2008). Automatic acoustic detection of the red palm weevil. *Computers and Electronics in Agriculture, 63*(2), 131-139. doi:https://doi.org/10.1016/j.compag.2008.02.004

Plaza, A., Benediktsson, J. A., Boardman, J. W., Brazile, J., Bruzzone, L., Camps-Valls, G., . . . Gualtieri, A. (2009). Recent advances in techniques for hyperspectral image processing. *Remote sensing of environment, 113*, S110-S122.

Pourkhak, B., Mireei, S. A., Sadeghi, M., & Hemmat, A. (2017). Multi-sensor data fusion in the nondestructive measurement of kiwifruit texture. *Measurement, 101*, 157-165.

Pu, Y. Y., Feng, Y. Z., & Sun, D. W. (2015). Recent progress of hyperspectral imaging on quality and safety inspection of fruits and vegetables: a review. *Comprehensive Reviews in Food Science and Food Safety, 14*(2), 176-188.

Pu, Y. Y., Feng, Y. Z., & Sun, D. W. (2015). Recent progress of hyperspectral imaging on quality and safety inspection of fruits and vegetables: a review. *Comprehensive Reviews in Food Science Food Safety, 14*(2), 176-188.

Qin, J., Burks, T. F., Ritenour, M. A., & Bonn, W. G. (2009). Detection of citrus canker using hyperspectral reflectance imaging with spectral information divergence. *Journal of Food Engineering, 93*(2), 183-191.

Qu, J.-H., Liu, D., Cheng, J.-H., Sun, D.-W., Ma, J., Pu, H., & Zeng, X.-A. (2015). Applications of near-infrared spectroscopy in food safety evaluation and control: a review of recent research advances. *Critical Reviews in Food Science and Nutrition, 55*(13), 1939-1954.

Rady, A., & Adedeji, A. (2018). Assessing different processed meats for adulterants using visible-near-infrared spectroscopy. *Meat science, 136*, 59-67.

Rady, A., Ekramirad, N., Adedeji, A., Li, M., & Alimardani, R. (2017). Hyperspectral imaging for detection of codling moth infestation in GoldRush apples. *Postharvest Biology Technology, 129*, 37-44.

Rajendran, S. (2005). Detection of insect infestation in stored foods. *Advances in food nutrition research, 49*, 163-232.

Rao, X., Ying, Y., Lv, F., & Jin, B. (2004). Development of a fruit quality inspecting system based on acoustic properties. *T. CSAM, 2*, 69-71.

Report, U. A. (2017). *USDA Annual Report*. Retrieved from https://www.aphis.usda.gov/publications/plant_health/report-ppq-2017.pdf

Rozsypal, J., Koštál, V., Zahradníčková, H., & Šimek, P. (2013). Overwintering strategy and mechanisms of cold tolerance in the codling moth (Cydia pomonella). *PLoS One, 8*(4), e61745.

Ruiz-Altisent, M., Ruiz-Garcia, L., Moreda, G., Lu, R., Hernandez-Sanchez, N., Correa, E., . . . García-Ramos, J. (2010). Sensors for product characterization and quality of specialty crops—A review. *Computers electronics in agriculture, 74*(2), 176-194.

Saeys, W., De Ketelaere, B., & Darius, P. (2008). Potential applications of functional data analysis in chemometrics. *Journal of Chemometrics: A Journal of the Chemometrics Society, 22*(5), 335-344.

Salehi, F., & Aghajanzadeh, S. (2020). Effect of dried fruits and vegetables powder on cakes quality: A review. *Trends in Food Science & Technology, 95*, 162-172.

Saranwong, S., Haff, R. P., Thanapase, W., Janhiran, A., Kasemsumran, S., & Kawano, S. (2011). A feasibility study using simplified near infrared imaging to detect fruit fly larvae in intact fruit. *Journal of near infrared spectroscopy, 19*(1), 55-60.

Schatzki, T., Haff, R., Young, R., Can, I., Le, L., & Toyofuku, N. (1997). Defect detection in apples by means of X-ray imaging. *Transactions of the ASAE, 40*(5), 1407-1415.

Shi, J., Zhang, F., Wu, S., Guo, Z., Huang, X., Hu, X., . . . Zou, X. (2019). Noise-free microbial colony counting method based on hyperspectral features of agar plates. *Food Chemistry, 274*, 925-932.

Silwal, A., Gongal, A., & Karkee, M. (2014). Apple identification in field environment with over the row machine vision system. *Agricultural Engineering International: CIGR Journal, 16*(4), 66-75.

Singh, C. B., Jayas, D. S., Paliwal, J., & White, N. D. (2010). Identification of insect-damaged wheat kernels using short-wave near-infrared hyperspectral and digital colour imaging. *Computers electronics in agriculture, 73*(2), 118-125.

Singh, D., & Sharma, R. R. (2018). Chapter 1 - Postharvest Diseases of Fruits and Vegetables and Their Management. In M. W. Siddiqui (Ed.), *Postharvest Disinfection of Fruits and Vegetables* (pp. 1-52): Academic Press.

Sirisomboon, P., Hashimoto, Y., & Tanaka, M. (2009). Study on non-destructive evaluation methods for defect pods for green soybean processing by near-infrared spectroscopy. *Journal of Food Engineering, 93*(4), 502-512.

Smyth, H., & Cozzolino, D. (2013). Instrumental methods (spectroscopy, electronic nose, and tongue) as tools to predict taste and aroma in beverages: advantages and limitations. *Chemical reviews, 113*(3), 1429-1440.

Sonka, M., Hlavac, V., & Boyle, R. (2014). *Image processing, analysis, and machine vision*: Cengage Learning.

Soroker, V., Nakache, Y., Landau, U., Mizrach, A., Hetzroni, A., & Gerling, D. (2004). Note: Utilization of sounding methodology to detect infestation by Rhynchophorus ferrugineus on palm offshoots. *Phytoparasitica, 32*(1), 6-8.

Stone, M., Armstrong, P., Zhang, X., Brusewitz, G., & Chen, D. (1996). Watermelon maturity determination in the field using acoustic impulse impedance techniques. *Transactions of the ASAE, 39*(6), 2325-2330.

Su, Z., Tu, K., Zou, X., Jing, W., & Pan, L. (2008). Detection of internal defect in apples by acoustic impulse technique. *Science and Technology of Food Industry, 29*(7), 235-238.

Suffert, M., Wilstermann, A., Petter, F., Schrader, G., & Grousset, F. (2018). Identification of new pests likely to be introduced into Europe with the fruit trade. *EPPO Bulletin, 48*(1), 144-154.

Sun, D.-W. (2010). *Hyperspectral imaging for food quality analysis and control*: Elsevier.

Sun, Y., Wei, K., Liu, Q., Pan, L., & Tu, K. (2018). Classification and discrimination of different fungal diseases of three infection levels on peaches using hyperspectral reflectance imaging analysis. *Sensors, 18*(4), 1295.

Susič, N., Žibrat, U., Sinkovič, L., Vončina, A., Razinger, J., Knapič, M., . . . Gerič Stare, B. (2020). From genome to field—observation of the multimodal nematicidal and plant growth-promoting effects of Bacillus firmus I-1582 on tomatoes using hyperspectral remote sensing. *Plants, 9*(5), 592.

Sutin, A., Flynn, T., Salloum, H., Sedunov, N., Sinelnikov, Y., & Hull-Sanders, H. (2017). *Vibro-acoustic methods of insect detection in agricultural shipments and wood packing materials*.

Paper presented at the 2017 IEEE International Symposium on Technologies for Homeland Security (HST).

Sutin, A., Yakubovskiy, A., Salloum, H. R., Flynn, T. J., Sedunov, N., & Nadel, H. (2019). Towards an Automated Acoustic Detection Algorithm for Wood-Boring Beetle Larvae (Coleoptera: Cerambycidae and Buprestidae). *Journal of economic entomology, 112*(3), 1327-1336.

Sutin, A., Yakubovskiy, A., Salloum, H. R., Flynn, T. J., Sedunov, N., & Nadel, H. (2019). Towards an Automated Acoustic Detection Algorithm for Wood-Boring Beetle Larvae (Coleoptera: Cerambycidae and Buprestidae). *Journal of Economic Entomology, 112*(3), 1327-1336. doi:10.1093/jee/toz016

Swietlicka, I., Muszynski, S., & Marzec, A. (2015). Extruded bread classification on the basis of acoustic emission signal with application of artificial neural networks. *International agrophysics, 29*(2). doi:doi: 10.1515/intag-2015-0022

Szymańska-Chargot, M., Chylińska, M., Pieczywek, P. M., Rösch, P., Schmitt, M., Popp, J., & Zdunek, A. (2016). Raman imaging of changes in the polysaccharides distribution in the cell wall during apple fruit development and senescence. *Planta, 243*(4), 935-945.

Tian, X., Fan, S., Li, J., Huang, W., & Chen, L. (2020). An optimal zone combination model for on-line nondestructive prediction of soluble solids content of apple based on full-transmittance spectroscopy. *Biosystems engineering, 197*, 64-75.

Tian, X., Li, J., Wang, Q., Fan, S., Huang, W., & Zhao, C. (2019). A multi-region combined model for non-destructive prediction of soluble solids content in apple, based on brightness grade segmentation of hyperspectral imaging. *Biosystems engineering, 183*, 110-120.

Torres, I. D. A. (2006). *Estudio, aplicación y propuesta de automatización del procesamiento de imágenes por resonancia magnética para la evaluación y detección de defectos internos de calidad en cítricos y melocotones.* Universitat Politècnica de València,

Torres, M. T. R. (2008). *TRANSMISIÓN OPTICA E IMAGEN EN VISIBLE E INFRARROJO EN FRUTAS. ENSAYO DE EQUIPOS COMERCIALES.* Universidad Politécnica de Madrid,

Trifa, V. M., Kirschel, A. N., Taylor, C. E., & Vallejo, E. E. (2008). Automated species recognition of antbirds in a Mexican rainforest using hidden Markov models. *The Journal of the Acoustical Society of America, 123*(4), 2424-2431.

Ueda, M., Sasaki, K., Utsunomiya, N., Inaba, K., & Shimabayashi, Y. (2000). Changes in Physical and Chemical Properties during Maturation of Mango Fruit (<i>Mangifera indica</i> L. ‘Irwin’) Cultured in a Plastic Greenhouse. *Food Science and Technology Research, 6*(4), 299-305. doi:10.3136/fstr.6.299

Umeh, V., Olaniyan, A., Ker, J., & Andir, J. (2004). Development of citrus fruit fly control strategies for small-holders in Nigeria. *http://dx.doi.org/10.1051/fruits:2004025, 59*. doi:10.1051/fruits:2004025

USDA Annual Report. https://www.aphis.usda.gov/publications/plant_health/report-ppq-2016.pdf.

USDA Annual Report. https://www.aphis.usda.gov/publications/plant_health/report-ppq-2017.pdf.

USDA, E. R. C. (2015). Retrieved from https://www.ers.usda.gov/data-products/fruit-and-tree-nuts-data/fruit-and-tree-nuts-yearbook-tables/#General

USDA, E. R. C. (2020). Retrieved from https://www.ers.usda.gov/data-products/fruit-and-tree-nuts-data/fruit-and-tree-nuts-yearbook-tables/

USDA, E. R. C. (2020). Retrieved from https://www.ers.usda.gov/data-products/fruit-and-tree-nuts-data/fruit-and-tree-nuts-yearbook-tables/#General

Vasighi-Shojae, H., Gholami-Parashkouhi, M., Mohammadzamani, D., & Soheili, A. (2018). Ultrasonic based determination of apple quality as a nondestructive technology. *Sensing and bio-sensing research, 21*, 22-26.

Veena, T., Chidanand, D., & Alagusundaram, K. (2015). Quality analysis of mango fruit with fruit fly insect by non-destructive soft X-ray method. *International Journal of Agricultural Science Research, 5*(3), 37-45.

Waldron, K. W., Smith, A. C., Parr, A. J., Ng, A., & Parker, M. L. (1997). New approaches to understanding and controlling cell separation in relation to fruit and vegetable texture. *Trends in Food Science & Technology, 8*(7), 213-221. doi:https://doi.org/10.1016/S0924-2244(97)01052-2

Walker, J., Lo, P., Horner, R., Park, N., Hughes, J., & Fraser, T. (2013). Codling moth (Cydia pomonella) mating disruption outcomes in apple orchards. *New Zealand Plant Protection, 66*, 259-263.

Wang, J., Nakano, K., Ohashi, S., Kubota, Y., Takizawa, K., & Sasaki, Y. (2011). Detection of external insect infestations in jujube fruit using hyperspectral reflectance imaging. *Biosystems engineering, 108*(4), 345-351.

Wang, J., Nakano, K., Ohashi, S., Takizawa, K., & He, J. (2010). Comparison of different modes of visible and near-infrared spectroscopy for detecting internal insect infestation in jujubes. *Journal of Food Engineering, 101*(1), 78-84.

Wang, P., Zhuang, L., Zou, Y., & Hsia, K. J. (2015). Future Trends of Bioinspired Smell and Taste Sensors. In *Bioinspired Smell and Taste Sensors* (pp. 309-324): Springer.

Watanabe, H., Yanase, Y., & Fujii, Y. (2016). Relationship between the movements of the mouthparts of the bamboo powder-post beetle Dinoderus minutus and the generation of acoustic emission. *Journal of Wood Science, 62*(1), 85-92. doi:10.1007/s10086-015-1525-4

Webb, C., Litzkow, JC, & Slaughter, D. (1988). A computerized acoustical larval detection system. *Applied Engineering in Agriculture, 4*(3), 268-274.

Wen, T., Zheng, L., Dong, S., Gong, Z., Sang, M., Long, X., . . . Peng, H. (2019). Rapid detection and classification of citrus fruits infestation by Bactrocera dorsalis (Hendel) based on electronic nose. *Postharvest Biology and Technology, 147*, 156-165. doi:10.1016/j.postharvbio.2018.09.017

Witzgall, P., Stelinski, L., Gut, L., & Thomson, D. (2008). Codling moth management and chemical ecology. *Annu. Rev. Entomol., 53*, 503-522.

Wu, L., He, J., Liu, G., Wang, S., & He, X. (2016). Detection of common defects on jujube using Vis-NIR and NIR hyperspectral imaging. *Postharvest Biology and Technology, 112*, 134-142.

Xing, J., Guyer, D., Ariana, D., & Lu, R. (2008). Determining optimal wavebands using genetic algorithm for detection of internal insect infestation in tart cherry. *Sensing Instrumentation for Food Quality Safety, 2*(3), 161-167.

Yang, C.-C., Kim, M. S., Millner, P., Chao, K., Cho, B.-K., Mo, C., . . . Chan, D. E. (2014). Development of multispectral imaging algorithm for detection of frass on mature red tomatoes. *Postharvest biology and technology, 93*, 1-8.

Yang, S. F., Xue, L., & Zhao, J. M. (2014). *Detecting system of crop disease stress based on acoustic emission and virtual technology.* Paper presented at the Applied mechanics and materials.

Yu, D., & Li, J. J. I. C. J. o. A. S. (2017). Recent progresses in deep learning based acoustic models. *4*(3), 396-409.

Zdunek, A., & Bednarczyk, J. (2006). Effect of mannitol treatment on ultrasound emission during texture profile analysis of potato and apple tissue. *Journal of texture studies, 37*(3), 339-359.

Zdunek, A., Cybulska, J., Konopacka, D., & Rutkowski, K. (2011). Evaluation of apple texture with contact acoustic emission detector: A study on performance of calibration models. *Journal of Food Engineering, 106*(1), 80-87.

Zdunek, A., Konopacka, D., & Jesionkowska, K. (2010). Crispness and crunchiness judgment of apples based on contact acoustic emission. *Journal of texture studies, 41*(1), 75-91.

Zdunek, A., & Konstankiewicz, K. (2004). Acoustic emission in investigation of plant tissue micro-cracking. *Transactions of the ASAE, 47*(4), 1171.

Zhang, B., Li, J., Fan, S., Huang, W., Zhao, C., Liu, C., & Huang, D. (2015). Hyperspectral imaging combined with multivariate analysis and band math for detection of common defects on peaches (Prunus persica). *Computers and Electronics in Agriculture, 114*, 14-24.

Zhang, B., Zhang, M., Shen, M., Li, H., Zhang, Z., Zhang, H., . . . Xing, L. (2021). Quality monitoring method for apples of different maturity under long-term cold storage. *Infrared Physics & Technology, 112*, 103580.

Zhang, D., Xu, Y., Huang, W., Tian, X., Xia, Y., Xu, L., & Fan, S. (2019). Nondestructive measurement of soluble solids content in apple using near infrared hyperspectral imaging coupled with wavelength selection algorithm. *Infrared Physics & Technology, 98*, 297-304.

Zhang, H., & Wang, J. (2007). Detection of age and insect damage incurred by wheat, with an electronic nose. *Journal of stored products Research, 43*(4), 489-495.

Zhang, L., & McCarthy, M. J. (2013). Assessment of pomegranate postharvest quality using nuclear magnetic resonance. *Postharvest Biology and Technology, 77*, 59-66.

Zhang, W., Lv, Z., & Xiong, S. (2018). Nondestructive quality evaluation of agro-products using acoustic vibration methods—A review. *Critical Reviews in Food Science and Nutrition, 58*(14), 2386-2397.

Zhou, B., & Wang, J. (2011). Discrimination of different types damage of rice plants by electronic nose. *Biosystems engineering, 109*(4), 250-257.

Zhou, J., Hong, X., & Jin, P. (2019). Information Fusion for Multi-Source Material Data: Progress and Challenges. *Applied Sciences, 9*(17), 3473.

Zhou, L., Zhang, C., Qiu, Z., & He, Y. (2020). Information fusion of emerging non-destructive analytical techniques for food quality authentication: A survey. *TrAC Trends in Analytical Chemistry, 127*, 115901. doi:https://doi.org/10.1016/j.trac.2020.115901

Žibrat, U., Gerič Stare, B., Knapič, M., Susič, N., Lapajne, J., & Širca, S. (2021). Detection of root-knot nematode Meloidogyne luci infestation of potato tubers using hyperspectral remote sensing and real-time PCR molecular methods. *Remote Sensing, 13*(10), 1996.

VITA

Education

Master of Science (MS), University of Tehran, 09/17/2008

Bachelor of Science (BS), Tabriz University, 09/22/2005

PROFESSIONAL EXPERIENCE

Researcher/Lecturer, University of Mohaghegh Ardabili, Ardabil, Iran.
R&D Expert, AVA-Pezeshk Company, Research and Development Department, Iran.

PROFESSIONAL PUBLICATIONS

1. Ekramirad, N., Khaled, A. Y., Doyle L. E., Loeb J. R., Donohue K. D., Villanueva R. T., and Adedeji A. A. (2022). Nondestructive Detection of Codling Moth Infestation in Apples Using Pixel-Based NIR Hyperspectral Imaging with Machine Learning and Feature Selection. Foods 11(1), 8. https://doi.org/10.3390/foods11010008

2. Ekramirad, N., Khaled, A. Y., Parrish, C. A., Donohue, K. D., Villanueva, R. T., & Adedeji, A. A. (2021). Development of pattern recognition and classification models for the detection of vibro-acoustic emissions from codling moth infested apples. Postharvest Biology and Technology 181, 111633. https://doi.org/10.1016/j.postharvbio.2021.111633.

3. Adedeji, A. A., Ekramirad, N., Rady, A., Hamidisepehr, A., Donohue, K. D., Villanueva, R. T., ... & Li, M. (2020). Non-destructive technologies for detecting insect infestation in fruits and vegetables under postharvest conditions: a critical review. Foods, 9(7), 927. https://doi.org/10.3390/foods9070927.

4. Li, M., Ekramirad, N., Rady, A., & Adedeji, A. (2018). Application of acoustic emission and machine learning to detect codling moth infested apples. Transactions of the ASABE, 61(3), 1157-1164. doi: 10.13031/trans.12548.

5. Ekramirad, N., Rady, A., Adedeji, A. A., & Alimardani, R. (2017). Application of Hyperspectral imaging and acoustic emission techniques for apple quality prediction. Transactions of the ASABE, 60(4), 1391-1401. doi: 10.13031/trans.12184.

6. Rady, A., Ekramirad, N., Adedeji, A. & Alimardani, R. (2017). Hyperspectral imaging for detection of codling moth infestation in GoldRush apples. Postharvest Biology and Technology, 129, 37–44. https://doi.org/10.1016/j.postharvbio.2017.03.007.

7. Ekramirad, N., Adedeji, A. A., & Alimardani, R. (2016). A review of non-destructive methods for detection of insect infestation in fruits and vegetables. Innovations in Food Research, 2, 6-12.

8. Ekramirad, N., Khazaei, J., & Khoshtaghaza, M. H. (2011). Selected mechanical properties of pomegranate peel and fruit. International Journal of Food Properties, 14(3), 570-582. https://doi.org/10.1080/10942910903291920.

9. Khazaei, J., Ekrami-Rad, N., Safa, M., & Nosrati, S. Z. (2008). Effect of air-jet impingement parameters on the extraction of pomegranate arils. Biosystems engineering, 100(2), 214-226. https://doi.org/10.1016/j.biosystemseng.2008.02.010.

Nader Ekramirad